Non-invasive Fetal RhD Type Prediction by Direct qPCR

by

Kellar Bastian Klein

A thesis submitted in partial fulfillment of the requirements for the degree of

Master of Science

Department of Laboratory Medicine and Pathology

Abstract

Hemolytic disease of the fetus and newborn (HDFN), characterized by anemia, jaundice, and edema, can lead to fetal/neonatal death in its most severe form. Linked to maternal immune response to the RhD antigen, the disease can be prevented by administering Rh immune globulin (RhIg) to D-negative pregnant women. Current Canadian guidelines recommend an antepartum dose be given at 28 weeks' gestation. However, up to 40% of these antepartum injections are unnecessary because the fetus is also D-negative and incapable of causing RhD sensitization. Unnecessary RhIg treatment could be avoided if the fetal blood type were known. Some international regions use non-invasive prenatal testing (NIPT), a genetic test that detects the small amount of cell-free fetal DNA that circulates in maternal blood, to predict fetal RhD type and determine RhIg eligibility, but the technique has not been widely adopted in North America. There are many factors that could contribute to this, including cost and availability of technical expertise.

NIPT is a quantitative polymerase chain reaction (qPCR) method and current protocols require purified DNA. An inhibitor-resistant polymerase eliminates the DNA purification step and can be used to perform PCR directly from whole blood, plasma or other "dirty" sample types. By eliminating the DNA purification step, direct qPCR (dqPCR) can reduce costs, improve turnaround times and make fetal RhD typing easier to perform. This thesis examined the hypothesis that dqPCR using maternal blood from D-negative women can accurately predict fetal RhD type at or before 28 weeks' gestation.

The work presented in this thesis has provided insight into the impact of sample matrix on whole blood dqPCR and demonstrated that whole blood dqPCR for RhD antigen typing was comparable to traditional qPCR using extracted DNA. Additionally, this work described the development of a plasma-based dqPCR protocol. Finally, this thesis described the first use of dqPCR for RhD NIPT.

Preface

This thesis is an original work by Kellar Klein. The research project, of which this thesis is a part, received the research ethics approval from the University of Alberta and Canadian Blood Services as detailed below.

University of Alberta, "A microfluidics device for ABO and RhD testing", Study ID: Pro00001114, 13May2007

University of Alberta, "Validation of a method for non-invasive fetal RhD phenotype prediction by qPCR directly from blood samples without DNA extraction", Study ID: Pro00047045, 04Jan2014

Canadian Blood Services, "Blood group antigen identification using DNA-based technology", Protocol reference # 2001-010, 10Aug2011

Canadian Blood Services, "Validation of direct qPCR for non-invasive fetal RhD typing", Protocol reference # 2014.018, 23Feb2014

The inclusion, contents, and placement of Table 30 in this document were dictated by the examining committee. The author of this thesis does not consider the table to be his own work and thus, acknowledges the origin of it here.

Acknowledgements

I would like to thank the following people and organizations:

My supervisor, Dr. Jason Acker, and the members of my supervisory committee, Dr. Gwen Clarke and Dr. Stephanie Yanow, for their guidance

Canadian Blood Services
- CBS netCAD for donor selection, consent and collections
- CBS Graduate Fellowship Program for scholarship funding
- CBS and Health Canada for research funding
- Diagnostic Services – Edmonton Centre, especially:
  - Kirsten Hannaford, Jean Ashdown & crossmatch lab staff for sample phenotyping
  - Gerri Barr and Celsie Mallard for NIPT study sample procurement
- Dr. Qi-Long Yi for NIPT study sample size calculations

Humirah Sultani for technical work on the whole blood fragmented DNA LOD experiment

Women & Children's Health Research Institute for generous support of the NIPT study through the Clinical Seed Grant program:

This research has been funded by the generosity of the Stollery Children's Hospital Foundation and supporters of the Lois Hole Hospital for Women through the Women and Children's Health Research Institute.

The following people deserve very special recognition:

Staff and students of Acker Lab, past and present, for friendship, encouragement and distractions ☺

Dr. Jelena Holovati for support and guidance when I was struggling to write

Dr. Lisa Ross-Rodriguez for wisdom and clarity of thought when the going was toughest

Tracey Turner for understanding me and being the best friend in the world

My parents, Al and Diane Allenby, for their unwavering support, understanding, encouragement and unconditional love

Thank you seems like too small a thing to say, for without you, this thesis would not exist.

Table of Contents

List of Tables

List of Figures

Abbreviations/List of Symbols

bp	base pairs
cffDNA	cell-free fetal DNA
DEL	a class of RHD alleles with very weak antigen expression, detectable only by adsorption-elution techniques or genetic testing
dqPCR	direct quantitative polymerase chain reaction
EG	EvaGreen fluorescent dye
FBS	fetal bleed screen
HDFN	hemolytic disease of the fetus and newborn
HTR	hemolytic transfusion reaction
IAT	indirect antiglobulin test
IBGRL	International Blood Group Reference Laboratory
IS	immediate spin
KMB	Klentaq Mutant Buffer, a PCR buffer for use with OmniKlentaq polymerase
LOD	limit of detection
MCA	melt curve analysis
MoAb	monoclonal antibody
NIPT	non-invasive prenatal testing
OKT	Omni Klentaq polymerase
PCR	polymerase chain reaction
PEC	PCR enhancement cocktail
PL	plasma
qPCR	quantitative polymerase chain reaction
RBC	red blood cell
RFLP	restriction fragment length polymorphism
RhAG	Rh associate glycoprotein
RhIg	Rh immune globulin
SG	SYBR Green I fluorescent dye
SRA	specific research aim
UTR	untranslated region
WB	whole blood

Chapter 1: Introduction

Every year, pregnant women in Canada receive unnecessary treatment with a blood product[1], a practice that raises ethical concerns as well as questions of appropriate allocation of healthcare resources. The treatment is given to prevent complications arising from blood group differences between the mother and fetus[2].

The matching of human blood groups, defined by proteins and sugars located on the surface of red blood cells (RBC), is extremely important for modern medical treatments. The proteins and sugars, called antigens, are organized into over 30 different blood group systems[3] based on their genetic origin and are the foundation of matching blood. For patients with anemia or traumatic blood loss due to injury or disease, transfusion of correctly matched blood components can have a significant impact on their recovery. Incorrect matches, however, can present significant problems in a variety of therapeutic contexts[4]. In pregnancy, blood group mismatches between the mother and fetus can cause the mother to become immunized and form antibodies against the fetus' blood group antigens[5]. This may result in hemolytic disease of the fetus and newborn (HDFN), with severity ranging from mild anemia at birth to fetal death[6].

Though many blood group antigens can cause problems during pregnancy, the D antigen of the RH blood group system is of significant concern[6]. A D-negative woman carrying a D-positive fetus is at risk of becoming immunized against the D antigen. Anti-D antibodies can cross the placenta and interact with fetal red blood cells causing anemia and, in severe cases, fetal death. To prevent immunization, Rh immune globulin (RhIg), a product derived from human blood, is administered during pregnancy at about 28 weeks gestation and again at delivery if testing of umbilical cord blood indicates that the baby is D-positive[7]. However, as a D-negative fetus poses no risk of maternal immunization, the antenatal RhIg treatment is unnecessary for some women[1].

Although RhIg is generally viewed as safe[8], the risks associated with it being a blood product cannot be completely eliminated. As the manufacturing process for RhIg may include deliberate immunization of volunteers, there are also ethical reasons for reducing unnecessary usage. Usage reduction hinges on knowing the fetal D type, as only D-positive fetuses are capable of triggering immunization in a D-negative mother. Due to the complexity of the RH blood group system, the traditional serologic testing technique can be inadequate, especially in terms of identifying and differentiating variant D antigens[9, 10]. DNA testing addresses some of these shortcomings, but also

has challenges, including prediction of D-type when non-functional gene sequences are present[11]. Additionally, obtaining cells or DNA directly from the fetus for testing can be difficult and risky[12].

In light of these challenges, some countries have begun using non-invasive prenatal testing (NIPT) to determine fetal RhD type by detecting the small amount of fetal DNA that exists in the mother's blood[13, 14]. Often, however, NIPT is used only if the mother has already been immunized. The cost and complexity of testing likely contribute to the slow adoption of routine NIPT for predicting fetal RhD type and determining RhIg eligibility.

Direct PCR, a testing technique that eliminates the need for steps to purify DNA from blood samples[15], could simplify and reduce the costs of NIPT. Accordingly, the purpose of this thesis is to explore the hypothesis that direct PCR using maternal blood from D-negative women can predict fetal RhD type at or before 28 weeks gestation.

In the pages that follow, I will provide background information on the RH blood group system, describe the problematic condition caused by perinatal RhD immunization and discuss the attempt to eliminate its effects through the use of RhIg. I will also provide information on testing methods and their limitations, including serologic D antigen phenotyping, *RHD* genotyping and non-invasive perinatal testing. Finally, I will introduce the objectives that create the framework for the original research presented in this thesis.

RH Blood Group System

Though most people have a passing familiarity with the RH blood group system (i.e. they know that some individuals are positive for the "Rh factor" and others are negative), they would likely be surprized at the complexities of RH genetics and the resultant phenotypic variations. Given that specialists in the field of transfusion medicine consider RH the most complex of the blood group systems[1], it seems fitting that the antigen originally given the moniker of Rh by Landsteiner and Wiener in 1940[16] was later found to be completely unrelated to the RH system[17]. Nevertheless, the name persisted. Since then, 54 antigens have been ascribed to the RH system[3]. The use of human polyclonal antibodies, monoclonal antibodies, and molecular analyses as well as the study of null phenotypes have all been important in identifying and characterizing the antigens assigned to the

RH system[18]. The five main antigens of the system are D, C, c, E, and e, with C/c and E/e being antithetical pairs[19].

Structure and Function of Rh Proteins

The proteins that express the Rh antigens, RhD and RhCcEe, are comprised of 417 amino acids[20, 21] and differ by 31 to 35 amino acids[1]. Part of a superfamily of homologous proteins that include Rh-associated glycoprotein (RhAG) and two non-erythroid proteins (RhBG and RhCG)[22], they are characterized by 12 transmembrane domains with six extracellular loops. There is evidence that RhD, RhCcEe and RhAG proteins form an Rh complex in the red cell membrane[22, 23] though specific details of the multimeric interaction are still to be elucidated[24]. RhAG, the basis of a separate blood group system[25], is required for the expression of RhD and RhCcEe proteins and individuals with Rh-deficiency syndrome (Rh_{null}) lack all Rh antigens due to failure of Rh complex formation[22]. The lack of the Rh complex has been associate with changes in RBC morphology, supporting a structural role for the Rh proteins[18, 22, 23]. Based on structural similarity to Mep and Amt proteins, it has been proposed that the Rh complex may function as an ammonium or carbon dioxide transporter[18, 22], though definitive data is lacking.

Gene Structure of the RH Blood Group System

The two genes that code for Rh proteins, *RHD* and *RHCE*, are located on the short arm of chromosome 1[26] and code for the RhD and RhCcEe proteins respectively. Separated from *RHCE* by the unrelated *SMP1* gene, *RHD* is flanked by two very similar regions known as Rhesus boxes[27] and lies in reverse orientation to *RHCE* (Figure 1). *RHAG* is located on chromosome 6. All three genes have ten exons and while *RHAG* has approximately 40% of its sequence in common with *RHD* and *RHCE*[28], there are very few differences between *RHD* and *RHCE* (~97% homology)[10]. The translated regions of corresponding exons even have the same number of base pairs (bp). Despite the similarities between *RHD* and *RHCE*, there is at least one *RHD*-specific nucleotide in each of exons 3 to 7 and 9[29]. There are no differences in exon 8 and exon 2 is the same for *RHD* and *RHCE/e*.

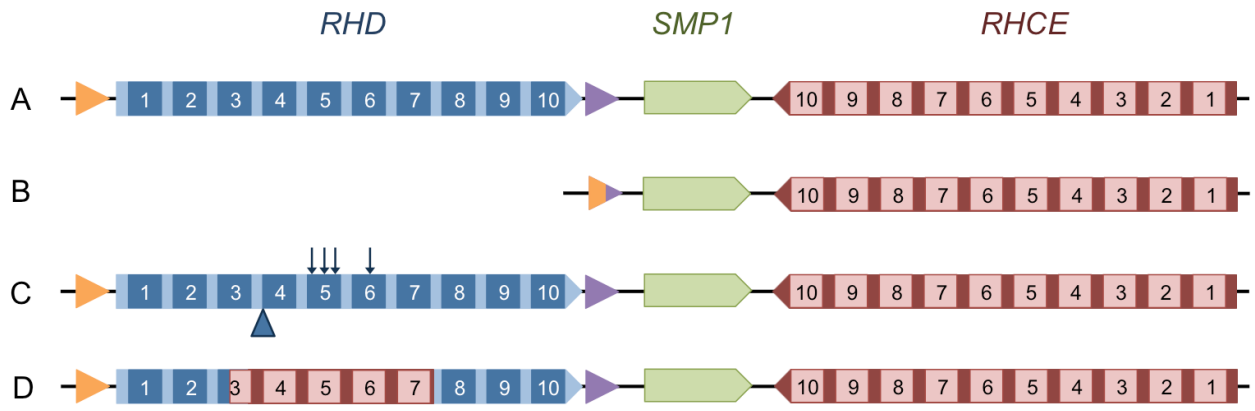

Figure 1. Genetic arrangement of the most common RhD phenotypes. The RH locus structures are depicted for A) D-positive showing Rhesus boxes (orange and purple triangles); B) D-negative by *RHD* gene deletion showing the hybrid Rhesus box; C) D-negative by RHDΨ indicating the 37 bp insertion (blue triangle) and polymorphisms (arrows); D) D-negative by *RHD-CE(3-7)-D* hybrid (*Cde*^{S}) showing the duplicated *RHCE* sequences (red boxes). The *SMP1* gene (shown in green) is unrelated to RH.

RHD and its Variants

The presence of the RhD protein denotes the D-positive phenotype, but the highly variable nature of the *RHD* gene gives rise to a number of phenotype alterations. The first D variant was identified just six years after discovery of the antigen[30], and by 2006 over 150 variants had been classified as partial D, weak D or DEL[31]. Unique variants continue to be discovered, with at least 22 reported in the past year[32].

Although there are inconsistencies in classification stemming from problematic definitions of weak D and partial D, an alternative term (D variant) has not yet been widely adopted[1]. By a common definition, based on the ability of an antigen to elicit an immune response, partial D antigens lack one or more epitopes thus individuals with such antigens have the potential to form anti-D if exposed to normal D-positive blood[22]. The inverse orientation of *RHD* and *RHCE* is believed to contribute to generation of hybrid alleles (e.g. *RHD-CE-D* hybrids) commonly seen in partial D variants through the formation of a hairpin structure in which the exons of the two genes line up facilitating conversion events[33]. Weak D are quantitative variants which have decreased antigen density but normal antigen structure[34] eliminating the possibility of alloimunization. The DEL phenotype, first reported in 1984[35], is generally an extreme form of weak D, though partial DEL variants with extremely low antigen density as well as altered epitopes have been reported[36].

The molecular foundation of the D-negative phenotype also shows variations. Wagner and Flegel[27] reported that the most common D-negative allele in Caucasians is a complete deletion of *RHD* characterized by the presence of a hybrid Rhesus Box (Figure 1). The homology and identical orientation of the upstream and downstream Rhesus boxes likely contributed to the deletion event[27]. Further investigation by Wagner, Moulds and Flegel[37] found that there is significant variation in both upstream and downstream Rhesus boxes, complicating detection of the hybrid Rhesus box. The D-negative phenotype is slightly more complicated in people of African origin. In addition to the hybrid Rhesus box deletion allele, an *RHD* pseudogene (*RHD*Ψ)[38] or *RHD*-CE-D^S hybrid (*Cde*^{S}) are found in D-negative individuals. *RHD*Ψ has a 37 bp duplication of the intron 3/exon 4 splice site and a number of point mutations including one that translates into a stop codon in exon 6[38]. For *Cde*^{S}, a 3´ section of exon 3 and exons 4 to 7 have been replaced with sequences from *RHCE*[39].

Anti-D Alloimmunization

Alloimmunization, the development of an antibody to an antigen that a person lacks, can occur upon exposure to RBCs. Alloimmunization to blood group antigens complicates matching blood for transfusion, as the antibody can cause destruction of transfused RBCs that carry the corresponding antigen. Hemolytic transfusion reactions (HTR) due to antibody/antigen interactions vary in severity depending on the specific conditions, including the characteristics of the antibody and antigen. Hemolysis can be intravascular, occurring within the blood vessels, or extravascular, with the reticuloendothelial system being the site of RBC destruction. In mild reactions, the transfused RBCs have a shortened lifespan and the anemic condition that prompted the transfusion may recur. Tissue damage due to arterial hypotension, disordered bleeding attributed to simultaneous activation of clotting and fibrinolytic cascades, and renal failure contribute to poor outcomes in severe reactions[40].

The D antigen is highly immunogenic and, although it does not occur for every exposure, anti-D alloimmunization is not uncommon. One study found anti-D in 79% of D-negative volunteers after a single exposure to D-positive RBCs[41]. Accurate determination of D status in blood donors, as well as those receiving transfusion, is very important in terms of preventing alloimmunization, which can produce potent antibodies. Evidence that DEL red blood cells can elicit an immune response, both primary[42] and secondary[43, 44], in D-negative transfusion recipients has led to the realization that unidentified DEL donors may be responsible for alloimmunization[22, 34].

Hemolytic transfusion reactions attributed to anti-D are most often associated with extravascular hemolysis and milder symptoms. With respect to pregnancy, prevention of Rh alloimmunization is of special importance because anti-D exhibits transplacental mobility. Consequences for an affected pregnancy can be disastrous.

Hemolytic Disease of the Fetus and Newborn

Hemolytic disease of the fetus and newborn (HDFN), or erythroblastosis fetalis, was first described in the literature in 1609[45]. It is characterised by anemia, jaundice, and edema and can lead to fetal/neonatal death in its most severe form. The notion of an antibody-antigen reaction traced to the mother and passed to the fetus via the placenta as the cause of HDFN was first proposed by Darrow[46] in 1938. A year later, Levine & Stetson[47] presented data that indicated pregnancy could elicit an immune response in the mother and by 1941 the disease had been linked to the newly discovered "Rh factor" (D antigen)[5]. It is now known, as suggested by Levine[48], that other antibodies can be implicated, though anti-D remains one of the most common[49].

The first antigen incompatible pregnancy is rarely affected by HDFN. Instead, it is usually the source of the RBCs that trigger alloimmunization in the mother (see Figure 2). In subsequent pregnancies, the antibody crosses the placental barrier and interacts with RBCs carrying the incompatible antigen causing hemolytic anemia. During pregnancy, the mother's liver clears excess unconjugated bilirubin produced from the breakdown of hemoglobin. After birth, the neonate's underdeveloped liver may not be able to adequately process the toxic unconjugated bilirubin. As a result, the newborn may become jaundiced. Kernicterus, a potentially fatal accumulation of toxic bilirubin in the brain, can occur if hyperbilirubinemia is left untreated. Clinical signs and sequelae include lethargy, high-pitched cry, opisthotonos[a], sensorineural deficits and intellectual disability. In cases of severe fetal anemia, extramedullary erythropoiesis, hepatosplenomegaly, and liver damage lead to hydrops fetalis, a condition characterized by edema, effusions and ascites and often results in death.

[a] Opisthotonos is a condition in which muscle spasms causes backwards arching of the body.

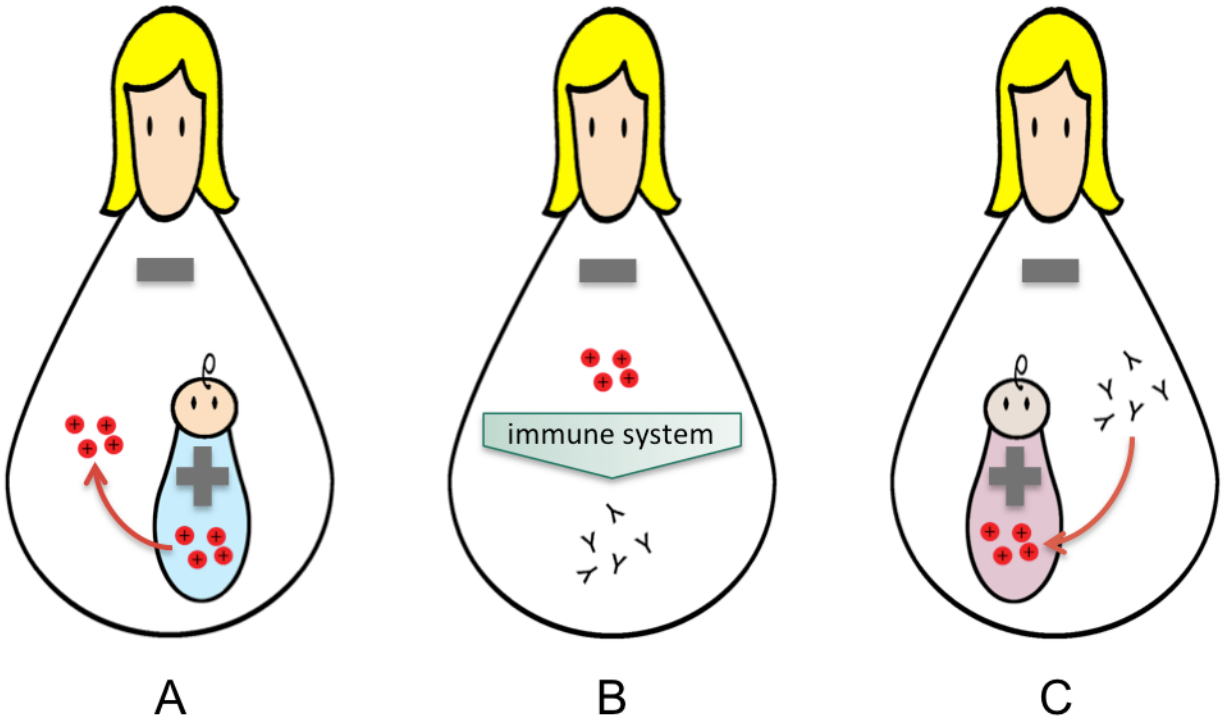

Figure 2: Anti-D alloimmunization mechanism of HDFN. D-positive fetal RBCs can enter maternal circulation during pregnancy or at delivery (A). The fetal RBCs are processed by the mother's immune system and anti-D is produced (B). During a subsequent pregnancy, maternal anti-D crosses the placenta and leads to destruction of D-positive fetal RBCs.

Rh Immune Globulin Prophylaxis for the Prevention of HDFN

The idea that an antibody could be used to remove fetal red cells (RBC) from maternal circulation before alloimmunization occurred was first presented in 1960 by Dr. Ronald Finn[50] after it was noted by Levine[48] that ABO incompatibility between the mother and father of HDFN children occurred less frequently than expected. It was postulated that the incompatibility afforded protection against D-immunization due to destruction of the fetal red cells by naturally occurring ABO antibodies[50].

The ability to differentiate fetal from adult RBC on a blood smear[51] aided research into the prevention of HDFN. Investigations of the incidence of transplacental hemorrhage[52], the class of immunoglobulin associated with the clearing of foreign RBC (IgM vs. IgG)[53] and clinical trials carried out in Liverpool, New York and Freiberg[54] in the 1960s led to the development of Rh Immunoglobulin (RhIg). RhIg, a human-sourced polyclonal anti-D preparation proven to be

successful in preventing D-negative women from becoming immunized by D-positive pregnancies[55], was granted North American licensure as a prophylactic treatment in 1968[45, 56].

Manufacture of RhIg from Human Plasma

Originally, RhIg was prepared using plasma from women who had developed potent anti-D through perinatal exposure. The success of RhIg prophylaxis reduced the availability of this source material. To maintain a sufficient supply of source plasma, healthy D-negative volunteers, men or post-menopausal women, are deliberately injected with D-positive RBCs to induce immunization. Although the RBCs are thoroughly tested to reduce the chance of disease transmission, the risk can never be completely eliminated. Being immunized also puts the volunteers at greater risk should they need a transfusion. This creates an ethical dilemma around usage of RhIg that has prompted interest in targeted RhIg prophylaxis and spurred research into monoclonal RhIg[45]. The lack of success with monoclonal antibodies to date is likely due to the fact that the mechanism by which RhIg works remains unclear.

Mechanism of Alloimmunization Prevention by RhIg

Anti-D prophylaxis exploits the ability of IgG antibodies to prevent an immune response when given at the same time as the corresponding antigen. This ability, termed antibody-mediated immune suppression (AMIS), is not well understood. Brinc et al.[57] discussed evidence for and against the three major mechanistic hypotheses of AMIS (antigen clearance, FcγRIIB-mediated B-cell inhibition and epitope masking) and ultimately proposed an alternate theory in which B-cell antigen processing altered by the presence of IgG prevents full activation of B-cells by reducing T-cell help. The precise mechanism of AMIS is yet to be elucidated and could prove to be an important step towards successful development of monoclonal anti-D for prophylaxis.

Perinatal Administration of RhIg

RhIg was initially administered after delivery only (within 72 hours as is standard today). Work at the Rh Laboratory in Winnipeg revealed that some women who were not immunized at the outset of pregnancy had developed anti-D sometime before delivery so Bowman et al. suggested prophylaxis be given during pregnancy as well[56]. Current clinical practice guidelines from the Society of Obstetricians and Gynaecologists of Canada recommend RhIg be administered at 28 weeks' gestation when specific eligibility conditions are met[7](Table 1). The Alberta Prenatal Screening Program and others like it test expectant mothers for ABO/Rh type and the presence of blood group

antibodies prenatally and at delivery to ensure that D-negative women receive antenatal and post-delivery Rh prophylaxis.

Although blood group typing is part of routine prenatal care to determine eligibility to receive RhIg, the lack of routine testing to determine fetal D status means that up to 40%[1] of D-negative women will be unnecessarily exposed to this blood product. This number is approximate because of race-dependent variations in antigen frequency (Table 2).

Table 1: Antenatal RhIg eligibility conditions for pregnancy women

Condition	Routine Testing
D-negative	serologic D phenotyping
no evidence of D alloimmunization	antibody screen
fetal D type unknown or known to be D-positive	none

Table 2: Occurrence of the D antigen in various populations[17]

Population	Frequency
Caucasians	85%
Blacks	92%
Asians	99%
Native Americans	99%

Advantages of Knowing Fetal D Type

There are two situations where knowing the fetal D type could alter perinatal treatment. For unimmunized women, knowing the fetal D-type allows the antenatal RhIg dose to be targeted to only those women at risk of immunization. If maternal immunization has already occurred, frequent monitoring of fetal health and measurement of maternal antibody titre is standard treatment for all women to ensure that timely intervention occurs if needed. However, because a D-negative fetus is not at risk for complications related to HDFN, determining the fetal D type can indicate which patients need additional follow-up care.

D Antigen Phenotyping

Basic D typing, an immediate spin (IS) technique performed by adding patient red cells to reagent anti-D followed by a brief centrifugation step and inspection for agglutination (graded from negative to 4+), differentiates D-positive (agglutination) from D-negative (no agglutination) phenotypes. Though a simple procedure, complications arise due to genetic mutations, the exact method performed, and reagent specificity[58].

Stratton[30] described the first example of variant D, which he termed D^u, in 1946. To this day, detection of weakened D variants by serologic methods is challenging, though considered optional in certain circumstances (e.g. perinatal testing)[59]. The weak D test is an indirect antiglobulin test (IAT), which includes an incubation step (to sensitize the red cells with anti-D), the use of an antihuman globulin reagent and a second agglutination reading in addition to the immediate spin procedure. It was first described by Coombs, et al.[60] as a means to detect IgG ("incomplete") antibodies. Although many variant D forms can be detected by this method, there is no way to differentiate those that at are risk of forming alloanti-D from those that are not[61]. This remains a significant limitation. Partial and fully automated systems now exist that use gel-filled microtubes (e.g. ID-Micro Typing System™ from Ortho-Clinical Diagnostics) or solid phase technology (e.g. Capture® from Immucor Gamma). Although these automated systems are based on the same hemagglutination principles as tube tests, discrepancies between them have been noted[62]. An earlier report found no discrepancies between the manual tube method and the gel system in parallel testing of known weak D samples[63] however, the particular weak D variants tested were not indicated.

In addition to weak D and partial D, variants with both characteristics (e.g. partial DEL[36] and DVI[64]), D epitopes on RHCE proteins[58] and DEL variants are difficult if not impossible to identify serologically. For example, DEL types require adsorption-elution studies as they are not detected by either IS or IAT testing. Further complicating matters is the example of weak D type 4.2 and partial D DAR. Daniels et al.[65] pointed out that the two are phenotypically identical (differentiated by a single silent mutation) and suggested that separate nomenclature for partial and weak D should be abandoned in favour of a single "D variant" category. Westhoff states that genetic polymorphisms are only important when they identify a specific phenotype that has been associated with antibody formation[10] but if we know that a mutation is likely to have altered epitopes then there is always a chance that somebody will become immunized.

D variant phenotypes can pose significant challenges in the transfusion medicine laboratory. Historically, blood group typing has been a serologic hemagglutination method. Indeed, the mixing of red blood cells with serum containing an agglutinin (antibody) was how Landsteiner first discovered blood types in 1901[66]. Although standard serologic techniques can detect many weak and partial D variants, interpretation of results to determine D antigen status is not always straightforward. Depending on the particular reagent and technique in use, some variants are deliberately typed as positive or negative (according to their propensity to cause or become immunized), some are completely undetected, and others manifest as discrepancies where they type as positive by one reagent/technique combination and D-negative by another protocol[58]. Even if detected without difficulty, serology cannot differentiate partial D (risk of forming alloanti-D) from weak D[61]. Identification of DEL variants is especially difficult because the number of antigens present on the red cell is so low that routine serologic methods are insufficient and adsorption/elution is required to identify them[35].

Reagent Specificities

FDA-licensed reagent specificities vary widely and this affects the results obtained with D variants[58, 67]. Most are a mixture of monoclonal IgM and monoclonal or polyclonal IgG. In contrast, most European facilities have switched to IgM monoclonal antibody (MoAb) reagents[68]. Studies with these reagents have revealed MoAb families having specific reaction patterns with D variants[69, 70].

Donor vs. Recipient

Regarding D variants as D-positive or D-negative depends upon their status as blood donor or recipient. In some regions, identification cards are provided that indicate the individual is D-positive as donor but should be considered D-negative for transfusion or RhIg prophylaxis purposes[71]. Transfusion laboratory personnel have been reluctant to assign different D types to an individual for different situations[10]. The "D variant" category could address this as well, and Westhoff[10] reports on one hospital that essentially does this.

Flegel et al.[64] seem to support building a negative bias into testing methods and reagents used for recipient testing (i.e. no IAT testing, limited specificity reagent) in an effort to classify those with variants susceptible to alloimmunization as D-negative. While this seems like a wise idea, the lack

of measures to guarantee the D-negative blood supply (i.e. no unidentified DEL or other potential immunizing phenotype in D-negative donor pool) and potential to increase unnecessary exposure to RhIg make me question the value and ethics of such a bias.

Despite these issues, error rates reported by the UK National External Quality Assessment Scheme for simple RhD typing did not change significantly from 1984 to 2000 and remain quite low (approximately 0.2%)[68]. The same report indicates that discrepant results are still a problem for weak D phenotypes but a common immunization susceptible partial D (DVI) posed no difficulties while Denomme et al.[72] showed that other partial D types are not adequately identified by serologic techniques. *RHD* genotyping in concert with serological testing offers solutions to many of these problems but requires a robust, rapid and cost effective method in order to gain acceptance in mainstream transfusion medicine laboratories.

Fetal D Phenotyping

Although serologic testing can be performed on fetal RBC, obtaining samples is invasive and carries substantial risks. Complications of fetal blood sampling (FBS) include fetal bradycardia, umbilical hematoma or bleeding, chorioamnionitis, and fetal death[73].

RHD GENOTYPING

Non-invasive fetal antigen typing, zygosity determination and resolution of weak or discrepant results (e.g. variant phenotypes) are areas where molecular diagnostics outshine serologic testing methods[9]. Genotyping is useful since serologic methods alone cannot adequately identify weak D or partial D[74], but Reid[9] points out that the genotype itself is of limited value unless it can be used to accurately predict blood group antigen expression.

Molecular Techniques

Polymerase chain reaction (PCR) with restriction fragment length polymorphism (RFLP) analysis has been a useful tool in discovering, characterizing and differentiating new *RHD* alleles[29]. For example, the hybrid Rhesus box has been detected by observation of an additional *Pst*I restriction site when compared to the downstream Rhesus box[37]. However, the availability of sequence information for *RHD* and *RHCE* made qPCR methods possible.

The general approach for many *RHD* genotyping studies in the last few years has been to subject samples with weak or negative D phenotypes to molecular testing for a few known variant alleles. Any samples not specifically identified at this point would be further analysed by exon screening and sequencing. This basic strategy was outlined by Seltsam and Doescher[75]. Polin et al.[76] used this tactic to successfully genotype weak D types 1, 2 and 3 and identify the first documented incidence of weak D type 49[76].

Exon screening verifies the presence or absence of exons by using primers designed to amplify nearly the entire exon sequence. Gassner et al.[77] reported a sequence-specific primer polymerase chain reaction (PCR-SSP) exon screening protocol that used seven *RHD*-specific primer sets (exons 3 to 10). These primer sets allowed differentiation of *RHD* sequences from those of *RHCE* despite the nearly identical nature of the two genes.

While exon screening can identify a number of *RHD-CE-D* hybrids (e.g. DVI), SNPs within the amplified sequence cannot be detected[77]. However, unexpected results in exon screening (e.g. the presence of exons in D-negative samples) can be used to identify samples appropriate for genetic sequencing, aiding in the characterization of new variant D alleles. Such characterization allows for positive identification of known alleles by PCR-SSP. While electrophoresis of amplified products is often used, real-time PCR with TaqMan probes and melting curve analysis (MCA) are proving useful in *RHD* genotyping[78].

Differentiation of *RHD* from *RHCE*

Since *RHD* and *RHCE* are so closely related in sequence, it is important to be able to differentiate them. Two differences occur in the 5´ untranslated region (UTR) of exon 1 and the 3´ UTR of exon 10 as these regions are different for each gene (Table 3). In addition to differences in exons, *RHD* has a 600-bp deletion in intron4[79] and a single primer set (one in exon 4 and one in exon 5) will yield two differently sized products, the larger coming from *RHCE*[80]. If differentiating standard *RHD* from the gene deletion D-negative allele was sufficient for accurate RhD phenotype prediction, any of the *RHD*-specific sequences could be used. Since the RH system is not that simple, consideration must be given to D-negative alleles when choosing *RHD*-specific targets.

Table 3. Comparison of Exon Regions

Region	Length of region (bp)		Number of *RHD* specific alleles[77]
	RHD	*RHCE*	
5´ UTR of exon 1	58	86	n/a
Exon 1 translated	148	148	0*
Exon 2	187	187	5 (*RHD/C*)**
Exon 3	151	151	4
Exon 4	148	148	7
Exon 5	167	167	8
Exon 6	138	138	2
Exon 7	134	134	15
Exon 8	80	80	0
Exon 9	74	74	1
Exon 10 translated	27	27	0
3´ UTR of exon 10	1521	295	large sequence

* exon 1 has one RHC specific allele

** *RHD* exon 2 is identical to RHC exon 2

Detection of D-negative Genotypes

In a review of non-invasive prenatal *RHD* typing by Daniels et al.[81], the most common targets were exons 7 and 10, both together and individually. This is problematic because *RHDΨ* has standard *RHD* sequences in these regions resulting in an incorrect phenotype prediction. Finning et al.[82] observed very low false positive and false negative rates (0.8% and 0.2% respectively) by pairing exon 5 with exon 7. In addition to the 37 bp insertion, *RHDΨ* has three point mutations in exon 5 and one in exons 4 and 6. Daniels et al.[81] suggests the use of *RHD*-specific primers for exons 4 and 5 so that negative PCR reactions (i.e. no amplification) are obtained for *RHDΨ* variants. The goal of having negative PCR reactions for genotypes corresponding to D-negative phenotypes may be too simplistic given the complex molecular structure of the RH genes. Another approach would be to also target the 37 bp repeat sequence specifically (i.e. absolute specific detection of the variant type). There is an *RHD*-specific SNP in exon 4 just beyond the duplicated sequence that, when paired with an intron 3 primer would give differently sized products for *RHD* and *RHDΨ* (*RHDΨ* product will be 37 bp longer) without amplifying *RHCE* sequences.

A similar direct detection strategy for other D-negative phenotypes (e.g. the *RHD*/*RHCE* breakpoint in exon 3 could be targeted for detection of the Cde^{s} allele) though application to hybrid Rhesus box detection may not be possible. Although direct detection of the hybrid Rhesus Box would allow definitive identification of D-negative phenotype, amplification of the entire hybrid Rhesus box (~9000 bp) as proposed by Wagner and Flegel[27] is technically challenging. Another method exploits

the differences in the upstream and downstream Rhesus Boxes but variations in these sequences and the existence of hybrid Rhesus Boxes with different breakpoints[37] indicates that phenotype prediction based on Rhesus box genotyping should be approached with caution.

Detection of D Variant Genotypes

Molecular typing of weak and partial D variants poses a challenge simply because there are so many. Many are exceedingly rare. By choosing the most appropriate targets for differentiation of *RHD* from RHCE and detection of D-negative genotypes, testing for only the more common D variant alleles may still allow accurate phenotype prediction in nearly every case. Primer sets for weak D types 1, 2 and 3 have already been reported[76] (Table 4).

Since many DEL variants are the result of single nucleotide polymorphisms, they can easily be detected by PCR-SSP methods. A study comparing PCR-SSP for the *RHD*1227A DEL allele with adsorption/elution reported sensitivity and specificity of 96.9% and 97.5% respectively[83].

Table 4. Weak D-specific Primer Sequences

Weak D type	Nucleotide change	Primers[76] (5' → 3')
1	809T>G	CAGGGTTGCCTTGTTCCCA TAGTTTCTTACCGGCAGGT
2	1154G>A	TGGTCCAGGAATGACAGGGCT CTTGGTCATCAAAATATTTAGCCT
3	8G>C	ATAGAGAGGCCAGCACAA GCTATTTGCTCCTGTGACCACTT

Fetal *RHD* Genotyping

Fetal genetic testing can be done on samples obtained by amniocentesis and chorionic villus sampling. Although slightly less invasive than fetal blood sampling, these methods carry similar risks.

NON-INVASIVE PRENATAL TESTING

As discussed above, knowing the fetal RhD type has important implications for management of pregnancy in D-negative women. If the fetus is also D-negative, a previously immunized woman may require less medical monitoring and intervention. For a non-immunized woman, unnecessary

exposure to a blood product (RhIg) could be prevented, but fetal blood sampling, amniocentesis, and chorionic villus sampling are too risky to be performed on a routine basis. In 1993, Lo et al.[84] presented the first proof that cellular DNA extracts from maternal peripheral blood could be used to determine fetal RhD type. Four years later, cell free fetal DNA (cffDNA) present in maternal plasma was identified as a potential source for NIPT of fetal RhD status[85]. A UK study in 2008 showed that NIPT can be used successfully to reduce the frequency of unnecessary RhIg treatment but illustrated concerns over false-negative results that would leave women at risk for immunization[81].

Anstee acknowledged the usefulness of blood group genotyping for HDFN (e.g. determining fetal blood type and paternal zygosity), but does not see it as a replacement for conventional serologic methods due to cost[86]. He suggests that red cell genotyping would be most useful if it could be targeted to immune responders (individuals likely to form alloantibodies)[86]. While this is true, definitive determination of immune responder status is not yet possible.

Assumptions & Challenges of NIPT for Prediction of Fetal D Type

NIPT for fetal D type prediction is based on three assumptions: (1) the mother is D-negative by the *RHD* deletion allele, (2) the fetus is D-positive by the standard RHD allele, and (3) a positive reaction is predictive of a D-positive fetal phenotype. For the majority of cases, these assumptions hold true. Challenges arise when either mother or fetus carries a variant allele. For example, if the mother carries the *RHDΨ* allele, most exon specific reactions will be positive because the *RHDΨ* sequences are identical to those of the standard *RHD* allele (Figure 1). The use of multiple, carefully chosen targets can detect and differentiate common D-negative alleles. In some circumstances, the use of quantitative polymerase chain reaction (qPCR) methods can indicate the source of the D-negative allele, either maternal or fetal. Despite the challenges, RHD NIPT has been successfully implemented in a number of regions internationally[13, 87] and a recent cost-benefit analysis indicated RhIg usage in Alberta could be reduced by over 4000 doses annually by implementing targeted prophylaxis[88].

Notable Fetal RhD Typing Methods

The International Blood Group Reference Laboratory (IBGRL) in Bristol, England was one of the first laboratories to offer fetal blood group genotyping and has been providing the service since 2001[89]. The IBGRL performs two slightly different *RHD* NIPT protocols depending on the maternal immunization status. For alloimmunized women, the reported method involved manual extraction

of DNA from maternal plasma followed by qPCR for *RHD* exons 4, 5 and 10 as well as non-RH control sequences and included a detailed interpretation algorithm[90]. Although the published protocol contains no reference to the recommended gestational age for testing, the IBGRL Blood Group Genotyping User Guide states that samples can be drawn as early as 16 weeks' gestation[91]. For determination of RhIg eligibility for non-immunized women, a high throughput automated method is used for extraction of cffDNA[82] from maternal plasma samples collected as early as 11 week's gestation[92]. Though the technical approach used is nearly identical, the two protocols have unique interpretation algorithms. For immunized women, the algorithm is designed to minimize false negative results, while the algorithm for the RhIg eligibility testing is designed to maximize the accuracy of both D-positive and D-negative fetal type predictions (Finning K, personal communication, 17Mar2016).

The first national program using NIPT to determine RhIg eligibility was implemented in Denmark in 2010. In the reported method, maternal samples were drawn at 25 weeks' gestation and extracted DNA was tested for two exon targets which were limited to exons 5, 7 and 10 but the combination of targets varied depending on the testing site, of which there were five[13].

Direct PCR

Although the benefits of *RHD* NIPT are clear, adoption in North America lags compared to European nations. Cost and availability of the required expertise can be factors affecting adoption. A common response employed to find a balance between limiting factors and a desire to implement genetic testing is to set up centralized/reference laboratories. While this approach can be adequate in other pathology disciplines, the often emergent nature of transfusion medicine demands timely access to genotyping results if they are to be of value in treatment decisions.

For transfusion services, nucleic acid testing platforms with on-demand testing and simplified protocols may be preferable to those designed for high-throughput. To bring nucleic acid testing out of reference labs and into hospital labs, a platform that is less expensive and easier to perform (e.g. less sample manipulation needed) than current molecular diagnostics but able to provide comparable quality results is needed. The ability to use instrumentation that may already be on-site (e.g. quantitative PCR analysers) could reduce the implementation cost. One way to make testing easier to use is to remove the DNA extraction step and use direct PCR, wherein unprocessed blood is added to PCR reactions. Although prenatal fetal typing for the purpose of determining RhIg

eligibility is not an emergency situation, simplification of testing by using direct PCR may overcome barriers to implementation.

Previous reports of direct PCR employed specialized buffers[93] or additives[94], heat pre-treatment[15, 95], inhibitor-tolerant polymerases[96] and inhibitor-resistant polymerases[97, 98], though the majority of protocols used endpoint PCR followed by electrophoresis rather than quantitative PCR.

Omni Klentaq (OKT) polymerase (DNA Polymerase Technology, St. Louis, USA) is an inhibitor-resistant polymerase that, when used in conjunction with a PCR enhancement cocktail (PEC), can be used to perform PCR directly from whole blood, plasma or other "dirty" sample types[99]. Taylor et al.[100] demonstrated the use of OKT polymerase in a direct qPCR protocol for the detection of *Plasmodium spp.* from whole blood and filter paper samples. This protocol serves as the starting point for the application of direct PCR to fetal *RHD* genotyping and the original research presented in this thesis.

Project Rationale and Framework

With NIPT, it is possible to determine a fetus' *RHD* status. This information, when included in antenatal RhIg prophylaxis eligibility criteria, can reduce unnecessary blood product exposure in D-negative women carrying D-positive fetuses. Although the approach has been implemented in other regions, routine *RHD* NIPT is not available in Canada. A recent cost/benefit analysis suggests that approximately 4000 antenatal doses of RhIg could be saved annually if *RHD* NIPT were implemented as part of the Alberta Perinatal Testing Program[88].

Cost and complexity of testing likely contribute to slow adoption, despite very good protocols being available for a decade or more. Direct PCR offers a means to simplify the testing protocol and eliminate costs associated with DNA extraction. Although the majority of studies exploring direct PCR employ electrophoresis, quantitative PCR is easier and faster to perform.

The aim of this thesis is to investigate the practicability of using direct quantitative PCR (dqPCR) to non-invasively predict fetal RhD type as part of a targeted antenatal RhIg prophylaxis program. The simplest approach to dqPCR is to use whole blood (WB) samples, eliminating sample manipulation altogether. This approach is reflected in the first Project Objective. As hemoglobin is an optically active compound, there may be interference that limits the practical use of WB dqPCR. In the

second Project Objective, the use of plasma (PL) samples eliminates the potential for hemoglobin interference while limiting sample manipulation. Together, the first two Project Objectives comprise the method development phase of the project. The application phase of the project, covered by the final Project Objective, is a clinical investigation that includes a pilot study to determine which dqPCR testing mode, whole blood or plasma, is to be used for the full clinical study. The project hypothesis, objectives and specific research aims (SRA) are presented below.

Research Hypothesis

DqPCR using maternal blood from D-negative women can accurately predict fetal RhD type at or before 28 weeks gestation.

Project Objectives

A. Determine performance characteristics of WB dqPCR.

SRA A-1: To investigate the impact of sample matrix on WB dqPCR.
SRA A-2: To determine PCR efficiency and limit of detection of WB dqPCR.
SRA A-3: To compare WB dqPCR, DNA qPCR, and serologic phenotyping and determine sensitivity, specificity, precision and accuracy of WB dqPCR.

B. Develop a method for dqPCR using plasma samples.

SRA B-1: To modify the WB direct qPCR protocol for use with plasma samples.
SRA B-2: To determine PCR efficiency and limit of detection of PL dqPCR.

C. Apply dqPCR to non-invasive prenatal testing for the prediction of fetal RhD type.

SRA C-1: To evaluate the appropriateness of WB and PL dqPCR for RhD NIPT (pilot study)
SRA C-2: To compare WB and PL dqPCR in the context of NIPT
SRA C-3: To compare dqPCR performed on clinical prenatal samples to cord blood RhD phenotyping and determine sensitivity, specificity, precision and accuracy

Chapter 2: Methods

This chapter is divided into five sections. The first two sections, Procurement and Processing of Samples and Finalized dqPCR Protocols, describe method details that are applicable to a number of experiments. The remaining three sections describe procedures used in experiments related to each of the three Project Objectives.

Procurement and Processing of Samples

Volunteer Donor Samples

Whole blood samples collected in EDTA were obtained from staff and student volunteers at the University of Alberta or from healthy volunteers at Canadian Blood Services' (CBS) Network Centre for Applied Development. CBS staff performed serologic RhD phenotyping by immediate spin only; weak D typing was not performed. Aliquots of whole blood were removed and the remainder was centrifuged at 2500 x *g* for 10 min at 4 °C. Plasma aliquots were removed and buffy coat was collected for DNA extraction. Whole blood, plasma and buffy coat aliquots were stored in 1.5 mL flip-top microtubes at -20 °C.

DNA Extraction and Quantification

DNA was extracted from buffy coat samples using a spin column-based method (QIAamp DNA Blood Mini kit), or a precipitation-based method (FlexiGene DNA kit) (both from QIAGEN, Toronto, Canada).

The QIAamp DNA Blood Mini kit has four stages: lysis, binding, washing, and elution (see Appendix A) for the detailed extraction protocol used for this project). The lysis reagents include a protease and chaotropic salts, which contribute to conditions that will allow DNA to bind to the spin column membrane. The addition of RNAse A (not included in the kit) reduces RNA contamination of the extracted DNA. In the binding stage, chaotropic salts and ethanol in the kit reagents cause DNA to bind to the spin column membrane. Washing removes impurities that can affect the yield and purity of the extracted DNA. In the final stage, the elution buffer formulation alters the conditions surrounding the spin column membrane, releasing the DNA.

The FlexiGene kit also has a lysis stage, including a protease reagent (see Appendix B for the detailed extraction protocol used for this project). Following lysis, the addition of isopropanol

causes the DNA to precipitate. A 70% v/v ethanol wash removes salts and other contaminants before the DNA is dissolved in a hydration buffer.

The QIAamp DNA Blood Mini kit was used for extraction from small sample volumes (200 µL). The FlexiGene kit was used for both large (1 mL) and small (100 µL) sample volumes and was also used for re-extraction of a sample if the extract from the Blood Mini kit was of inadequate yield or purity.

DNA concentration of each extract was determined by triplicate measurement on a NanoDrop 2000 spectrophotometer (Thermo Scientific, Wilmington, USA) using the appropriate DNA extraction kit elution or hydration buffer as a measurement blank. DNA extracts were stored in 1.5 mL flip-top microtubes at -20 °C.

RHD Zygosity Testing

BAGene D-Zygosity TYPE kit (Gen Trak, Inc., Liberty, USA) was used to determine the *RHD* zygosity of selected DNA extracts. The kit includes two PCR reactions for each sample, one specific for the downstream Rhesus Box, the other for the hybrid Rhesus box found in *RHD* gene deletion alleles (Figure 1). Both reactions contain a control primer set which the PCR product size is 659 bp. The PCR product size for both Rhesus Box products is 2760 bp.

The concentrations of DNA extracts were adjusted to 40 ng/µL. For each sample being tested, a reaction mixture containing 5 µL DNA extract, 0.4 µL *Taq* polymerase, 5 µL 10x PCR buffer (supplied with *Taq* polymerase), and 40 µL molecular grade water was prepared. Reactions were prepared by adding 10 µL of the mixture to the wells of the reaction strip provided in the kit.

PCR was performed using a Mastercycler Gradient thermal cycler (Eppendorf). Following an initial 10-minute denaturation step at 95 °C, PCR proceeded for 35 cycles of denaturation for 20 s at 92 °C, annealing for 30 s at 64 °C and extension for 5 min at 68 °C with a final extension step for 5 min at 72 °C.

A 2% agarose gel in 1x SB low-conductive electrophoretic buffer (Faster Better Media LLC, Hunt Valley, USA) containing 1x GelRed nucleic acid gel stain (Biotium, Hayward, USA). The entire volume of D-zygosity reactions (10 µL) and 5 µL of DNAmark 100bp Plus Ladder (G-Biosciences, St. Louis, USA) were loaded into wells of the gel and run at 30 V/cm for 30 min. An AlphaInnotech

FluorChem imagining system was used to photograph the gel. D-zygosity was determined by observing the pattern of the two PCR reactions (Figure 3).

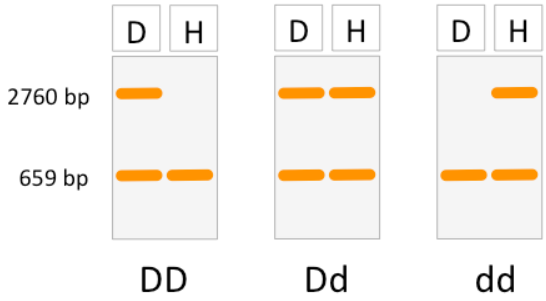

Figure 3: Interpretation of electrophoretic gels for BAGene D Zygosity-Type kit. The 2760 bp product in the downstream Rhesus Box reaction (D) is present on the standard *RHD* gene allele while the same size product in the hybrid Rhesus Box reaction (H) is only present when the *RHD* gene has been deleted. The 659 bp products are control targets and must be present for zygosity typing to be valid.

Pooled Controls

D-positive and D-negative pooled whole blood and plasma controls were prepared by combining equal volumes of whole blood or plasma from eight donors for each control. The same donors were used for whole blood and plasma controls. Aliquots were stored at -20 °C. Controls were thawed at room temperature and mixed well before use.

Prenatal Samples for NIPT study

Maternal prenatal EDTA samples (n=205) were chosen from samples submitted to CBS for routine prenatal testing. Sample size[b] was determined for non-inferiority testing using Equation 1. Sample sizes were calculated for two objectives: 1) to confirm non-inferiority in sensitivity with 95% confidence and 80% power, and 2) to confirm that D-positive rate is not lower than that in reference method with assumed sensitivity of 90%. Both calculations were made assuming that 60% of D-negative pregnant women would be carrying D-positive babies. The samples sizes were 196 and 207 respectively.

[b] Sample size calculations were performed by Dr. Qi-Long Yi, Senior Epidemiologist at Canadian Blood Services.

Equation 1: Sample size calculation formula for NIPT study. Z_{α} and $Z_{1-\beta}$ are the normal deviance value at significance level of α and power (1-β); p is the assumed sensitivity rate; delta is the allowed margin. In the calculation, p was assumed to be 95% and the delta value was assumed to be 0.05.

$$n = \frac{(Z_{\alpha} + Z_{1-\beta})^2 \, p(1-p)}{\text{delta}^2}$$

CBS staff identified samples meeting the study inclusion criteria (Table 5), anonymized them and labelled the samples with pre-printed study ID numbers. Gestational age at collection and information required for retrieval of postnatal cord blood RhD phenotyping results were recorded. The CBS Associate Medical Director for Clinical Services in Edmonton obtained cord blood phenotype results, which were not revealed until dqPCR testing was complete.

Samples were received two to five days after collection and were processed into aliquots of whole blood, plasma and buffy coat. During clinical testing, samples had been centrifuged and stored at 4 °C. Samples were allowed to warm to room temperature and placed on a rotating mixer for 15 minutes. Whole blood was aliquoted and the remaining sample was centrifuged at 2500 x *g* for 10 min at 4 °C. Plasma aliquots were removed and buffy coats were saved. All aliquots were stored in sterile 2 mL screw-top cryovials at -80 °C.

Ethics Approval

Ethics approvals for volunteer donor collections and prenatal sample procurement were obtained from CBS and the University of Alberta.

Table 5: NIPT study participant inclusion criteria and justification.

Criteria	Justification
perinatal testing completed	no impact to routine patient care, samples would normally be discarded
D-negative	the purpose of fetal RhD typing is to identify D-negative women who are carrying D-positive babies
antibody screen negative	maximizes sample volume for study and decreases time from collection to availability to researchers
from Edmonton & northern Alberta regions	allows access to cord blood phenotype through laboratory information system
≥ 8 weeks gestational age at time of collection	literature indicates fetal DNA concentration before this time is too low for reliable detection

FINALIZED QPCR PROTOCOLS

RHD specific primer sets

Primers for *RHD* exons 5[82], 7[77] and 10[101] were prepared and purified by Integrated DNA Technologies (Coralville, USA) using standard desalting. Stock solutions of 200 µM concentrations were prepared by adding molecular grade water. Aliquots of working solutions with concentrations of either 10 µM or 20 µM were prepared. Stock and working solutions were stored at -20 °C. Primer sequences and amplicon details are shown in Table 6.

Table 6: Primers and amplicon characteristics. Previously published primer sets for *RHD* exon 5[82], exon 7[77] and exon 10[101] were used for this study. Geneious[102] bioinformatics software was used to annotate the *RHD* gene sequence (NCBI Reference Sequence: NG_007494.1) with primer sequences and determine the length and predicted T_m of the PCR products.

Target	Primers	Predicted T_m (°C)	Product Length (bp)
Exon 5	5'-CGCCCTCTTCTTGTGGATG-3' 5'-GAACACGGCATTCTTCCTTTC-3'	72.2	82
Exon 7	5'-GTTGTAACCGAGTGCTGGGGATTC-3' 5'-TGCCGGCTCCGACGGTATC-3'	82.1	123
Exon 10	5'-CCTCTCACTGTTGCCTGCATT-3' 5'-AGTGCCTGCGCGAACATT-3'	76.9	74

DNA qPCR and Melt Curve Analysis

PCR master mix was prepared containing 1x PCR buffer (supplied with *Taq* polymerase), 2.5 mM $MgCl_2$, 0.1 µL of Invitrogen Platinum *Taq* DNA Polymerase (all from ThermoFisher Scientific, Burlington, Canada), 200 uM deoxynucleotide mix (dNTP; Sigma Aldrich, Oakville, Canada), 0.33x SYBR Green I (SG; Invitrogen Life Technologies, Carlsbad, USA) and 0.04% bovine serum albumin (BSA; Sigma Aldrich, Oakville, Canada). Primers for *RHD* exons 5[82], 7[77] and 10[101] (Integrated DNA Technologies, Coralville, USA) were used at 100 nM concentrations (see Table 6 for primer and amplicon details). The reaction volume was 20 µL and DNA samples were added at 5% of total reaction volume. Master mix was prepared fresh each day or stored at -20 °C and used within two days of preparation.

PCR and melt curve analysis (MCA) were performed on a StepOne real-time PCR system (Applied Biosystems, USA). PCR was run with a pre-denaturation step of 80 s at 95 °C followed by 40 cycles of denaturation at 95 °C for 15 s, annealing at 65 °C for 15 s and elongation at 72 °C for 40 s. Step-and-hold MCA was performed between 70 °C and 90 °C using the default ramp increment setting (0.3 °C). Automatic baseline selection and a common threshold of 1000 fluorescence units were used for PCR analysis. D-positive, D-negative and no-template (water) control samples were included with each PCR run to determine run validity. Runs with control failures were rejected from further analysis.

Whole Blood dqPCR and Melt Curve Analysis

PCR master mix was prepared containing 1x Klentaq Mutant buffer, 1x PCR Enhancement Cocktail 1 (PEC-1), 0.3 µL of OKT polymerase (DNA Polymerase Technology, St. Louis, USA), 200 µM dNTPs, 40x SYBR Green I and 0.03% BSA (Sigma Aldrich, Oakville, Canada). *RHD* primers were used at 400 nM in a reaction volume of 10 µL and whole blood samples were added at 8% (v/v) of reaction volume. Master mix was prepared fresh each day.

PCR and MCA were performed on the StepOne system. For PCR, a pre-denaturation step of 80 s at 95 °C preceded 40 cycles of denaturation at 95 °C for 15 s, annealing at 62 °C for 15 s and elongation at 72 °C for 40 s. Continuous MCA was performed between 75 °C and 95 °C with the default ramp rate[c] (0.3%) for dilution, interference and efficiency studies. For all other whole blood dqPCR experiments, step-and-hold MCA between 75 °C and 90 °C was used with the default ramp increment (0.3 °C).

PCR results were analyzed using automatic baseline determination and a common threshold for each of the three *RHD* targets. A threshold of 6000 fluorescence units was used for dilution studies, interference studies, amplicon control experiments and efficiency studies. A threshold of 1000 fluorescence units was used for all other whole blood dqPCR experiments[d].

---

[c] The StepOne software help file states that the ramp rate for continuous melt curves can be set from 0.3% (the default setting) to 100% and the ramp increment is "the rate at which the temperature ramps until the target temperature is reached." The ramp rate for step-and-hold MCA is 100% and cannot be adjusted, however, the ramp increment is adjustable and determines the number of degrees between each step.

[d] The threshold change was necessary following recalibration of the StepOne PCR system. The StepOne instrument requires recalibration annually.

Pooled whole blood D-positive and D-negative control samples were included with each PCR run to determine run validity. Runs with control failures were rejected from further analysis. Results were interpreted as described in PCR Interpretation.

Plasma dqPCR and Melt Curve Analysis

The development phase for plasma dqPCR began by simply changing the type of sample used in the whole blood dqPCR protocol and continued through modification of several reaction parameters. In the definitive plasma dqPCR protocol used in this manuscript, the reaction mixture contained 1x KMB, 1x PEC-2, 0.3 µL OKT polymerase, 200 µM dNTPs, 0.04% BSA, 400 nM forward and reverse primers, and 25% plasma.

PCR and MCA were performed on the StepOne system. For PCR, a pre-denaturation step of 80 s at 95 °C preceded 40 cycles of denaturation at 95 °C for 15 s, annealing at 62 °C for 15 s and elongation at 72 °C for 40 s. Fluorescence data capture was disabled for the first eight cycles. Step-and-hold MCA was performed between 75 °C and 90 °C using the default ramp increment (0.3 °C). PCR results were analyzed at a threshold of 1000 fluorescence units with baseline set at $3\text{-}15_{mod}$ cycles[e].

Pooled plasma D-positive and D-negative controls were included with each PCR run to determine run validity. Runs with control failures were rejected from further analysis. Results were interpreted as described in PCR Interpretation.

PCR interpretation

In general, and particularly for protocol development and experiments with unique parameters, reactions were considered positive when $C_q < 40$ without consideration of the product melt temperature. Reactions with undetermined C_q values were considered negative

For experiment where the presence of non-specific products might alter outcomes or impede analysis, such as limit of detection and method comparisons, reactions with C_q values were considered positive (i.e. $C_q < 40$) only when the T_m fell within a laboratory established control range. Reactions with $C_q < 40$ and T_m outside the control range were deemed non-specific amplification and either omitted from analysis or interpreted as negative, depending on the experiment. Control

[e] When discussing plasma dqPCR, "mod" indicates that the cycle numbers refer to those reported by the StepOne software, which do not include cycles for which fluorescence data capture was disabled.

ranges were established by determining the cumulative mean T_m of all controls previously run using the same reaction mixture, sample type, and settings for PCR cycling, MCA, baseline, and threshold. The result of this approach is that there were slight differences in control ranges for different experiments. Where applicable, the specific control ranges used for an experiment are included in the method description.

Determining Performance Characteristics of Whole Blood dqPCR

Dilution studies to determine the effect of hemoglobin the melt temperature of WB dqPCR products

Two dilution approaches were used to evaluate dqPCR. For the first, D-positive whole blood was diluted in D-positive plasma from the same donor. In the second, D-negative whole blood was diluted with water and commercial human genomic DNA (Roche Diagnostics, Laval, Canada) was added to a concentration of 4 ng/µL. Three different whole blood samples were used for each approach. Eight solutions were prepared from each sample with dilution factors ranging from 1.0 (undiluted) to 0.3 at intervals of 0.1. Hemoglobin concentration of the undiluted solutions was measured on a Coulter AcT hematology analyzer and used to calculate the hemoglobin concentrations for the other solutions in each series. Triplicate PCR with MCA was performed on each dilution.

One-way analysis of variance for melt temperature was performed on data for both dilution approaches using SPSS Statistics (IBM, Markham, Canada). A test for homogeneity of variances was used to determine which approach to use for group comparisons. Where the homogeneity test revealed equal variances, Bonferroni analysis was used for comparisons. Tamhane's T2 was used where variances were unequal.

Interference studies to investigate the cause of T_m shift associated with hemoglobin in WB dqPCR

Four master mixes were prepared for *RHD* exon 5 with SYBR Green I concentrations of 40x, 30x, 20x and 10x. Five samples with DNA concentrations of 55.2 ng/µL, 27.6 ng/µL, 13.8 ng/µL, 6.9 ng/µL and 3.4 ng/µL were prepared by adding D-positive DNA extract to D-negative whole blood. Two 30% blood solutions were prepared by diluting D-negative whole blood with PCR grade water (30%-H_2O) or plasma from the same donor (30%-PL). D-positive DNA extract was added to each 30% blood solution to prepare samples with the same DNA concentrations as the whole blood samples. PCR with MCA was performed in triplicate on all samples for all four master mixes.

Three-way ANOVAs were performed using SPSS statistics to compare each dilution arm to the whole blood data. This experiment was also run using the same concentrations of EvaGreen (Biotium, Hayward, USA), which has similar spectral properties to SYBR Green I. For analysis of EvaGreen reactions, StepOne software was set to take baseline between cycles 10 and 17. Threshold was set at 100 fluorescent units.

Controlling for sample hemoglobin using an amplicon-spiked reaction

Amplicons were prepared for each *RHD* target by endpoint PCR using DNA extracted from a single D-positive donor. Multiple PCR reactions for each target were run using a Mastercycler Personal thermal cycler (Eppendorf, Mississauga, Canada). Each reaction mixture contained 1x PCR buffer, 0.02 U/µL Platinum Taq polymerase (Invitrogen), 1.5 mM $MgCl_2$, 200 µM dNTPs, 200 nM forward and reverse primers and 12 ng/µL DNA in a total volume of 50 µL. An initial 5 min denaturation step at 95 °C preceded 40 cycles of 30 s at 95 °C, 30 s at 62 °C and 60 s at 72 °C, followed by a final 5 min at 72 °C. Reactions were cleaned up by MinElute PCR Reaction Cleanup kit (QIAGEN) DNA eluted in water. Amplicon eluates for each *RHD* target were pooled. DNA concentration of each amplicon solution was measured using a NanoDrop 2000 spectrophotometer. Amplicon solutions were diluted with molecular grade water to concentrations of 12.6 pg/µL, 13.8 pg/µL and 13.1 pg/µL for exons 5, 7 and 10 respectively.

Whole blood and plasma from a single D-positive donor, different from the donor sample used to prepare amplicon solutions, were used to prepare Hb solutions of 70% and 50% whole blood in plasma. Triplicate PCR with MCA was performed on the Hb solutions and undiluted whole blood with and without the addition of 0.5 µL of amplicon dilution to the reaction mixture. For each *RHD* target and Hb solution, ANOVA was performed in SPSS to compare melt temperatures of reactions with and without amplicon added.

PCR efficiency and the effect of Hemoglobin Concentration

The PCR efficiency of each target was evaluated at three different hemoglobin levels. D-negative whole blood samples (n=3) were diluted with plasma from the same sample to prepare three hemoglobin solutions, neat (no dilution), 70% and 50%. The hemoglobin concentration of these solutions was measured on a Coulter AcT hematology analyzer (Beckman Coulter, Mississauga, Canada). D-positive DNA was added to the hemoglobin solutions to prepare dilution series that consisted of seven samples with a 3-log DNA concentration range (10^2 pg/µL to 10^5 pg/uL).

Triplicate PCR was performed for each target on each dilution series and the StepOne software created standard curves and determined the reaction efficiency. The hemoglobin solutions were run as additional negative PCR controls. A one-way ANOVA was performed on the data using SPSS Statistics.

WB dqPCR Limit of Detection

Serial dilutions were created by adding homozygous D-positive DNA from a single donor to D-negative whole blood. Five dilutions with DNA concentrations of 0.21 pg/µL, 1.03 pg/µL, 5.15 pg/µL, 25.78 pg/µL and 51.56 pg/µL were tested along with D-negative whole blood without D-positive DNA. Replicates with non-specific amplification (i.e. C_q < 40 and T_m outside control range; see Table 7 for T_m ranges) were omitted from further analysis. Additional replicates were run to obtain a minimum of 15 acceptable replicates for each dilution sample. For acceptable replicates, the total number of replicates for each dilution and the total number of positive results were tabulated. DNA concentrations were converted to target copies per PCR reaction (GE/PCR) and probit regression analysis using natural log transformation was performed on the tabulated data using SPSS Statistics. The limit of detection (LOD) was determined at the 95% level.

Table 7: *RHD* target specific melt temperature ranges for whole blood dqPCR genomic DNA limit of detection.

Whole blood dqPCR

Target	Acceptable T_m Range (°C)
D5	79.30 - 81.63
D7	82.78 - 85.30
D10	79.53 - 82.10

WB dqPCR limit of detection using fragmented DNA

Homozygous D-positive DNA from a single donor was fragmented by digestion with NEBNext dsDNA Fragmentase (New England Biolabs, Whitby, Canada) in 20 reactions of 5 µg DNA each. Digest reactions were cleaned up by MinElute Reaction Cleanup kit (QIAGEN) and eluted in the supplied buffer. Eluates were pooled and DNA was quantified on a NanoDrop. Fragmentation was confirmed by electrophoresis in 2% agarose in 1x SB buffer (Faster Better Media, Hunt Valley, USA) with GelRed nucleic acid stain (Biotium). The gel was run for 15 minutes at 300 V in a BioRad Mini apparatus.

D-positive fragmented DNA was added to D-negative whole blood and serial dilutions were prepared using whole blood from the same D-negative donor as diluent. For each *RHD* target, 21 replicates of five dilutions with DNA concentrations of 22 pg/µL, 44 pg/µL, 110 pg/µL, 220 pg/µL, and 440 pg/µL were tested. Seven replicates of the D-negative whole blood diluent were also tested for each target. The total number of replicates for each dilution and the total number of positive results were tabulated. DNA concentrations were converted to target copies per PCR reaction (GE/PCR) and probit regression analysis using natural log transformation was performed on the tabulated data using SPSS Statistics. The limit of detection was determined at the 95% level.

Whole blood dqPCR and DNA qPCR method comparison

DNA, adjusted to 15 ng/µL with molecular grade water, and whole blood samples from 60 participants were blinded independently. Single DNA qPCR and WB dqPCR reactions were performed on each sample. Reactions with non-specific amplification were repeated in duplicate and interpreted as negative if non-specific amplification persisted (see Table 8 for T_m ranges). Results for each exon were interpreted collectively to predict RhD phenotype. Samples with discrepancies (i.e. indeterminate RhD predictions) were repeated in duplicate for all targets and the final RhD prediction was made based on all nine replicates. The interpretation algorithm is shown in Table 9.

Data were input into SPSS to create contingency tables and calculate kappa statistics comparing whole blood dqPCR to DNA qPCR for each *RHD* target and well as RhD prediction. Where appropriate, 95% confidence intervals were calculated for the kappa statistic using Equation 2. Whole blood dqPCR and DNA qPCR were also compared to serologic RhD phenotype results by calculating, specificity and sensitivity including confidence intervals[103], agreement, precision, and accuracy. For sensitivity and specificity calculations, indeterminate RhD predictions were classified as false positives or false negatives depending on the serologic RhD phenotype (i.e. if the phenotype was negative, indeterminate RhD predictions were considered false positives).

Table 8: *RHD* target specific melt temperature ranges for whole blood dqPCR and DNA qPCR method comparison

Whole blood dqPCR

Target	Acceptable T_m Range (°C)
D5	80.92 - 83.23
D7	82.83 - 86.62
D10	79.32 - 83.69

DNA PCR

Target	Acceptable T_m Range (°C)
D5	82.55 - 83.55
D7	86.38 - 87.38
D10	82.77 - 83.77

Table 9: Interpretation algorithms for RhD prediction from *RHD* genotyping by whole blood dqPCR and DNA qPCR

Single replicate per PCR target

Conditions	RhD prediction
• reactions positive for all targets	Positive
• reactions negative for all targets	Negative
• 1/3 or 2/3 targets positive	Indeterminate

Three replicates per target

Conditions	RhD prediction
• all targets with ≥2/3 positive replicates • one target with 3/3 positive replicates & two targets with ≥1/3 positive replicates	Positive
• all targets with 0/3 positive replicates • one target with 1/3 positive replicates & two targets with 0/3 positive replicates	Negative
• all targets with 1/3 positive replicates • two targets with 1/3 replicates positive & one target with 0/3 replicates positive • one target with ≥2/3 replicates positive & two targets with 0/3 replicates positive • one target with 2/3 replicates positive & two targets with 1/3 replicates positive • D5 with 0/3 replicates positive, D7 & D10 with ≥2/3 replicates positive (possible *RHDΨ*) • D5 & D7 with 0/3 replicate positive & D10 with ≤2/3 replicates positive (possible Cde^s)	Indeterminate

Equation 2: 95% confidence interval calculation for kappa (κ) statistic where SE is the asymptotic standardized error calculated by SPSS.

$$95\%\ CI = \kappa \pm 1.96SE$$

Developing a Method for dqPCR using Plasma Samples

Plasma dqPCR Protocol Development

Plasma dqPCR protocol development: First trial of plasma dqPCR

For the initial trial of dqPCR using plasma, master mix contained 1x KMB, 1x PCR Enhancement Cocktail 2 (PEC-2), 0.3 µL OKT polymerase, 200 µM dNTPs, 40x SG, 0.03% BSA, 400nM forward and reverse *RHD* exon 5 primers, and 8% plasma in a 10 µL reactions volume. This is the same as the WB dqPCR mix replacing PEC-1 with PEC-2, which the manufacturer of OKT polymerase suggests for reactions using plasma.

D-positive and D-negative pooled controls were run in quadruplicate for *RHD* exon 5. Whole blood dqPCR was run for comparison.

Plasma and whole blood reactions were performed simultaneously on the StepOne instrument using cycling and MCA settings described in WB dqPCR and MCA. Whole blood reactions were analyzed as described previously. For plasma, various baseline and threshold settings were evaluated.

Plasma dqPCR protocol development: SYBR titration

Using the recipe described for the first trial of plasma dqPCR, six reaction mixes for plasma dqPCR of *RHD* exon 5 were prepared with SG concentrations of 40x, 20x, 10x, 5x, 2.5x, and 1x. D-positive and D-negative pooled plasma controls tested in duplicate for each SG concentration. PCR and MCA were performed on the StepOne as described for the first trial of plasma dqPCR. For analysis, baseline was set at cycles 11 to 23 and threshold at 1000 fluorescence units.

Plasma dqPCR protocol development: Sample volume study

The first of two master mixes targeting *RHD* exon 5 was prepared as described for previous experiments using 8% plasma. In the second mix, molecular grade water was replaced entirely by

plasma, bringing the concentration of sample in each reaction to 25.5%. Both reaction mixtures contained 5x SG.

By adding D-positive DNA to D-negative plasma and performing two-fold serial dilutions with D-negative plasma, five samples with DNA concentrations ranging from 6.25 pg/µL to 100 pg/µL were prepared. Pooled plasma controls, the five dilutions, and the plasma sample used to prepare the dilutions were run in single reactions for 8% and 25.5% reaction mixes. PCR and MCA were performed on the StepOne as described for the pilot study and analysed using baseline at 11-23 cycles and threshold of 1000 fluorescence units.

Plasma dqPCR protocol development: Dye Titration

Reactions were performed with either SYBR Green I or EvaGreen in concentrations of 10x, 5x, 2.5x or 1x. Each 10 µL reaction also contained 1x KMB, 1x PEC-2, 0.3 µL OKT polymerase, 200 µM dNTPs, 0.02% BSA, and 400 nM forward and reverse *RHD* exon 5 primers. Plasma sample was added at 26% of the reaction volume, representing a slight adjustment to the amount used in the sample volume experiment. The adjustment was made to simplify calculation of reagent volumes for reaction mix preparation. Pooled plasma controls were run in duplicate for each SYBR concentration. PCR and MCA were performed on the StepOne as described for the pilot study.

Plasma dqPCR protocol development: Run method modification

Duplicate pooled plasma control reactions were prepared for *RHD* exon 5. Each 10 µL reaction contained 1x KMB, 1x PEC-2, 0.3 µL OKT polymerase, 200 µM dNTPs, 0.04% BSA, 2.5x SG, and 400 nM forward and reverse primers. Plasma was reduced to 25% of reaction volume to further simplify reagent volume calculations. The PCR cycling and MCA settings were the same as described previously, however fluorescence data capture was disabled for the first eight cycles. Threshold was set at 1000 fluorescence units, but because the StepOne instrument did not count the first eight cycles[f], baseline was set at cycles $3\text{-}15_{mod}$, which was equivalent to the baseline of cycles 11-23 used for previous plasma dqPCR experiments. For comparison, control samples were also run with the standard run method using the same reaction mixture.

---

[f] In order to disable fluorescence data capture, the first eight cycles were programmed as a separate stage in the StepOne software. In the results, the StepOne software only reported cycles from the program stage in which fluorescence data was captured, which had 32 cycles. For clarity when discussing plasma dqPCR, "mod" will be added to indicate that the cycle numbers refer to the actual StepOne report and "adj" will be used to when referring to the total number of cycles.

Plasma DqPCR Protocol Evaluation

Plasma dqPCR Protocol Evaluation: PCR efficiency

D-positive DNA was added to D-negative plasma to prepare a series of six samples with a 5-log DNA concentration (10^0 pg/µL to 10^5 pg/µL). Samples were run in triplicate for each *RHD* target. Standard curves were created and reactions efficiency calculations were performed using Microsoft Excel.

Plasma dqPCR Protocol Evaluation: Limit of Detection

Homozygous D-positive DNA from a single donor was serially diluted in D-negative plasma to create six dilutions with DNA concentrations of 0.01 pg/µL, 0.06 pg/µL, 0.32 pg/µL, 1.62 pg/µL, 8.10 pg/µL, and 16.20 pg/µL. Multiple replicates of the dilutions and D-negative plasma without DNA added were run and replicates with non-specific amplification (i.e. $C_q < 40_{adj}$ and T_m outside control range; see Table 10 for T_m ranges) were omitted from analysis. Additional replicates were run to obtain a minimum of 11 acceptable replicate for each sample. Acceptable replicates were tabulated and probit regression without logarithmic transformation was performed using SPSS Statistics to determine LOD at the 95% level.

Table 10: *RHD* target specific melt temperature ranges for plasma dqPCR genomic DNA limit of detection.

Plasma dqPCR

Target	Acceptable T_m Range (°C)
D5	79.80 - 80.06
D7	83.56 - 83.90
D10	80.05 - 80.56

APPLYING DQPCR TO NON-INVASIVE PRENATAL TESTING FOR THE PREDICTION OF FETAL RHD TYPE

NIPT pilot study

A subset of the prenatal samples (n = 20) was identified by CBS staff such that the entire range of gestational ages would be represented yet remain blinded until testing was complete. Whole blood and plasma dqPCR were performed in triplicate for each *RHD* target. Each reaction was interpreted using T_m control ranges in Table 11 and RhD type predicted according to two predetermined algorithms (Table 12). Contingency tables were created to compare RhD predictions to cord blood

RhD phenotype results for all gestational ages and a subset with gestational ages of 27 weeks and greater.

Table 11: *RHD* target specific melt temperature ranges for whole blood dqPCR and plasma dqPCR NIPT pilot study

Whole blood dqPCR

Target	Acceptable T_m Range (°C)
D5	80.57 - 81.20
D7	83.55 - 85.28
D10	80.06 - 82.48

Plasma dqPCR PCR

Target	Acceptable T_m Range (°C)
D5	79.54 - 80.36
D7	83.21 - 84.12
D10	79.92 - 80.77

Table 12: RhD prediction algorithms for NIPT pilot study

Algorithm 1

Conditions	RhD prediction
• all targets with ≥2/3 positive replicates; OR • one target with 3/3 positive replicates & two targets with ≥1/3 positive replicates	Positive
• ≤ 1/9 positive replicates	Negative
• all other reaction patterns	Indeterminate

Algorithm 2

Conditions	RhD prediction
• ≥ 1/3 positive replicates for at least two targets; AND • ≥ 2/3 positive replicates for at least one target	Positive
• all replicates negative for all targets; OR • ≤ 2/9 replicates positive (total) for all targets combined	Negative

Plasma dqPCR NIPT study

The remaining 185 prenatal samples were tested in triplicate by plasma dqPCR and MCA. These results were combined with data from the plasma dqPCR arm of the NIPT pilot study and analyzed as a single sample set (n=205). Reactions with amplification (i.e. $C_q < 32_{mod}$) and T_m outside of the acceptable range (Table 13) were interpreted as negative.

Two interpretation algorithms were devised to interpret the plasma PCR results and predict the RhD type for each sample (Table 14). Algorithm 1 was developed using an approach similar to that used by Finning et al.[90] (i.e. all targets reporting a specified number of positive replicates and a specified number of positive reactions out of the total number of replicates). An arbitrary cut-off based on the number of positive reactions was chosen for Algorithm 2

Contingency tables were created to compare RhD predictions from each algorithm to the cord blood RhD phenotype for all samples and the subset of samples with gestational ages of 27 weeks or greater (third trimester) at the time of sample collection. Sensitivity, specificity, accuracy, false positive rate, false negative rate, positive predictive value and negative predictive value were calculated for each algorithm/sample set combination. For the purpose of calculating analytical performance measures, results interpreted as indeterminate were included in the false positive or false negative counts depending on the serologic RhD phenotype (i.e. if the phenotype was negative, indeterminate RhD predictions were considered false positives).

Table 13: RHD target specific melt temperature ranges for plasma dqPCR NIPT study.

Plasma dqPCR

Target	Acceptable T_m Range (°C)
D5	79.62 - 80.34
D7	83.37 - 84.32
D10	79.98 - 81.18

Table 14: RhD prediction algorithms for plasma dqPCR NIPT study.

Algorithm 1

Conditions	RhD prediction
• all targets with ≥1 positive replicates; AND • ≥5/9 positive replicates	Positive
• ≤ 1/9 positive replicates	Negative
• all other reaction patterns	Indeterminate

Algorithm 2

Conditions	RhD prediction
• ≥ 1/9 positive replicates	Positive
• 0/9 positive replicates	Negative

Chapter 3: Results

The three sections of this chapter, Determining Performance Characteristics of WB dqPCR, Developing a Method for dqPCR using Plasma Samples, and Applying dqPCR to Non-invasive Fetal RhD Type Prediction, describe the results of experiments related to each of the three Project Objectives outlined in Chapter 1.

Determining Performance Characteristics of Whole Blood dqPCR

The results presented in this section are from experiments related to the hypothesis that WB dqPCR can accurately predict RhD type. To fully evaluate this hypothesis, experiments were performed to investigate the impact of sample matrix, determine PCR efficiency and LOD, and to compare WB dqPCR to DNA qPCR and serologic phenotyping

Investigating the impact of sample matrix on WB dqPCR

Although there are many biochemical substances in whole blood that could affect WB dqPCR, hemoglobin is one of the most abundant. It is a known interfering substance in many diagnostic lab tests and has been shown to inhibit PCR. Its relatively high concentration in whole blood compared to other potentially interfering substances, known optical activity, and the ease with which it can be measured made hemoglobin a logical choice as a analyte representative of the whole blood sample matrix.

Determination of the Effect of Hemoglobin on the Melt Temperature of WB dqPCR Products

Dilution studies were performed to determine if changes in hemoglobin (Hb) levels would affect melt temperature of the PCR products. The range and mean hemoglobin concentration of the blood samples and dilutions and the corresponding mean hemoglobin present in PCR reactions for plasma and water dilution series are shown in Table 15 and Table 16.

Figure 4 shows representative melt curves for a single plasma dilution series of *RHD* exon 5 and illustrates the change in peak amplitude and T_m with various Hb levels. Both peak derivative fluorescence and T_m increased as the Hb concentration in the reaction decreased. The peak derivative fluorescence difference across the range of Hb concentrations tested was approximately 20,000 fluorescence units. This pattern was also seen in the water dilution series (data not shown). Both water and plasma dilution studies revealed an inverse relationship between Hb and T_m with a T_m shift of 2°C over the range of Hb concentrations tested for all targets (Figure 5). The observed

melt temperatures for the three *RHD* targets were higher than the calculated temperatures (Table 6). For both plasma and water dilutions, each *RHD* target showed a statistically significant difference in the melt temperature between dilutions (all $p<0.001$). Individual comparisons revealed no statistical differences between the melt temperatures of the undiluted, 0.9 and 0.8 hemoglobin dilutions (all $p>0.05$), which corresponded to mean Hb levels of 92 µg to 115 µg (Table 15) and 89 µg to 111 µg (Table 16) per PCR reaction for plasma and water dilution series, respectively.

As the amount of DNA in each reaction in the water dilution series was the same, the C_q values for each dilution were expected to be similar. Figure 6 reveals that this was not the case; rather, C_q values increased with higher Hb concentrations.

Table 15: Hemoglobin values for plasma dilution series

Dilution	Hb of blood samples[a] (g/L)	Mean Hb of blood samples (g/L)	Mean Hb per PCR reaction (µg)
1.0	140 - 148	143	115
0.9	126 - 133	129	103
0.8	112 - 118	115	92
0.7	98 - 104	100	80
0.6	84 - 89	86	69
0.5	70 - 74	72	57
0.4	56 - 59	57	46
0.3	42 - 44	43	34

[a] Represents Hb of clinical sample

Table 16: Hemoglobin values for water dilution series

Dilution	Hb of blood samples[a] (g/L)	Mean Hb of blood samples (g/L)	Mean Hb per PCR reaction (µg)
1.0	138 - 141	139	111
0.9	124 - 127	125	100
0.8	110 - 113	111	89
0.7	97 - 99	98	78
0.6	83 - 85	84	67
0.5	69 - 71	70	56
0.4	55 - 56	56	45
0.3	41 - 42	42	33

[a] Represents Hb of clinical sample

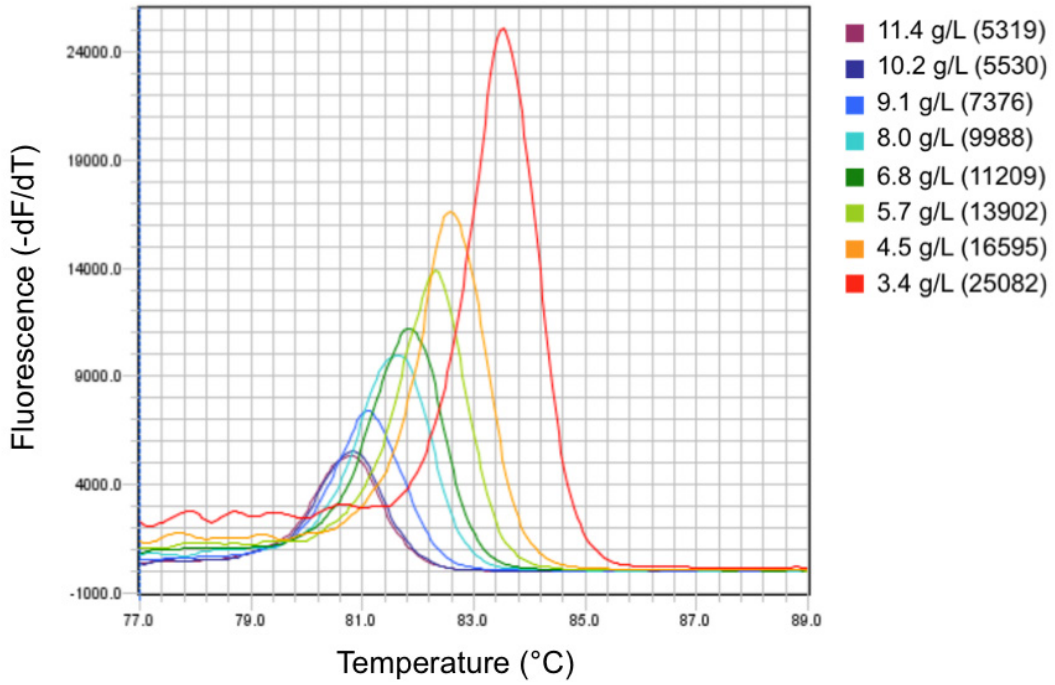

Figure 4: Melt curves for a representative plasma dilution series replicate for RHD exon 5. Legend shows the Hb concentration of each reaction with the peak derivative fluorescence in brackets.

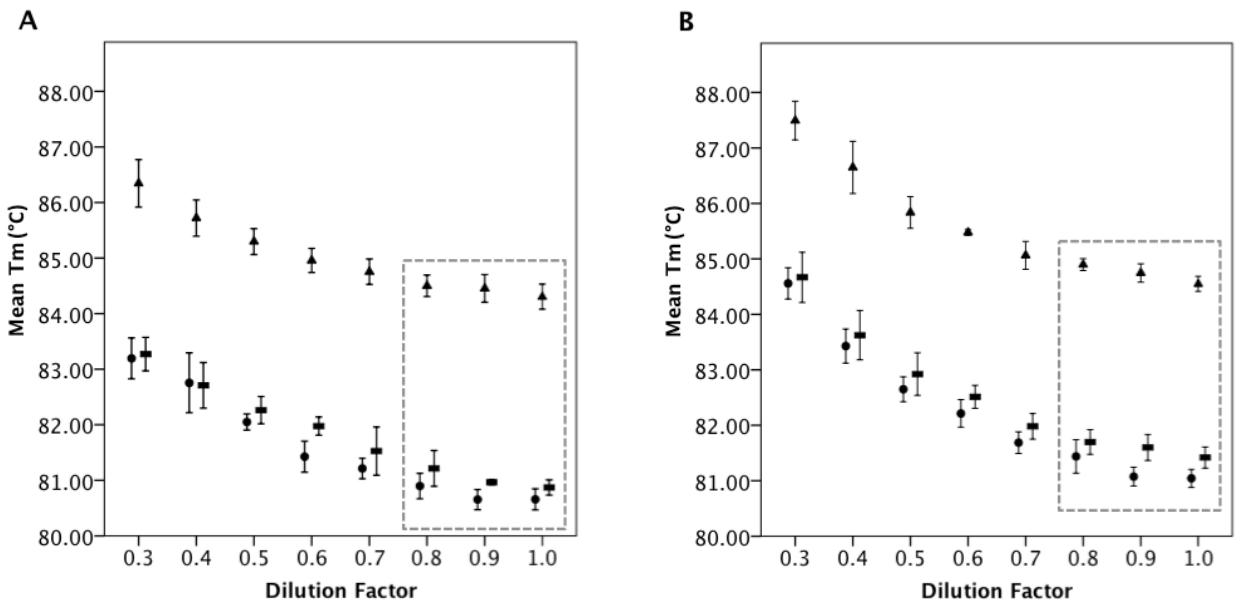

Figure 5: The effect of whole blood dilution with plasma (A) and water (B) on melt temperature is shown for *RHD* exon 5 (circle), exon 7 (triangle) and exon 10 (rectangle). Dashed boxes indicate dilution ranges for which there was no statistical difference in T_m ($p>0.05$). The Hb concentrations for each dilution are shown in Table 15. Error bars depict ±1 standard deviation.

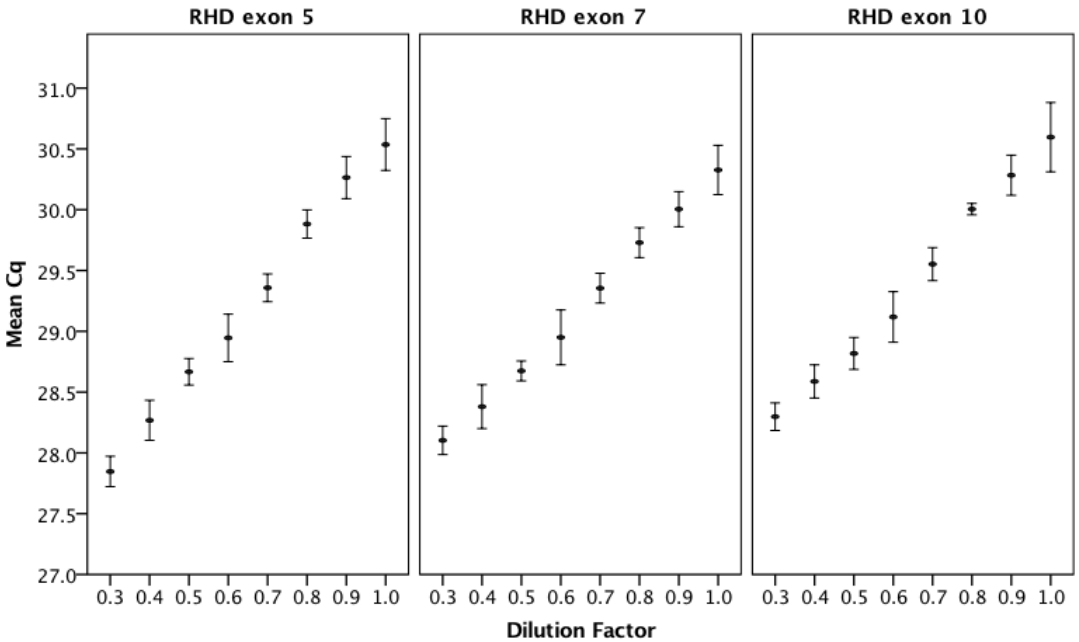

Figure 6: The effect of whole blood dilution with water on C_q is shown for *RHD* exon 5, exon 7 and exon 10. The Hb concentrations for each dilution are shown in Table 16. Error bars depict ±1 standard deviation.

Sample/Dye/DNA Interference Studies

The purpose of this experiment was to determine if the results of the dilution studies could be due to an interaction between hemoglobin, DNA and the fluorescent dyes, SYBR Green (SG) and EvaGreen (EG).

There were no statistically significant three-way interactions between SG, Hb and DNA when whole blood was compared to 30% whole blood in plasma (p=0.974) and 30% whole blood in water (p=0.894). However, there was a statistically significant two-way interaction between Hb and SG (p<0.001) for both plasma and water dilutions. The magnitude of the effect that SG had on T_m for 30% Hb in plasma or water was different from the effect of SG on T_m for whole blood (Figure 7). Data also showed a statistically significant interaction between Hb and SG affecting C_q for both plasma (p= 0.001) and water (p= 0.001) dilutions (Figure 8).

In the interference experiments using EvaGreen, there were no statistically significant three-way or two-way interactions (all p>0.05) affecting T_m (Figure 9). In addition, the observed T_m for *RHD* exon 5 agreed more closely with the calculated value.

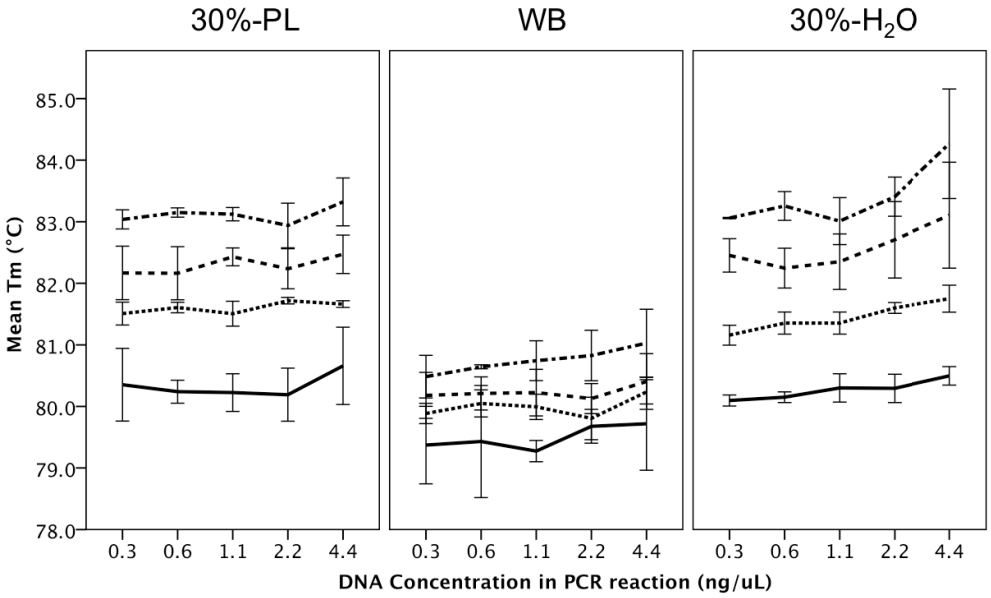

Figure 7: Mean T_m at various DNA concentrations is shown for whole blood (WB), 30% whole blood in plasma (30%-PL) and 30% whole blood in water (30%-H_2O) for reaction mixtures containing SYBR Green I dye concentrations of 10x (solid line), 20x (dotted line), 30x (dashed line) and 40x (dot and dash line). Error bars depict ±1 standard deviation.

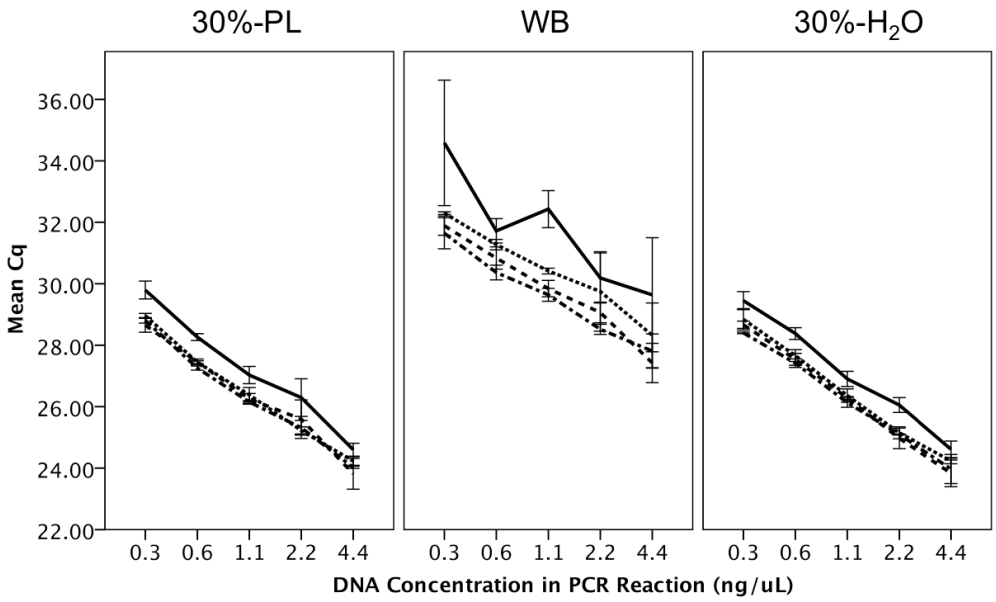

Figure 8: Mean C_q at various DNA concentrations is shown for whole blood (WB), 30% whole blood in plasma (30%-PL) and 30% whole blood in water (30%-H_2O) for reaction mixtures containing SYBR Green I dye concentrations of 10x (solid line), 20x (dotted line), 30x (dashed line) and 40x (dot and dash line). Error bars depict ±1 standard deviation.

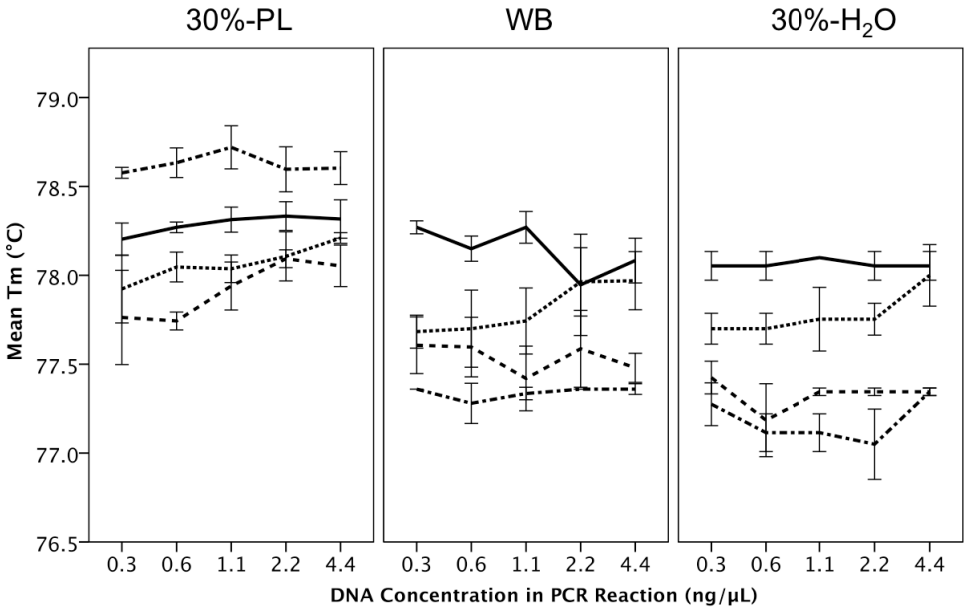

Figure 9: Mean T_m at various DNA concentrations is shown for whole blood (WB), 30% whole blood in plasma (30%-PL) and 30% whole blood in water (30%-H_2O) for reaction mixtures containing EvaGreen dye concentrations of 10x (solid line), 20x (dotted line), 30x (dashed line) and 40x (dot and dash line). Error bars depict ±1 standard deviation.

Amplicon control for sample hemoglobin

I explored the use of an amplicon control as a means of addressing the potential problems with T_m-based product verification in dqPCR. The premise of this approach is to add known, purified amplicon to a reaction with an unknown blood sample in sufficient quantity to ensure that a considerable portion of the PCR end product would come from the amplicon and therefore contribute substantially to the melt curve. The presence of the unknown sample would provide the same amount of Hb to the reaction with the additional amplicon as those without. The amplicon control, a separate reaction from the test reactions, would act as a basis for comparison to determine if an unexpected product was present. Figure 10 illustrates the difference in C_q values for samples with and without amplicon added to the reaction. The corresponding melt curves are shown in Figure 11.

Table 17 compares T_m for reactions where amplicon was either present or absent. Only one target/hemoglobin level combination showed a statistically significant difference in T_m for reactions with and without the additional amplicon. There was an increase in T_m in the 50% blood reactions for exon 7 with amplicon present ($p < 0.05$).

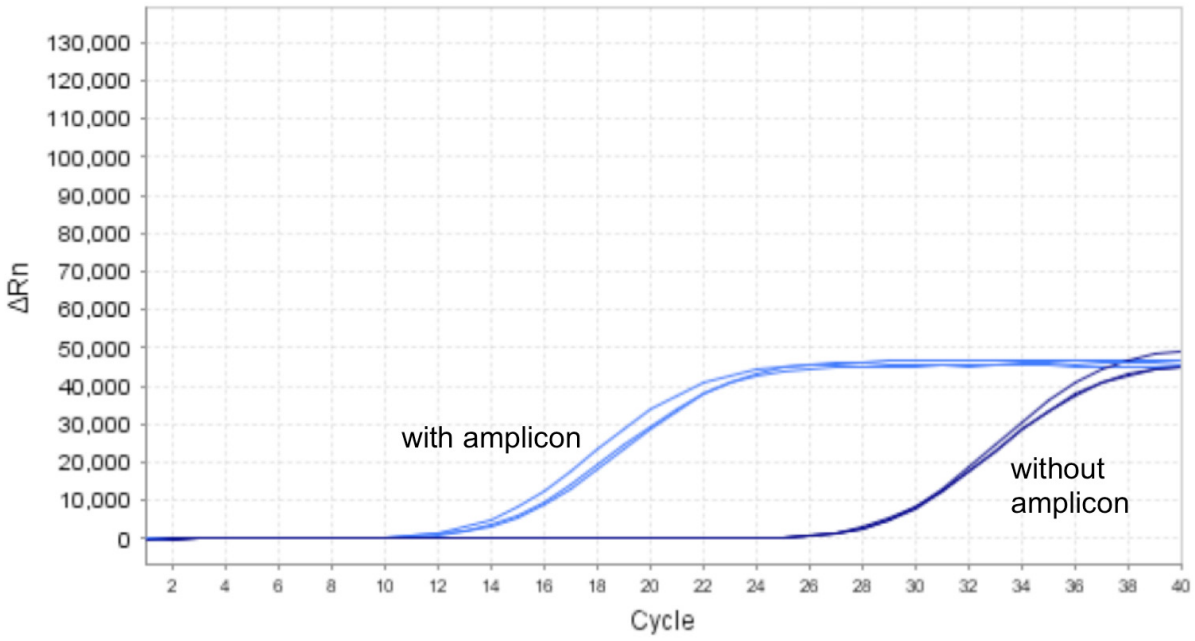

Figure 10: The amplification plots D7 WB reactions with (light blue) and without (dark blue) amplicon added to the reaction illustrates the difference in C_q due to the presence of the amplicon.

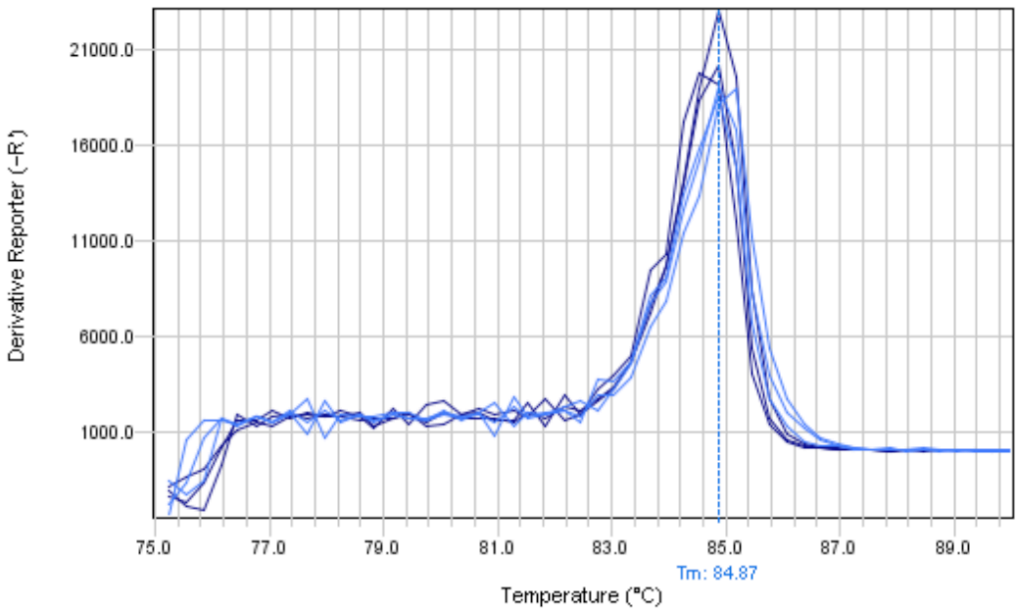

Figure 11: The melt curves for D7 WB reactions with (light blue) and without (dark blue) amplicon added to the reaction illustrate the similarity in T_m regardless of the presence of the amplicon.

Table 17: Comparison of T_m for reactions where amplicon was either present or absent.

Target	Hb	Amplicon	C_q mean	C_q SD	T_m mean	T_m SD	Between groups sig. (T_m)
D5	WB	Absent	29.51	0.17	81.41	0.00	0.374
		Present	16.74	0.24	81.45	0.08	
	70%	Absent	29.01	0.04	82.21	0.09	0.374
		Present	15.69	0.12	82.16	0.00	
	50%	Absent	29.01	0.20	83.30	0.44	0.891
		Present	14.37	0.24	83.35	0.40	
D7	WB	Absent	29.32	0.08	84.77	0.20	0.231
		Present	14.77	0.45	84.98	0.17	
	70%	Absent	28.72	0.05	85.27	0.16	0.108
		Present	13.79	0.47	85.55	0.18	
	50%	Absent	28.79	0.22	86.27	0.09	0.001
		Present	13.68	0.27	86.66	0.00	
D10	WB	Absent	29.53	0.19	81.55	0.00	0.984
		Present	15.63	0.22	81.55	0.26	
	70%	Absent	29.13	0.11	82.01	0.25	0.662
		Present	14.58	0.01	82.17	0.53	
	50%	Absent	28.98	0.11	83.20	0.25	0.277
		Present	14.02	0.08	83.40	0.08	

Determining PCR efficiency and Limit of Detection for WB dqPCR

Effect of hemoglobin concentration on reaction efficiency for WB dqPCR

Due to the interaction between Hb and SG affecting C_q seen in the interference studies (Figure 8), and the known PCR inhibition properties of hemoglobin[104], I evaluated the efficiency of PCR reactions for each *RHD* target at various HB concentrations. The range of PCR reaction efficiencies were 87% to 92% for all *RHD* targets across the three Hb levels tested. The mean efficiencies for each target/Hb level combination are displayed in Figure 12. For each *RHD* target, there was no statistical difference in efficiency between the three hemoglobin concentrations (exon 5, p=0.933; exon 7, p=0.843; exon 10, p=0.780). Representative standard curves are shown in Figure 13.

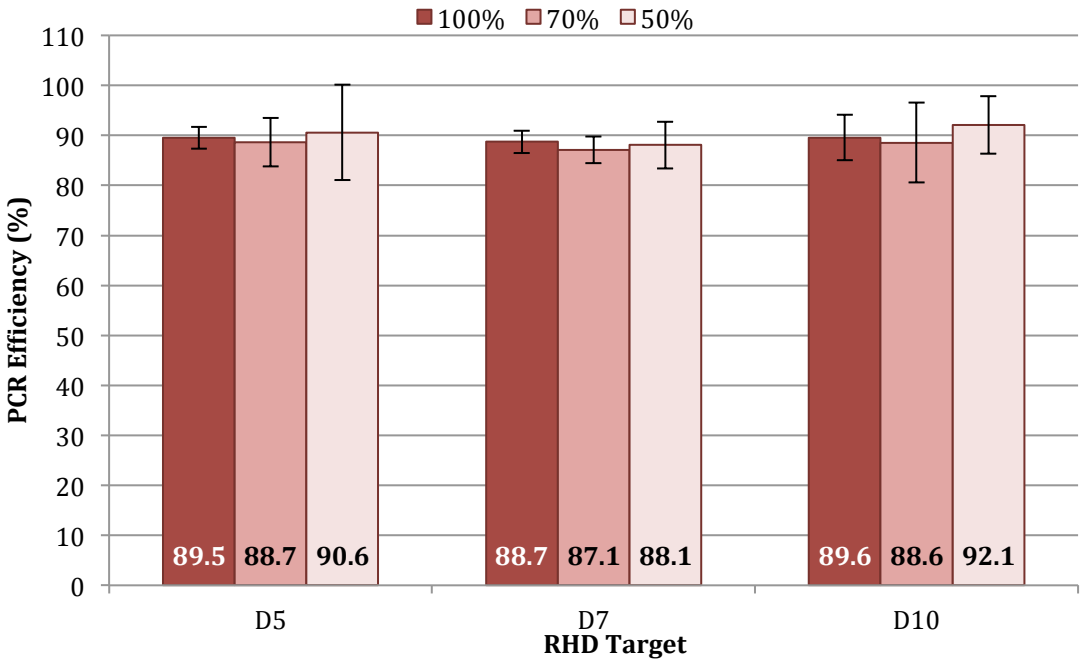

Figure 12: Efficiency Study. The Hb ranges for samples at 100%, 70% and 50% WB were 131-169 g/L, 93-111 g/L and 65-58 g/L, respectively.

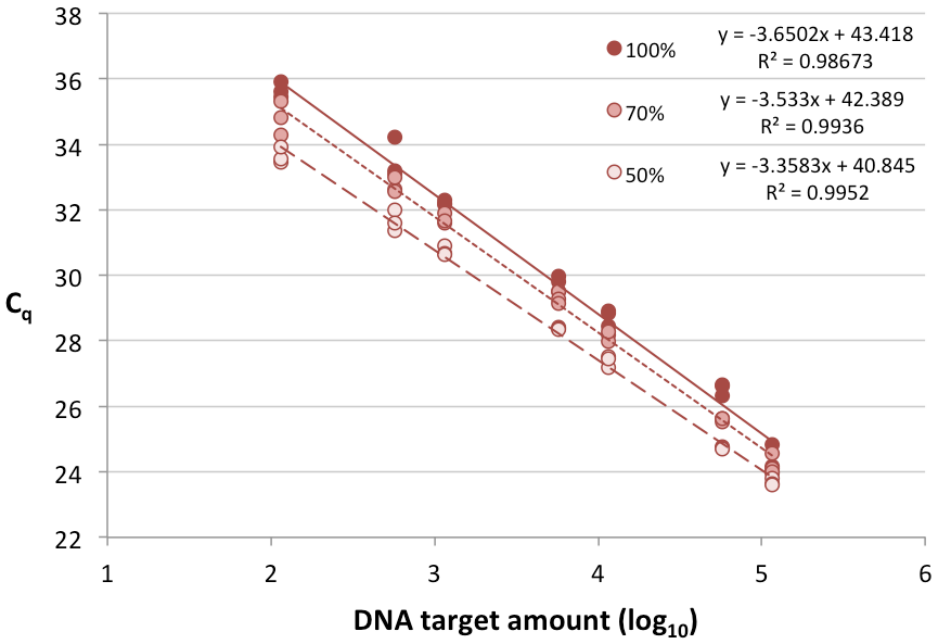

Figure 13: Representative *RHD* exon 5 standard curves for samples with Hb levels of 100% (solid line), 70% (dotted line), and 50% (dashed line) are shown along with the regression information used to determine reaction efficiency.

Limit of Detection for WB dqPCR

Probit analysis is based on the proportion of positive results observed for the various DNA concentrations tested and the SPSS Statistics program requires the data to be presented in a specific format, which is reflected in the tabulated results shown in Table 18. The output of probit analysis is a list of probabilities and the associated estimate and its 95% confidence interval. Excerpts of these tables can be seen in Figure 14. The 95% LOD for *RHD* exons 5, 7 and 10 were 17.2 GE/PCR (95% CI, 9.6 - 47.4), 11.1 GE/PCR (95% CI, 6.1 - 30.8), and 13.3 GE/PCR (95% CI, 8.0 - 30.5), respectively (Figure 14).

Table 18: Probit analysis input for whole blood dqPCR genomic DNA limit of detection.

Target	D-positive [DNA] (pg/µL)	Target Copies (GE/PCR)	Number of Replicates	Number of Positives
D5	0.0	0	16	0
	0.21	0.05	15	1
	1.03	0.25	17	1
	5.16	1.25	15	5
	25.78	6.25	15	11
	51.56	12.5	15	14
D7	0.0	0	15	0
	0.21	0.05	15	0
	1.03	0.25	15	2
	5.16	1.25	15	4
	25.78	6.25	15	14
	51.56	12.5	15	15
D10	0.0	0	16	0
	0.21	0.05	16	0
	1.03	0.25	20	3
	5.16	1.25	20	6
	25.78	6.25	21	19
	51.56	12.5	21	19

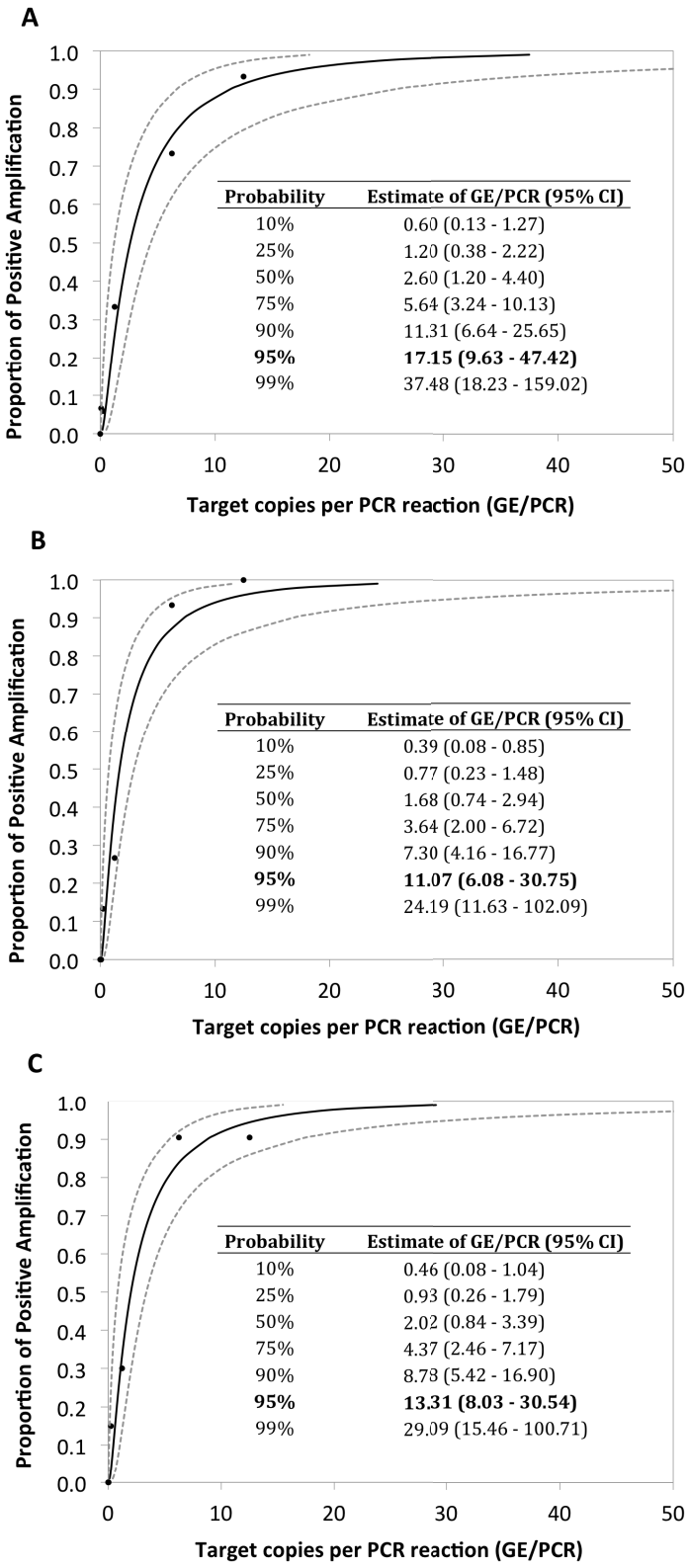

Figure 14: Whole blood dqPCR genomic DNA limit of detection probit estimates (black solid lines) and 95% confidence intervals (grey dashed lines) are shown for *RHD* exon 5 (A), exon 7 (B) and exon 10 (C). The proportions of positive observations from Table 18 are plotted as dots.

LOD using fragmented DNA

The purpose of performing the limit of detection experiment using fragmented DNA was to mimic the size range of cell-free fetal DNA (Figure 15). For each *RHD* target, 21 amplifications were performed on each dilution as well as seven negative control reactions. The number of positive reactions is shown in Table 19. The 95% LOD for *RHD* exons 5, 7 and 10 were 30, 34 and 29 GE/PCR (Figure 16).

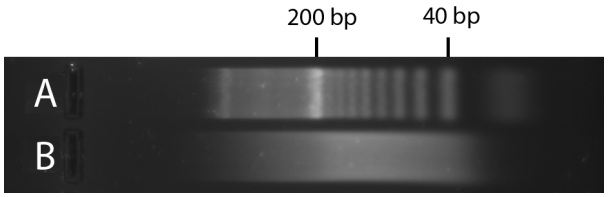

Figure 15: Fragmented DNA. Lane A: 20 bp DNA ladder (Lonza Rockland, Inc), lane B: NEBNext dsDNA Fragmentase-treated human DNA in 10 mM Tris-Cl pH 8.5.

Table 19: Probit analysis input for whole blood dqPCR fragmented DNA limit of detection

Target	D-positive [DNA] (pg/µL)	Target Copies (GE/PCR)	Number of Replicates	Number of Positives
D5	0	0	7	1
	22	5	21	12
	44	11	21	15
	110	27	21	21
	220	53	21	21
	440	107	21	21
D7	0	0	7	1
	22	5	21	12
	44	11	21	17
	110	27	21	19
	220	53	21	20
	440	107	21	21
D10	0	0	7	1
	22	5	21	12
	44	11	21	17
	110	27	21	20
	220	53	21	21
	440	107	21	21

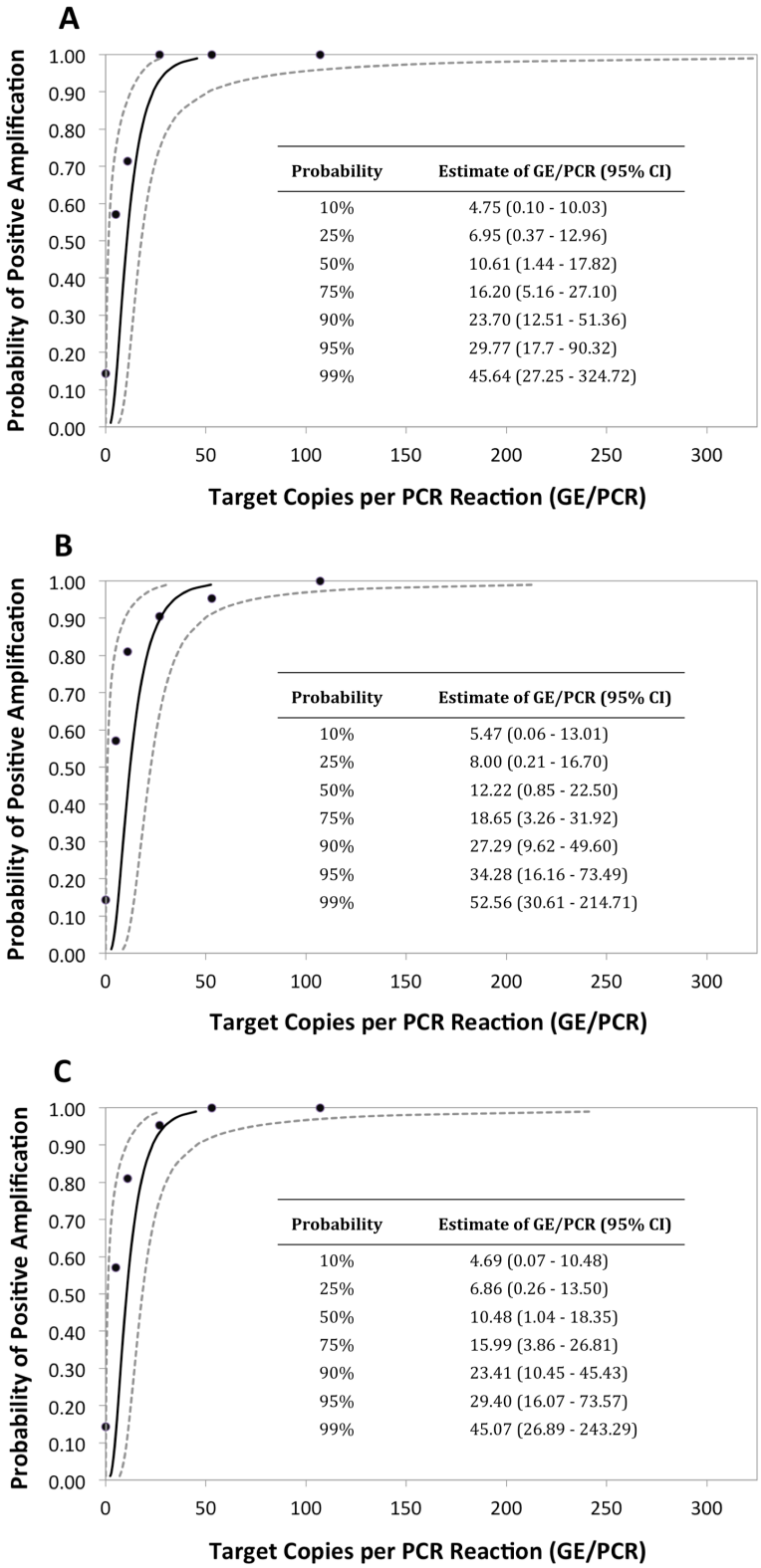

Figure 16: Whole blood dqPCR fragmented DNA limit of detection for *RHD* exon 5 (A), exon 7 (B) and exon 10 (C). Black (solid) lines are the probit estimates with 95% confidence intervals shown as grey (dashed) lines. Positive observations from Table 19 are plotted as dots.

Whole blood dqPCR and DNA PCR method comparison

Of the 60 samples tested, 37 were positive and 23 were negative by serologic RhD phenotyping, which was considered the "gold standard" for the comparison. There were 38 samples that required repeat testing because initial reactions showed amplification but the product T_m was outside of the acceptable range (see Table 8); 33 were for DNA PCR and five for WB dqPCR. For each method, there were four samples for which the RhD prediction was indeterminate after single replicate testing. Testing of additional replicates resolved most indeterminate RhD predictions leaving only two that had been tested by whole blood dqPCR.

To evaluate agreement between whole blood dqPCR and DNA PCR, kappa (κ) was run for each *RHD* target and RhD prediction. Contingency tables and kappa summaries are shown in Tables 7-14. For exons 5 and 10, there was 100% agreement between the two methods and κ = 1.000[g], p < 0.005. For exon 7 there were two samples that were positive by whole blood dqPCR but negative by DNA PCR. Despite this, there was 96.7% agreement and κ = 0.928 (95% CI, 0.830 - 1.026), p < 0.005. For RhD prediction, two samples were indeterminate by whole blood dqPCR. There was 96.7% agreement between the two methods and κ = 0.931 (95% CI, 0.841 - 1.021), p < 0.005. Comparing whole blood dqPCR RhD prediction to serologic RhD phenotype, there was 96.7% agreement and κ = 0.931 (95% CI, 0.841 - 1.021), p < 0.005. Sensitivity and specificity were 100% and 91.3%, (95% CI, 79.3 - 103.3), respectively. Precision was 94.9% and accuracy was 95.6%.

Table 20: Summary of whole blood dqPCR and DNA PCR results for *RHD* exon 5

		DNA PCR		
		Positive	Negative	Total
WB dqPCR	Positive	37	0	37
	Negative	0	23	23
	Total	37	23	60

[g] The 95% confidence intervals could not be calculated because the standard error was zero.

Table 21: Summary of whole blood PCR and DNA PCR results for *RHD* exon 7.

		DNA PCR		
		Positive	Negative	Total
WB dqPCR	Positive	37	2	39
	Negative	0	21	21
	Total	37	23	60

Table 22: Summary of whole blood dqPCR and DNA PCR results for *RHD* exon 10.

		DNA PCR		
		Positive	Negative	Total
WB dqPCR	Positive	37	0	37
	Negative	0	23	23
	Total	37	23	60

Table 23: Summary of SPSS output of kappa statistic calculation for *RHD* exons.

***RHD* target**	**Kappa (κ)**	**Standard Error**	**Approx. Sig.**
Exon 5	1.000	0.000	0.000
Exon 7	0.928	0.050	0.000
Exon 10	1.000	0.000	0.000

Table 24: Summary of whole blood dqPCR and DNA PCR results for RhD prediction

		DNA PCR RhD Prediction		
		Positive	Negative	Total
WB dqPCR RhD prediction	Positive	37	0	37
	Negative	0	21	21
	Indeterminate	0	2	2
	Total	37	23	60

Table 25: Summary of whole blood dqPCR RhD prediction and serologic RhD phenotype results

		Serologic RhD Phenotype		
		Positive	Negative	Total
WB dqPCR RhD prediction	Positive	37	0	37
	Negative	0	21	21
	Indeterminate	0	2	2
	Total	37	23	60

Table 26: Summary of DNA PCR RhD prediction and serologic RhD phenotype results

		Serologic RhD Phenotype		
		Positive	Negative	Total
DNA PCR RhD prediction	Positive	37	0	37
	Negative	0	23	23
	Total	37	23	60

Table 27: Summary of SPSS output of kappa statistic calculation for RhD prediction and phenotype

Comparison	Kappa (κ)	Standard Error	Approx. Sig.
WB dqPCR vs DNA PCR	0.931	0.046	0.000
DNA PCR vs Phenotype	1.000	0.000	0.000
WB dqPCR vs Phenotype	0.931	0.046	0.000

Developing a Method for dqPCR using Plasma Samples

The results presented in this section are from experiments related to the hypothesis that dqPCR can be performed using plasma samples. The first of two subsections describes the results of experiments that were performed during development of the PL dqPCR protocol, while the second focuses on evaluation of reaction efficiency and limit of detection for the PL dqPCR protocol.

Plasma dqPCR protocol development

The general approach to development of the plasma dqPCR protocol was to begin by substituting plasma into the whole blood protocol, followed by incremental changes to address specific issues or concerns arising from previous experiments.

Plasma dqPCR protocol development: First trial using plasma in WB dqPCR protocol

This experiment served as the starting point for PL dqPCR protocol development and provided insight into the variables that would need optimization.

Three PCR analysis conditions were evaluated for plasma dqPCR, each having a unique combination of baseline and threshold (Table 28). Condition A used the default settings provided by the StepOne software, condition B used the same settings as whole blood dqPCR, and condition C combined the threshold used for whole blood dqPCR and an empirically established baseline. For condition A, the software-selected threshold was 8260 fluorescence units and the mean C_q for the four D-positive replicates was 35.44 cycles ± 2.20 cycles. The mean C_q values for condition B and condition C were 33.42 cycles ± 2.24 cycles and 32.59 cycles ± 2.04 cycles, respectively. The mean C_q for the whole blood dqPCR D-positive replicates was 25.04 cycles ± 0.16 cycles. Regardless of the baseline setting, the amplification plots for plasma dqPCR show a "ramp up" effect in the first few cycles (see Figure 17 and Figure 18) that is not observed in whole blood PCR (Figure 19).

As T_m is unaffected by the choice of baseline, all three analysis conditions for plasma dqPCR had the same mean T_m of 87.33 °C ± 0.50 °C. The mean T_m for whole blood dqPCR was 80.97 °C ±0.00 °C (all 4 replicates had the exact same T_m).

Table 28: Analysis settings evaluated for first run of plasma dqPCR

Condition	Baseline	Threshold
A	automatic	automatic
B	automatic	1000
C	cycles 11-23	1000

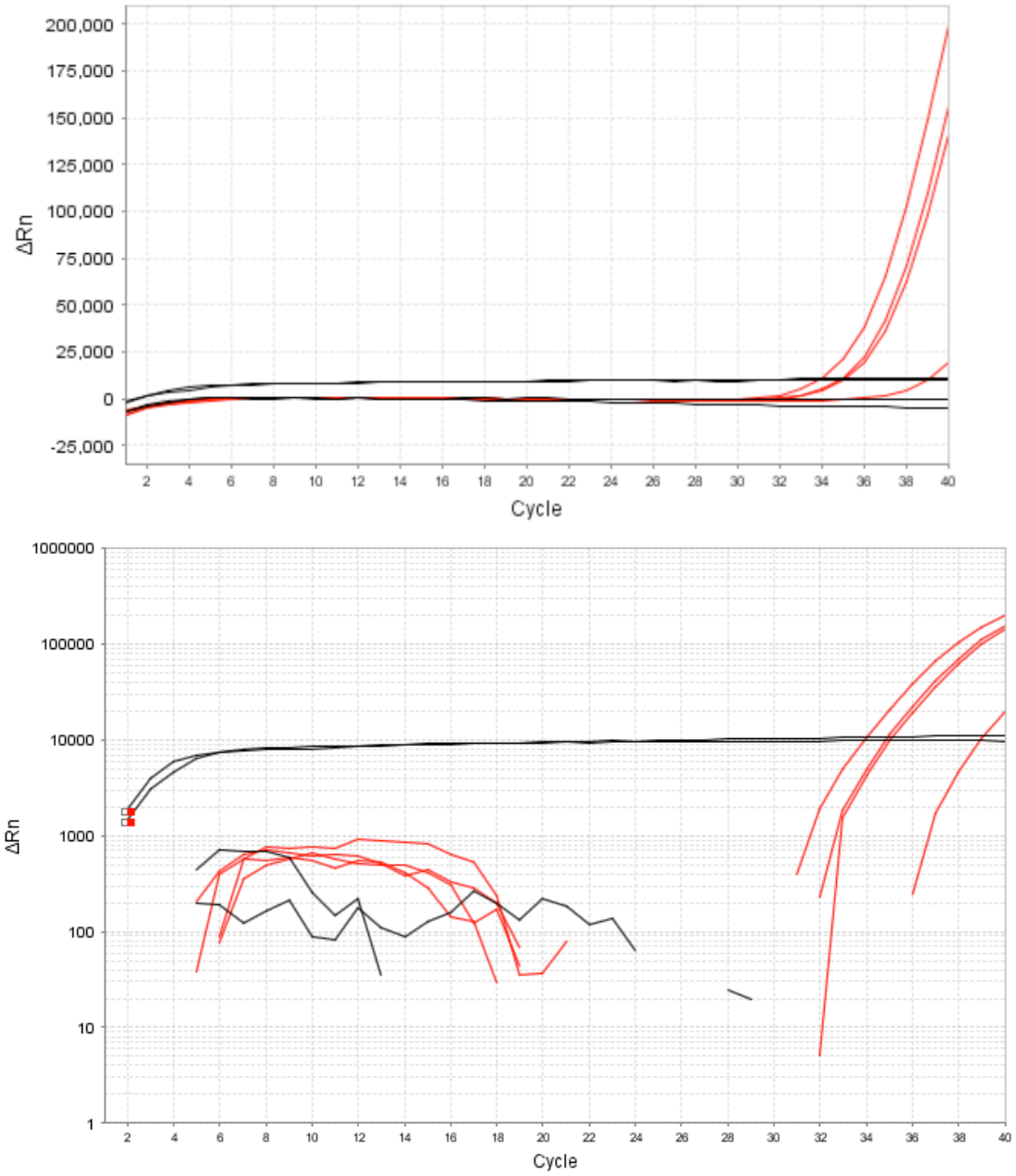

Figure 17: Linear (upper panel) and logarithmic (lower panel) amplification plots for plasma dqPCR as they appeared for conditions A and B, when baseline was automatically selected by StepOne software, are shown for D-positive (red) and D-negative (black) pooled control samples. Baseline end well is depicted by a white and red rectangle ( ). The logarithmic panel also shows the condition B threshold.

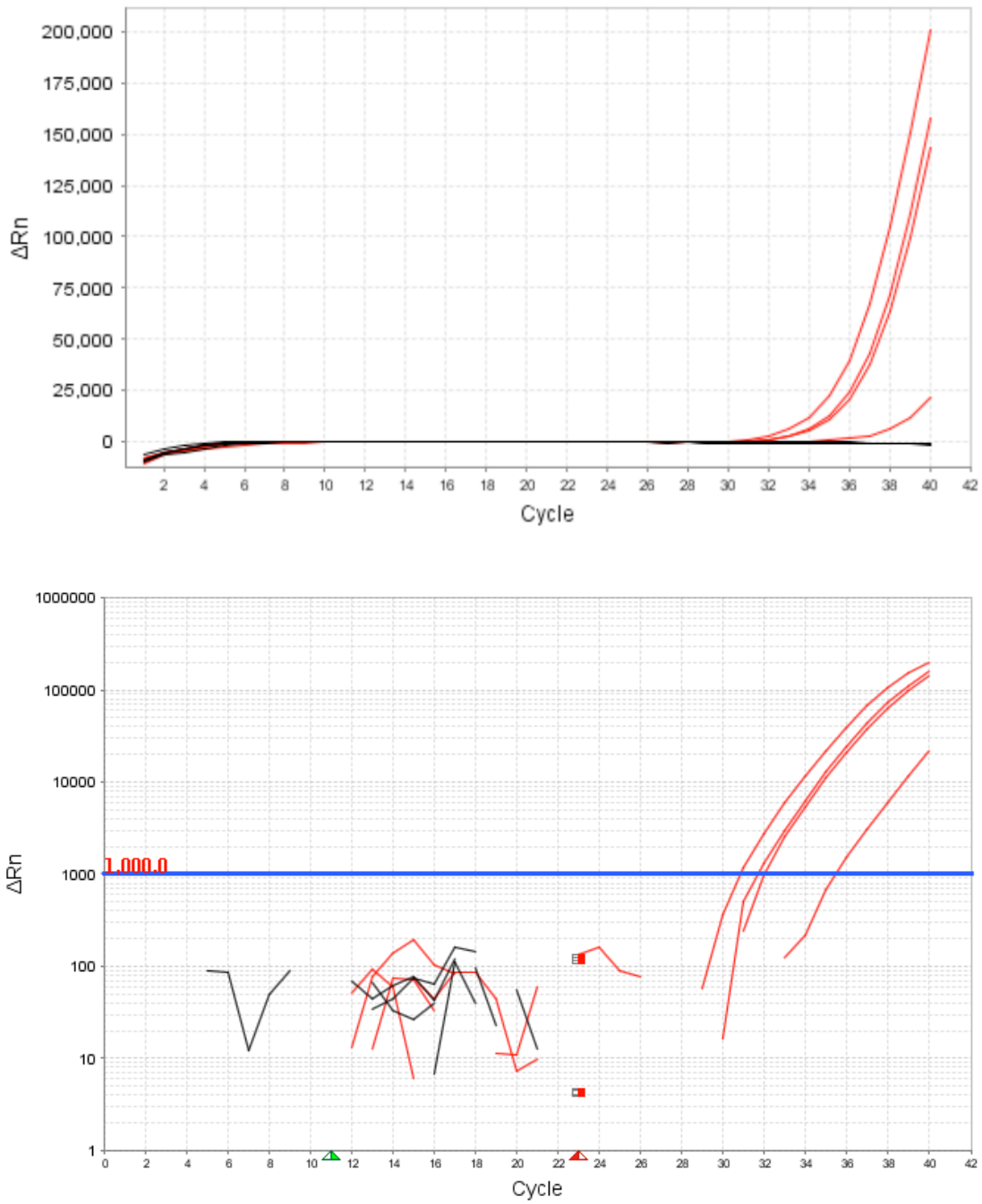

Figure 18: Linear (upper panel) and logarithmic (lower panel) amplification plots for plasma dqPCR as they appeared for condition C, when baseline was set between cycles 11 and 23, are shown for D-positive (red) and D-negative (black) pooled control samples. Green (▲) and red (▲) markers depict the common baseline start and end, respectively.

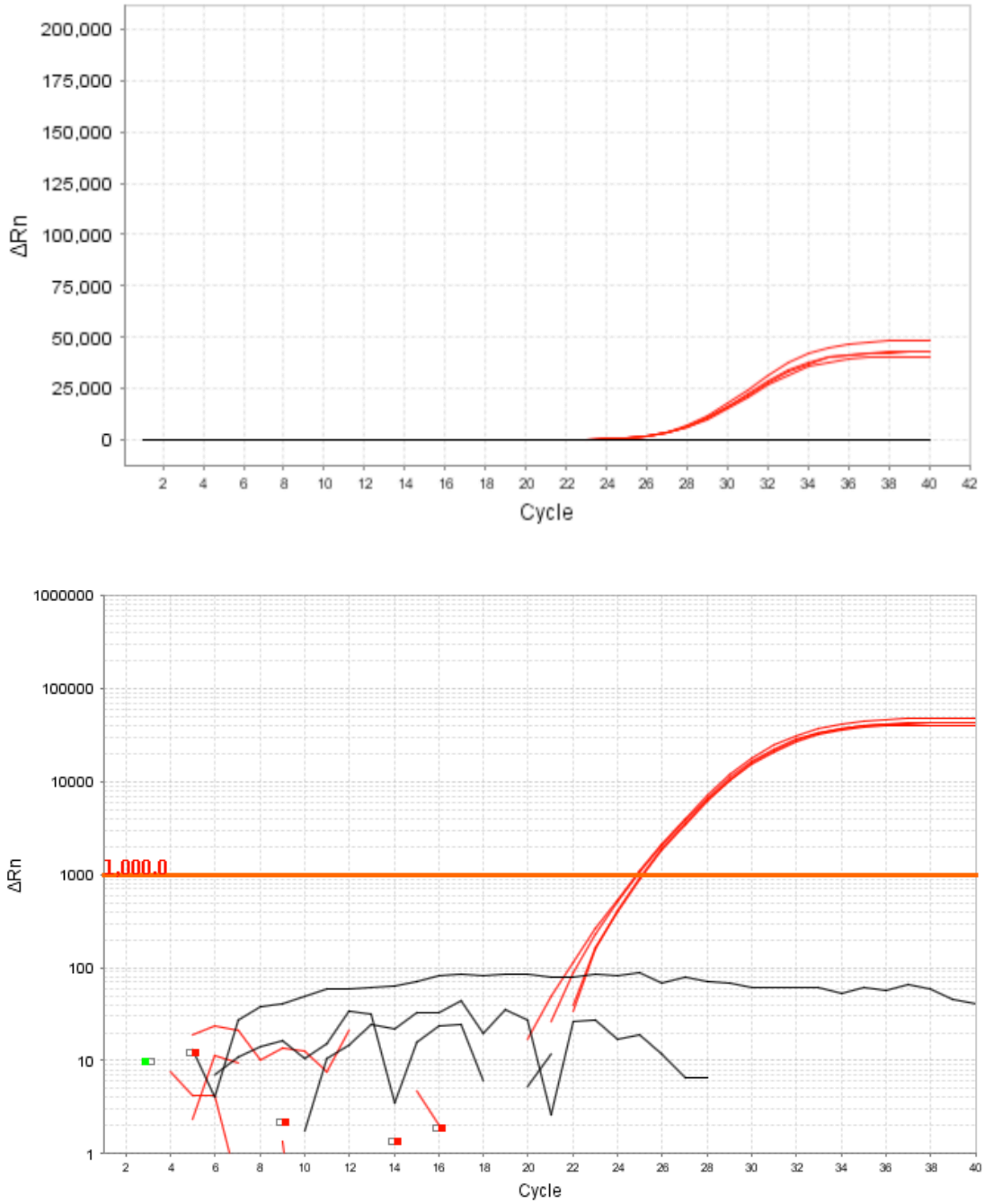

Figure 19: Linear (upper panel) and logarithmic (lower panel) amplification plots for whole blood dqPCR are shown for D-positive (red) and D-negative (black) pooled control samples. Green ( ) and red ( ) rectangular markers depict baseline start and end wells, respectively, as determined by the StepOne software.

Plasma dqPCR protocol development: SYBR Green I titration

The purpose of this experiment was to optimize the SG concentration for dqPCR reactions not containing hemoglobin. No amplification was seen for D-positive control reactions containing 40X SG; however, varying amplification was observed in the other SG concentrations tested (Figure 20). Mean C_q values ranged from 32.51 cycles for 1x SG to 29.75 cycles for 20x SG. The mean T_m for SG concentrations of 1x, 2.5x, 5x, 10x, and 20x were 79.46 °C, 80.19 °C, 81.03 °C, 83.35 °C, and 85.46 °C. Figure 21 illustrates the range of melt temperatures observed.

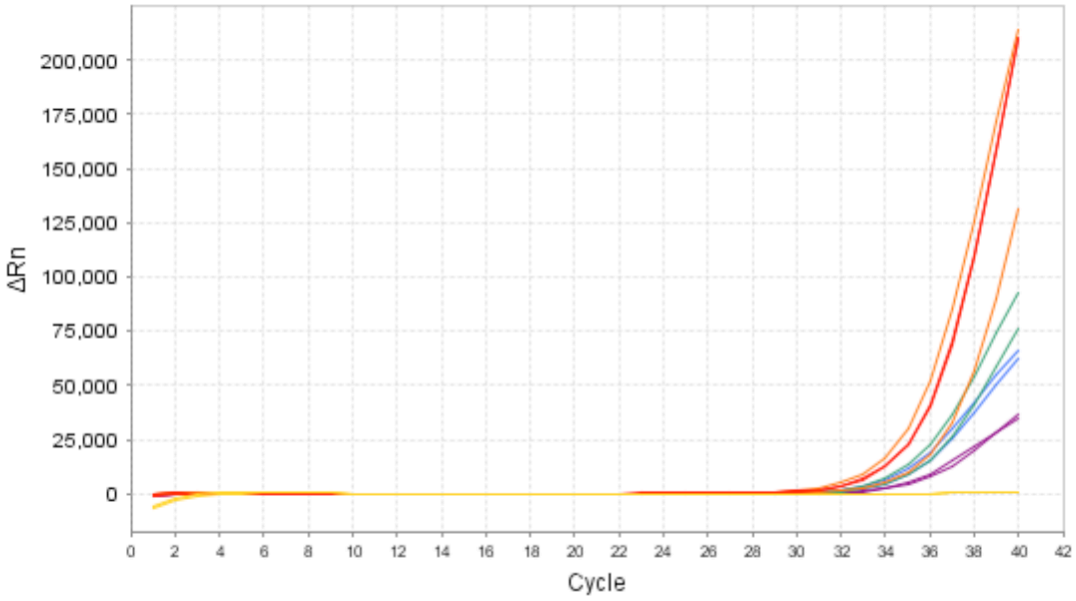

Figure 20: Amplification plots are shown for plasma dqPCR of D-positive pooled controls in reactions containing SYBR Green I in concentrations of 1x (purple), 2.5x (blue), 5x (green), 10x (orange), 20x (red), and 40x (yellow).

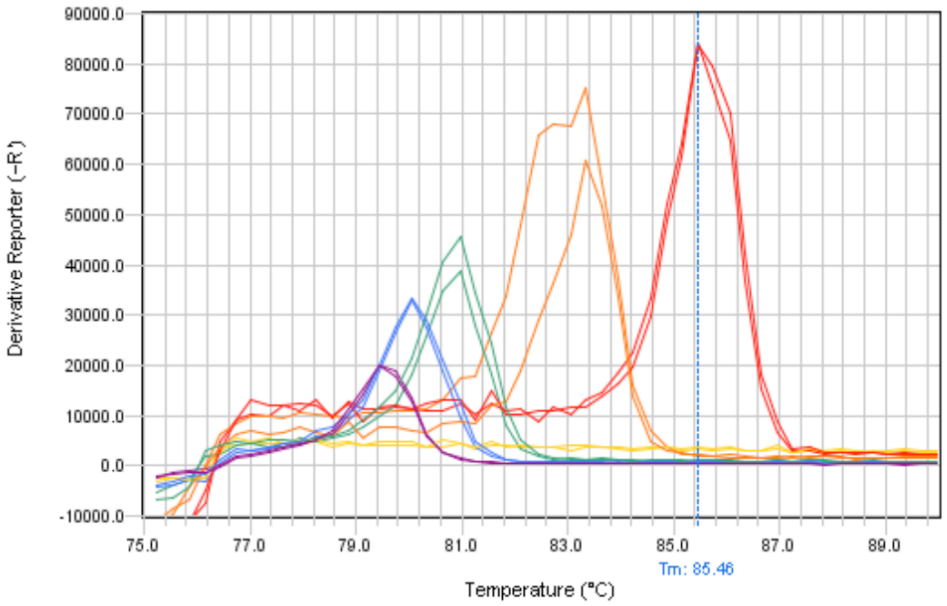

Figure 21: Melt curves are shown for plasma dqPCR of D-positive pooled controls in reactions containing SYBR Green I in concentrations of 1x (purple), 2.5x (blue), 5x (green), 10x (orange), 20x (red), and 40x (yellow).

Plasma dqPCR protocol development: Sample volume study

With the broader aim of improving the limit of detection, the purpose of this experiment was to increase the volume of plasma sample added to each reaction. The general approach was to compare 8% (v/v) plasma reactions to those containing the maximum possible volume. For the 8% plasma reactions, amplification occurred in all sample dilutions with C_q values ranging from 30.31 cycles to 32.92 cycles for the dilutions. The 6.25 pg/µL sample failed to amplify when sample volume was 25.5% of the reaction volume. The C_q values for the other sample dilutions ranged from 29.33 cycles to 33.25 cycles. Statistical comparison of the two sample volumes was not possible because samples were run as single reactions. The amplification plots for the pooled controls appear very similar regardless of sample volume though the "ramp up" effect seems more pronounced in reactions with greater plasma volume (see Figure 22 and Figure 23). The mean T_m for all positive reactions were 81.55 °C ± 0.06 °C and 80.73 °C ± 0.13 °C for 8% and 25.5% reactions, respectively.

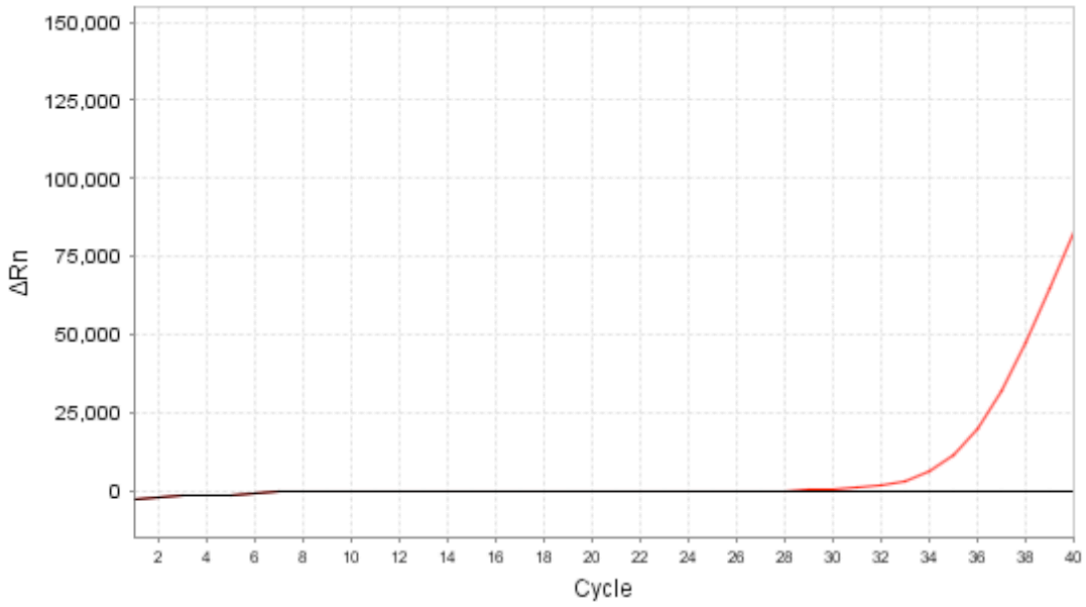

Figure 22: Amplification plots for plasma dqPCR with sample added at 8% of reaction volume is shown for D-positive (red) and D-negative (black) pooled controls.

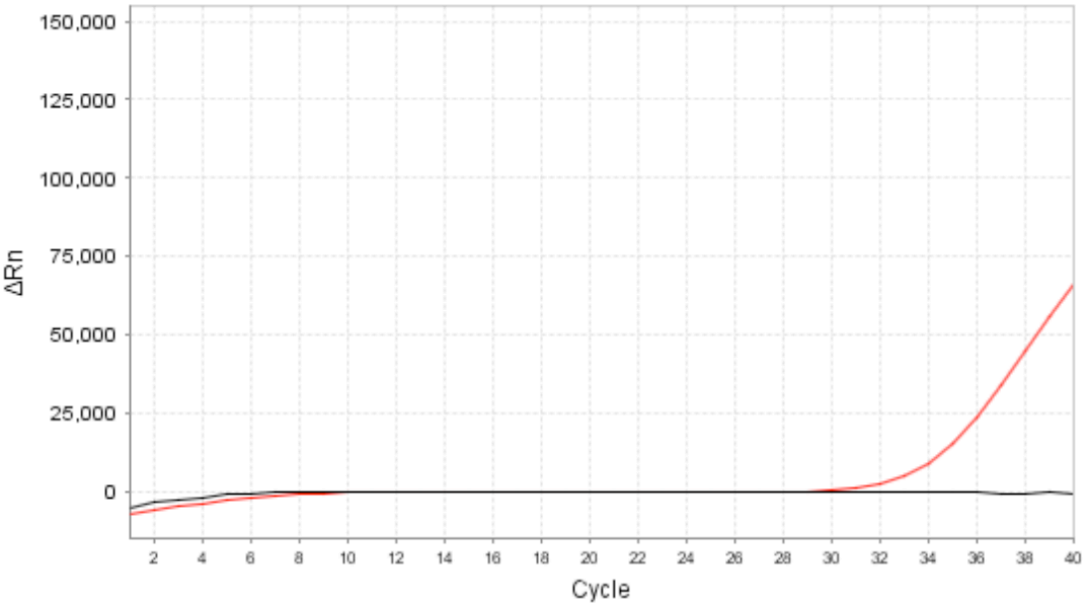

Figure 23: Amplification plots for plasma dqPCR with sample added at 25.5% of reaction volume is shown for D-positive (red) and D-negative (black) pooled controls.

Plasma dqPCR protocol development: Reporter dye titration and comparison

The purpose of this experiment was two-fold; to determine if the dye concentration needed to be adjusted in light of the larger sample volume, and to evaluate a second dye, EvaGreen, for possible use in the PL dqPCR protocol. Various concentrations of each dye were used in positive and negative control reactions targeting *RHD* exon 5. The mean C_q values for D-positive pool controls samples at SG concentrations of 1x, 2.5x, 5x and 10x were 33.80 cycles, 32.11 cycles, 31.14 cycles and 31.43 cycles. The corresponding melt temperatures were 79.24 °C, 79.92 °C, 80.57 °C, and 82.17 °C (Figure 24). For EvaGreen concentrations of 1x, 2.5x, 5x, and 10x, mean C_q values for D-positive pool controls were 38.40 cycles, 34.42 cycles, 33.51 cycles, and 34.59 cycles and T_m were 78.55 °C, 79.31 °C, 79.99 °C, and 80.72 °C (Figure 25). Figure 26 compares C_q and T_m values for SG and EG. Baseline-corrected amplification plots for both dyes show changes in fluorescent signal during the first few PCR cycles regardless of dye concentration. Figure 27 and Figure 28 illustrate the phenomenon. Amplification plots without baseline correction (Figure 29 and Figure 30) reveal that the increase in fluorescent signal continues throughout the reactions for both dyes, though the effect appears less pronounced for SG. The effect appears to be more pronounced in the first eight cycles and can be seen in previous experiments (see Figures 12, 13, 17 & 18).

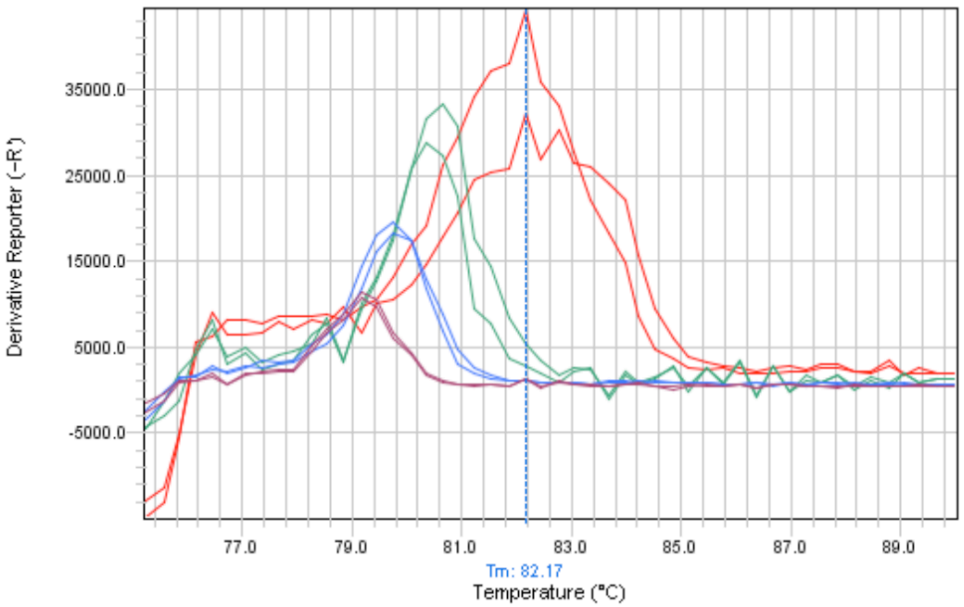

Figure 24: SG titration verification MCA showing melt curves for D-positive pooled control reactions containing SYBR Green I concentrations of 1x (purple), 2.5x (blue), 5x (green), and 10x (red).

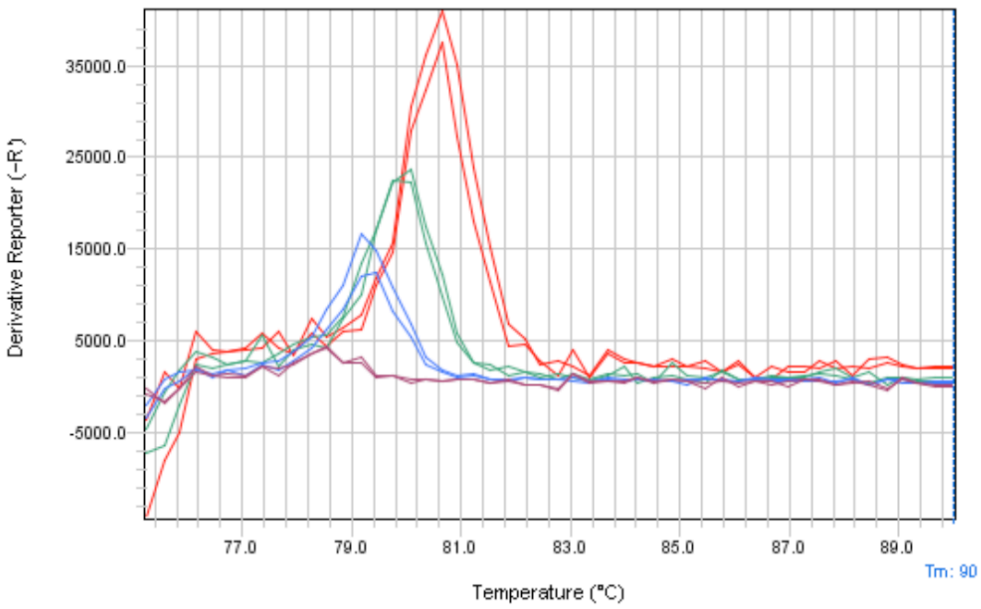

Figure 25: EvaGreen titration, melt curves for D-positive pooled control reactions containing EG concentrations of 1x (purple), 2.5x (blue), 5x (green), and 10x (red).

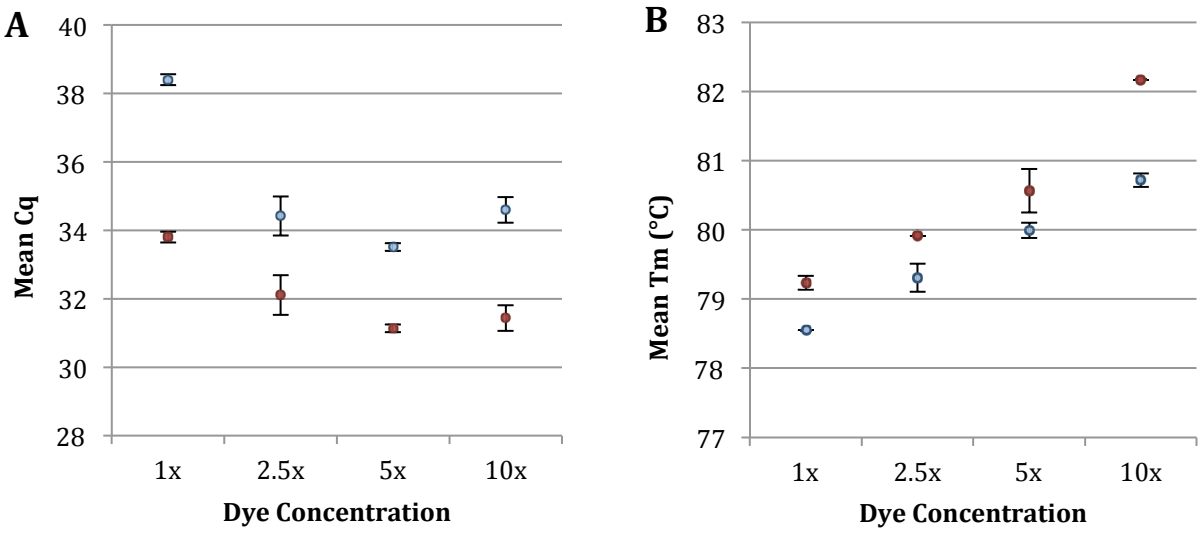

Figure 26: Plasma dqPCR reporter dye comparison. Mean C_q values (panel A) and mean T_m (panel B) are shown for reactions with various concentrations of SYBR Green I (red ●) and Evagreen (blue ●). Error bars depict ±1 standard deviation.

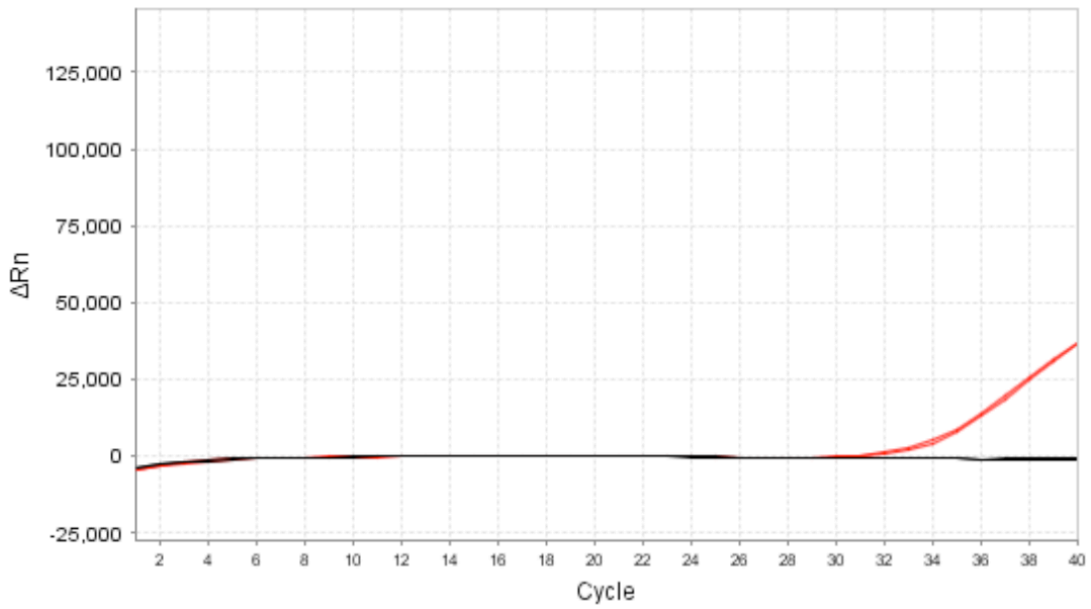

Figure 27: Amplification plot for SYBR Green I titration verification is shown for D-positive (red) and D-negative (black) pooled control reactions containing 2.5x SG.

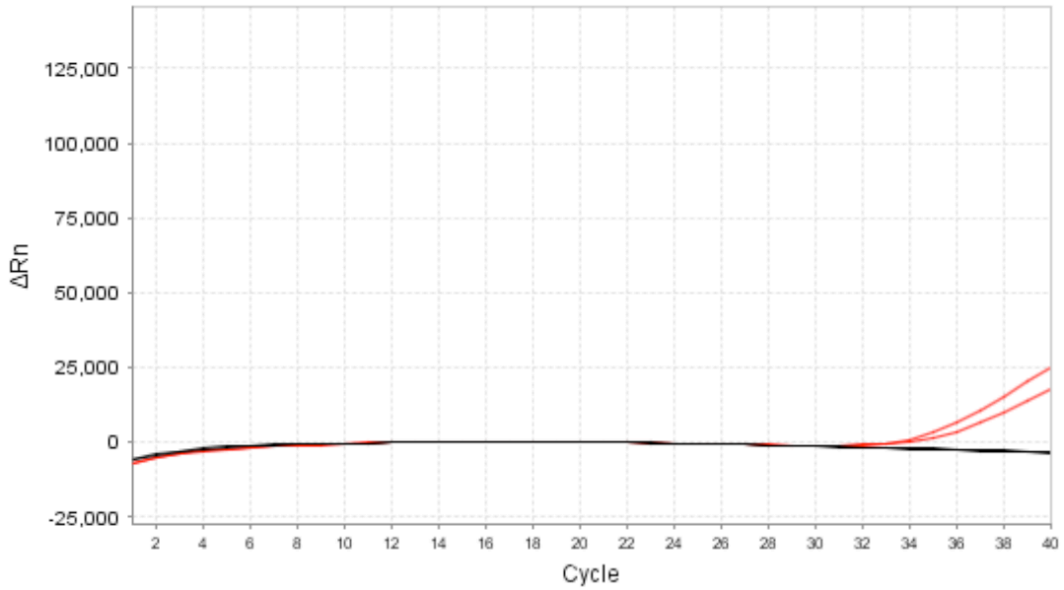

Figure 28: Amplification plot for EvaGreen titration is shown for D-positive (red) and D-negative (black) pooled control reactions containing 2.5x EG.

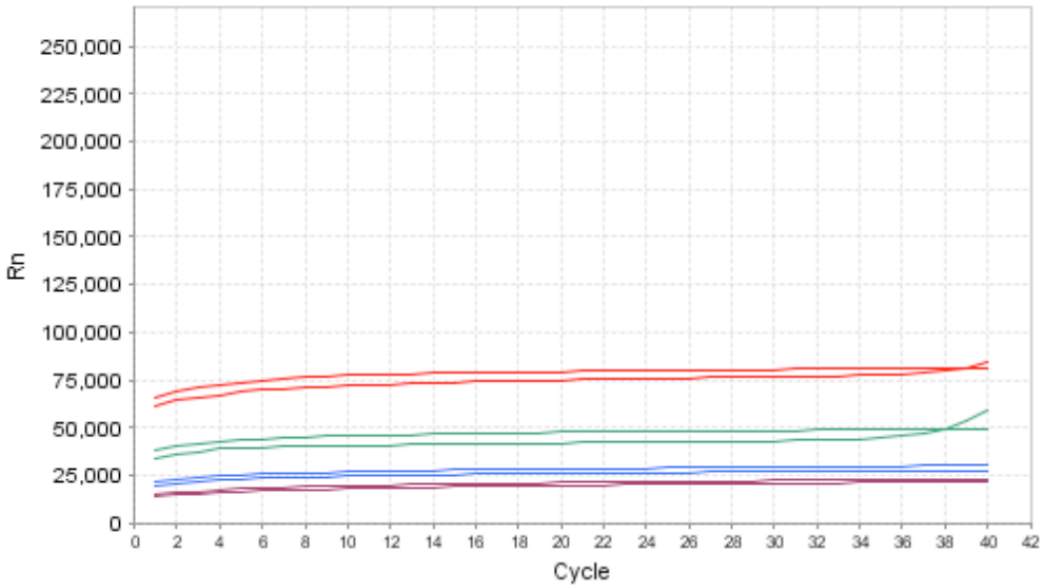

Figure 29: Amplification plots without baseline correction for D-negative pool reactions containing SYBR Green I concentrations of 1x (purple), 2.5x (blue), 5x (green), and 10x (red).

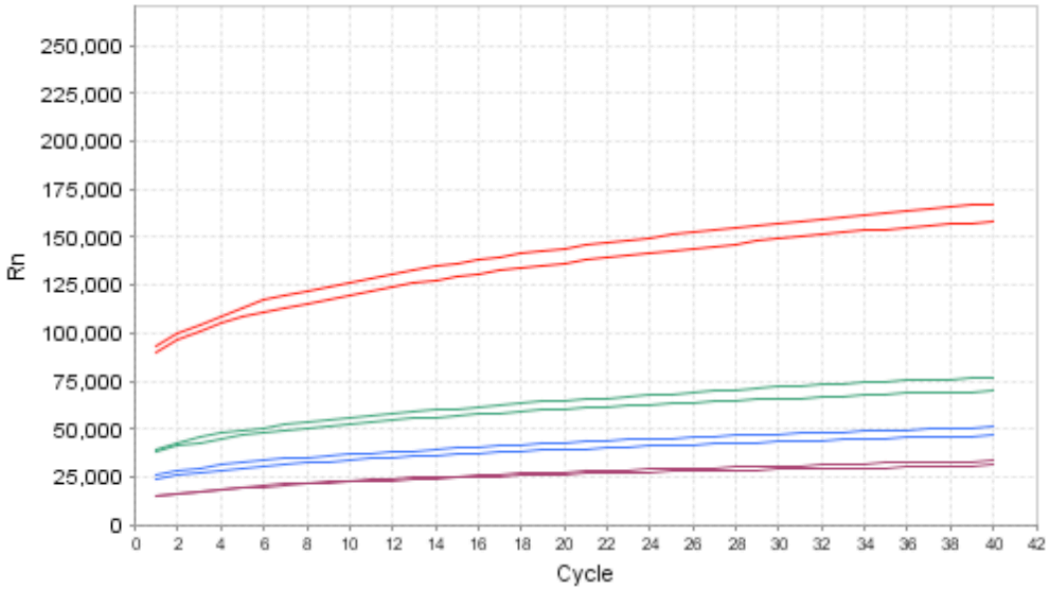

Figure 30: Amplification plots without baseline correction for D-negative pool reactions containing EvaGreen concentrations of 1x (purple), 2.5x (blue), 5x (green), and 10x (red).

Plasma dqPCR protocol development: Run method modification

The purpose of this experiment was to determine whether the StepOne software would correctly apply baselines in automatic mode if the fluorescent data from the first eight cycles were not collected. Because the StepOne software did not automatically include the cycles without fluorescent data capture in the total cycle count, C_q values were adjusted manually[h].

Figure 31 illustrates the effect of omitting fluorescent data capture on amplification plots prior to baseline correction. For comparison, Figure 32 shows amplification plots from similar reactions with fluorescent data collected for all cycles. Figure 33 and Figure 34 show the same amplification plots after baseline correction. With the baseline set at cycles 11-23$_{adj}$, the mean C_q value for D-positive pool samples tested with the modified run method was 32.24$_{adj}$ cycles. For the standard run method and the same baseline setting, the mean C_q value for the D-positive pooled control samples was 32.10 cycles.

[h] In the results, the StepOne software only reported cycles for which fluorescence data was captured, of which there were 32. For clarity when discussing plasma dqPCR, "mod" will be added to indicate that the cycle numbers refer to the actual StepOne report and "adj" will be used to when referring to the total number of cycles.

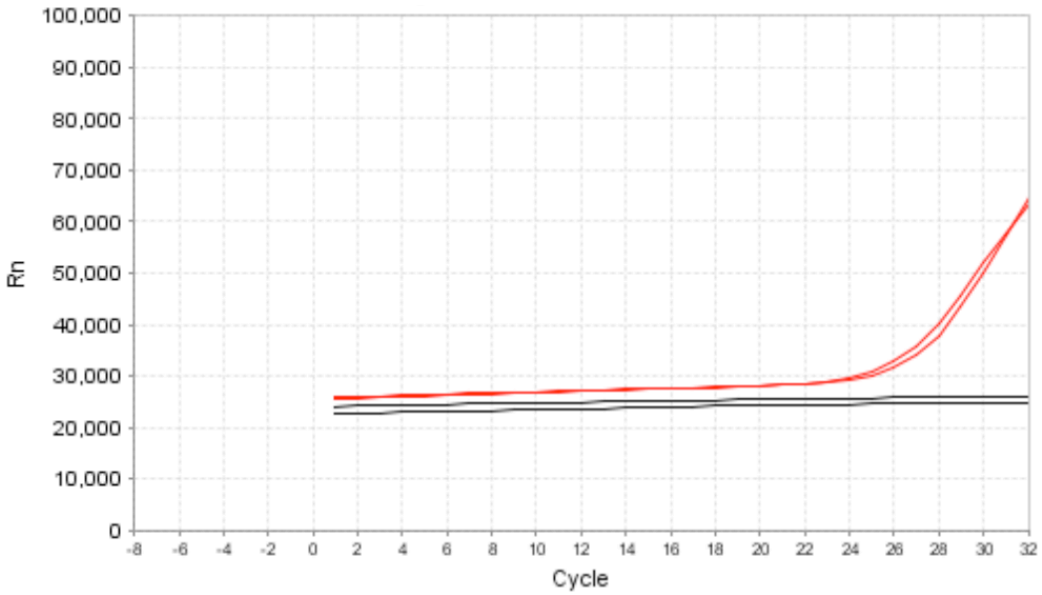

Figure 31: Amplification plots without baseline correction for D5 PL dqPCR with modified run method are shown for D-positive (red) and D-negative (black) pooled control samples. The x-axis has been adjusted to illustrate that fluorescent data was not collected for the first eight cycles (cycle -8 to cycle 0).

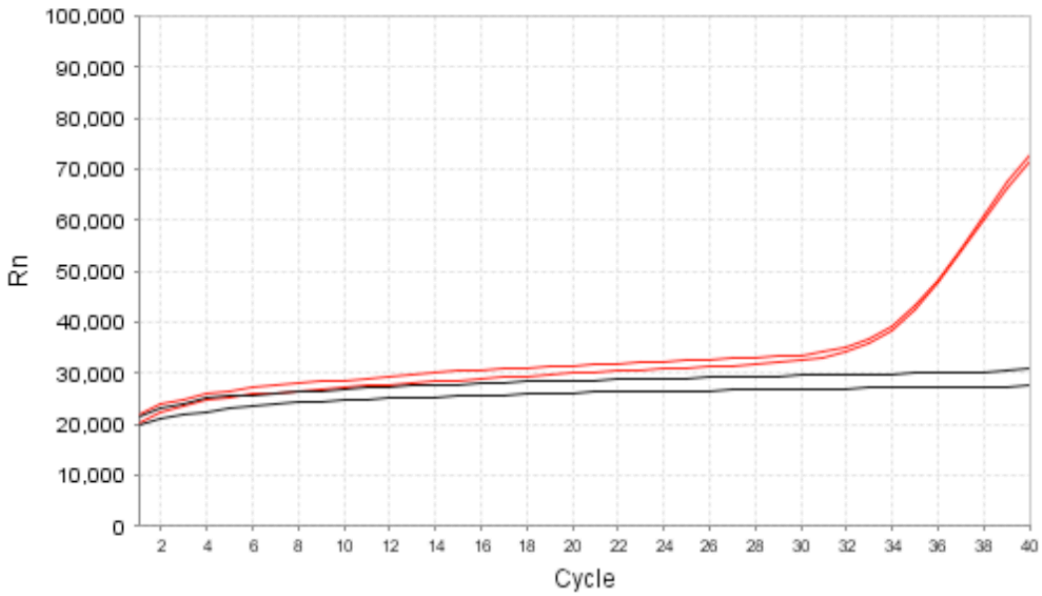

Figure 32: Amplification plots are shown for D5 PL dqPCR with the standard run method are shown for D-positive (red) and D-negative (black) pooled control samples.

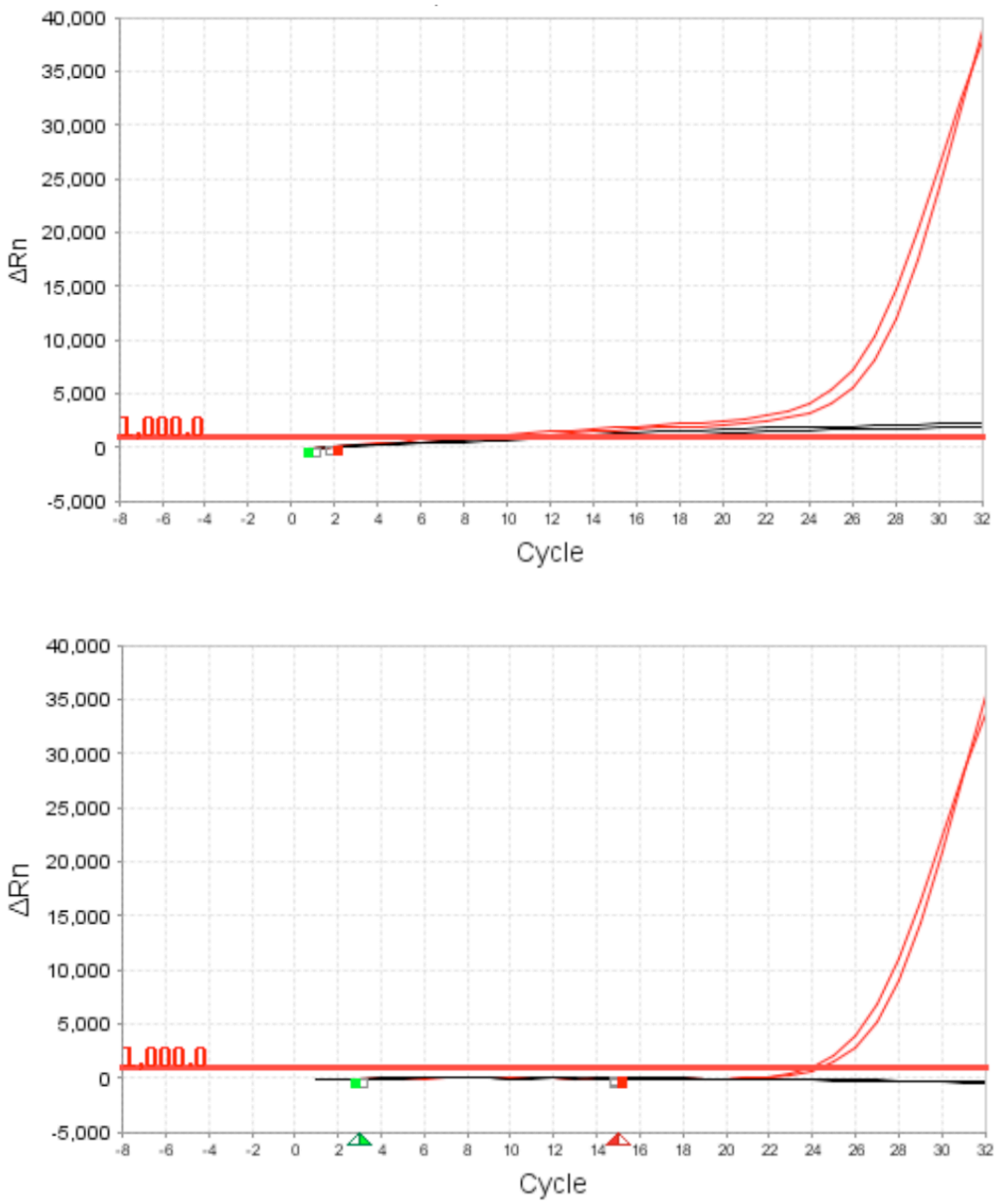

Figure 33: Amplification plots with baseline correction for D5 PL dqPCR with modified run method are shown for D-positive (red) and D-negative (black) pooled control samples. The x-axis has been adjusted to illustrate that fluorescent data was not collected for the first eight cycles (cycle -8 to cycle 0). Baseline settings were auto (upper panel) and cycles 11-23_{adj} (lower panel).

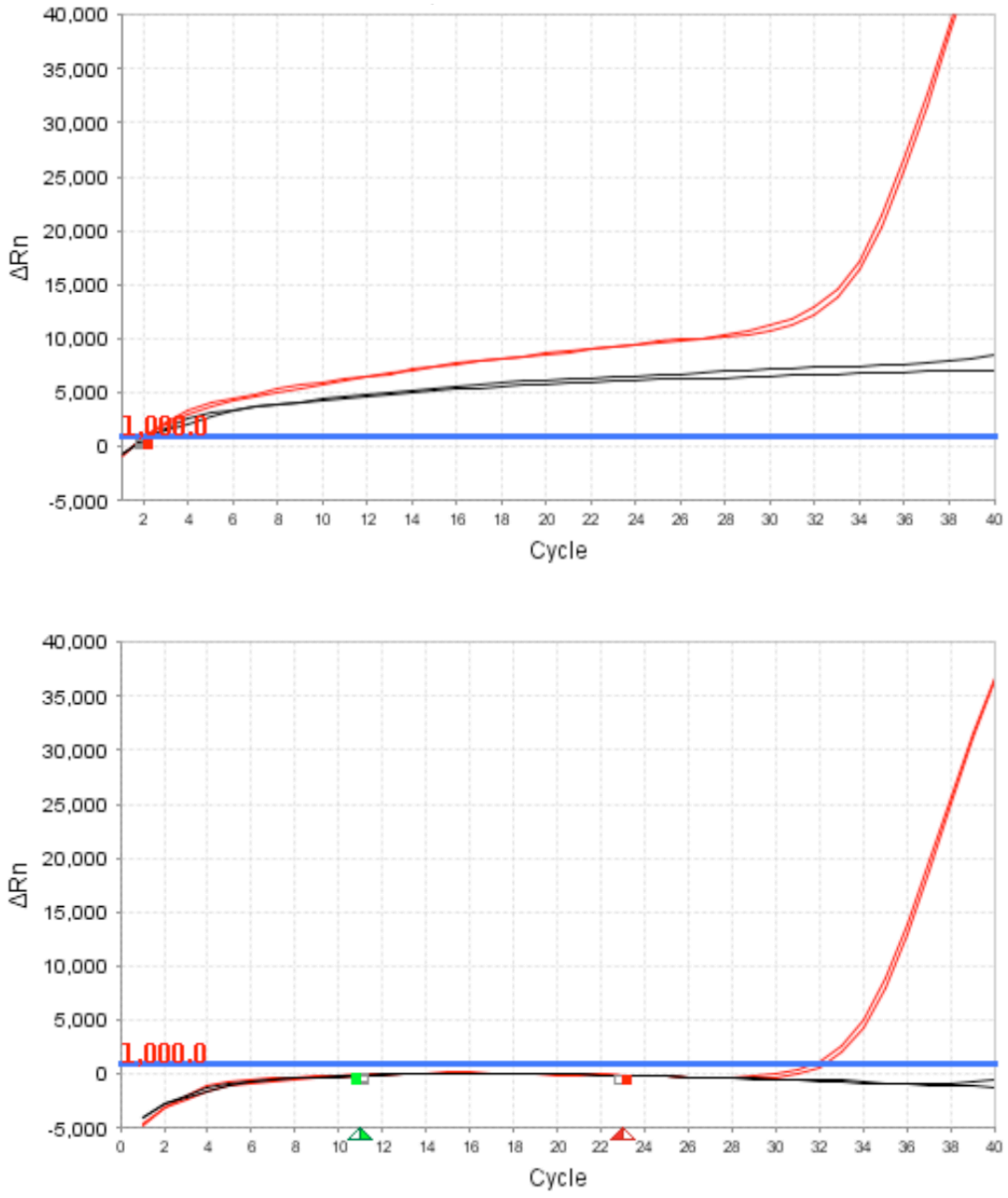

Figure 34: Amplification plots with baseline correction for D5 PL dqPCR with standard run method are shown for D-positive (red) and D-negative (black) pooled control samples. Baseline settings were auto (upper panel) and cycles 11-23$_{adj}$ (lower panel).

Determining PCR efficiency and Limit of Detection for PL dqPCR

PCR efficiency and limit of detection were utilized as means to evaluate the performance of the PL dqPCR protocol.

Plasma dqPCR Protocol Evaluation: PCR efficiency

Reaction efficiencies, calculated from standard curves (Figure 35) for PL dqPCR were 96.8%, 94.6%, and 94.2% for *RHD* exons 5, 7, and 10, respectively, with corresponding amplification factors of 1.97, 1.95 and 1.94.

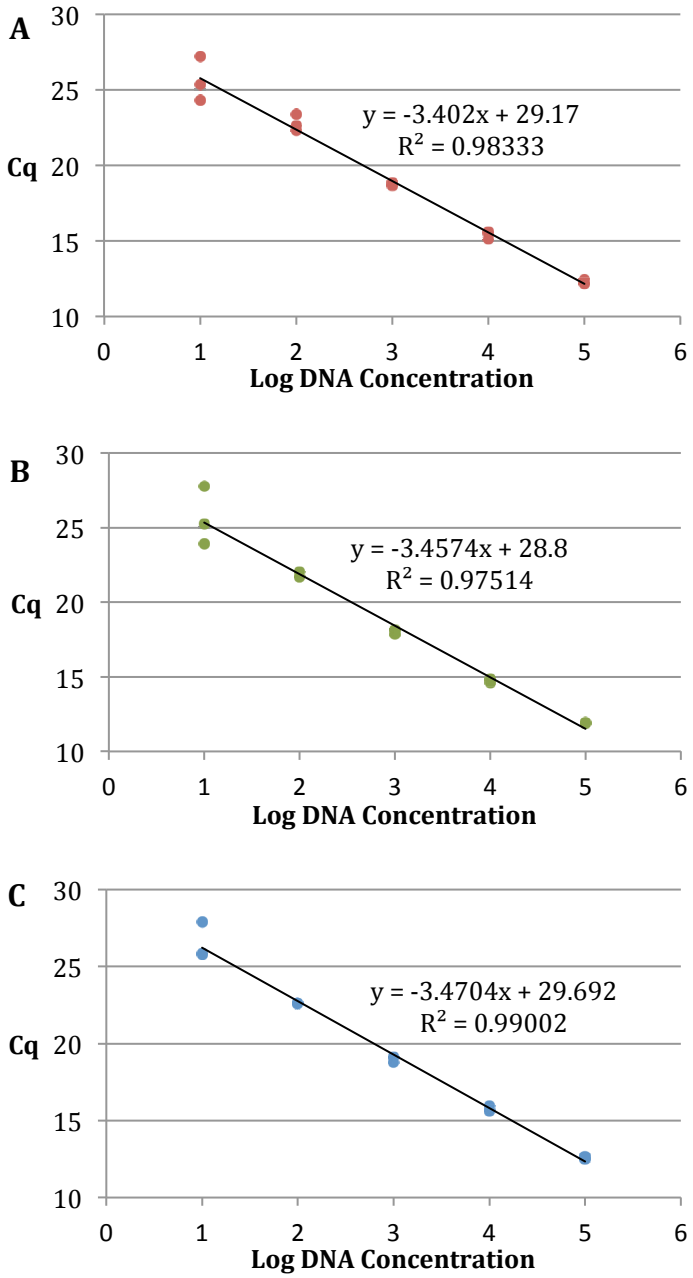

Figure 35: Plasma dqPCR standard curves for RHD exon 5 (A), exon 7 (B) and exon 10 (C).

Table 29: Probit analysis input for plasma dqPCR genomic DNA limit of detection.

Target	D-positive [DNA] (pg/µL)	Target Copies (GE/PCR)	Number of Replicates	Number of Positives
D5	0	0	15	0
	0.01	0.01	15	0
	0.06	0.05	15	0
	0.32	0.25	15	2
	1.62	1.23	15	6
	8.10	6.14	15	15
	16.20	12.28	12	12
D7	0	0	12	0
	0.01	0.01	12	0
	0.06	0.05	11	0
	0.32	0.25	14	2
	1.62	1.23	12	7
	8.10	6.14	15	15
	16.20	12.28	12	12
D10	0	0	14	1
	0.01	0.01	14	0
	0.06	0.05	13	0
	0.32	0.25	15	4
	1.62	1.23	15	6
	8.10	6.14	15	15
	16.20	12.28	11	11

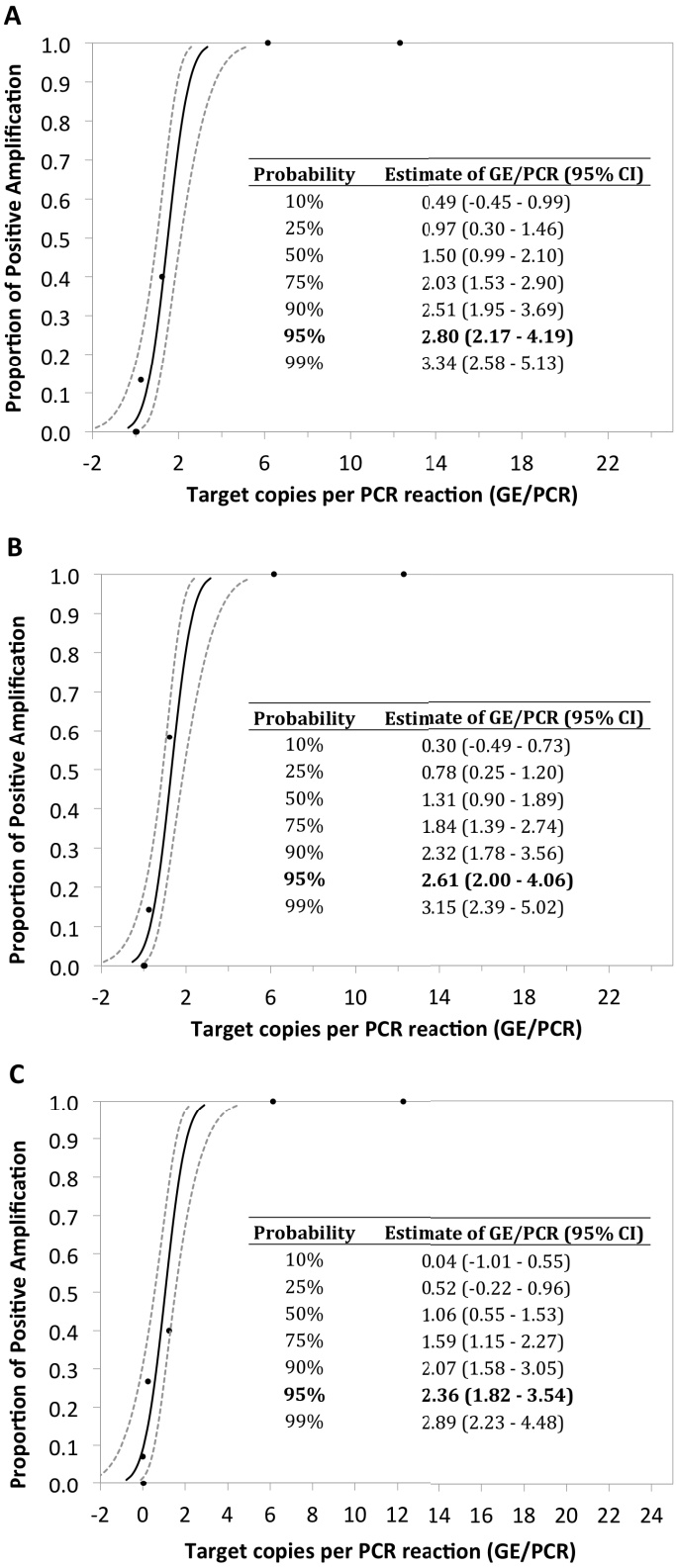

Figure 36: Plasma dqPCR limit of detection probit estimates (black solid lines) and 95% confidence intervals (grey dashed lines) are shown for *RHD* exon 5 (A), exon 7 (B) and exon 10 (C). The proportions of positive observations from Table 29 are plotted as dots.

Table 30: Direct qPCR summary

PCR Mix (µL)	**WB dqPCR**	**PL dqPCR**
PEC-1	5	-
PEC-2	-	5
PCR water	1.75	0.2
10x KMB	1	1
1000x SG in KMB	0.4	-
125x SG	-	0.2
OKT pol.	0.3	0.3
2% BSA	0.15	0.2
10 mM dNTPs	0.2	0.2
20 µM forward primer	0.2	0.2
20 µM reverse primer	0.2	0.2
whole blood sample	0.8	-
plasma sample	-	2.5
Total volume	10	10

Run Method		
PCR	hold: 95 °C for 1:20 40 cycles: 95 °C for 0:15 62 °C for 0:15 72 °C for 0:40	hold: 95 °C for 1:20 8 cycles: no data capture 95 °C for 0:15 62 °C for 0:15 72 °C for 0:40 32 cycles: 95 °C for 0:15 62 °C for 0:15 72 °C for 0:40
MCA	75 °C → 90 °C step & hold 0.3°C ramp	75 °C → 90 °C step & hold 0.3°C ramp

Efficiency (%)		
D5	89.5	96.8
D7	88.7	94.6
D10	89.6	94.2

95% LOD [CI] (GE/PCR)		
D5	17.2 [9.6-47.4]	2.8 [2.2-4.2]
D7	11.1 [6.1-30.8]	2.6 [2.0-4.1]
D10	13.3 [8.0-30.5]	2.4 [1.8-3.5]

Applying dqPCR to Non-invasive Prenatal Testing for the Prediction of Fetal RhD Type

The results presented in this section are from experiments related to the hypothesis that dqPCR can accurately predict fetal RhD type at all gestational ages. A pilot study and comparative analysis of PCR efficiencies and limits of detection for the two protocols were carried out in advance of applying dqPCR to the full set of clinical prenatal samples.

NIPT pilot study

The purpose of the NIPT pilot study was to obtain information that would aid in determining which of the dqPCR protocols to utilize for the full clinical study. The general approach was to run a subset of the clinical samples (n=20) using both protocols. Of the 20 samples tested in the pilot study, cord results were obtained for 15. Of the 15, nine were D-positive and six were D-negative.

Whole blood dqPCR

The whole blood PCR reaction patterns, RhD predictions, gestational age at the time of prenatal sample collection and cord blood RhD phenotype results for the 15 samples are shown in Table 31. Five samples had positive reactions with four having only a single positive reaction out of the nine replicates. The fifth sample had two positive reactions, both for the same *RHD* target (exon 10). There were no samples with positive reactions for more than one target.

Contingency tables for Algorithm 1 (Table 32 and Table 33) and Algorithm 2 (Table 34 and Table 35) reveal that neither algorithm correctly identified any samples for which the cord blood phenotype was D-positive regardless of gestational age subgroup. A single sample was predicted to have a positive fetal RhD type and only by Algorithm 2. The cord phenotype for this sample was D-negative.

Table 31: Results table for the whole blood dqPCR arm of the NIPT pilot study sorted by gestational age at the time of sample collection.

Sample	Number of positive reactions D5	D7	D10	ALG 1 RhD prediction	ALG 2 RhD prediction	Gestational Age (weeks)	Cord Rh Type
N002	1	0	0	NEG	NEG	8.9	POS
N023	0	0	0	NEG	NEG	10.7	POS
N011	1	0	0	NEG	NEG	10.9	NEG
N029	0	0	2	NEG	POS	22.9	NEG
N168	0	0	1	NEG	NEG	23.0	POS
N160	0	0	0	NEG	NEG	24.7	NEG
N145	0	0	0	NEG	NEG	25.0	POS
N032	0	0	0	NEG	NEG	27.3	POS
N024	0	0	0	NEG	NEG	28.7	POS
N025	0	0	0	NEG	NEG	29.3	NEG
N018	1	0	0	NEG	NEG	29.7	POS
N007	0	0	0	NEG	NEG	30.3	POS
N092	0	0	0	NEG	NEG	30.4	POS
N103	0	0	0	NEG	NEG	30.7	NEG
N101	0	0	0	NEG	NEG	35.0	NEG

Table 32: Contingency table for NIPT pilot study comparing whole blood dqPCR fetal RhD prediction (based on interpretation Algorithm 1) and cord blood RhD phenotyping for all gestational ages.

		Cord Rh Phenotype		
		Positive	Negative	Total
Whole blood dqPCR	Positive	0	0	0
	Negative	9	6	15
	Total	9	6	15

Table 33: Contingency table for NIPT pilot study comparing whole blood dqPCR fetal RhD prediction (based on interpretation Algorithm 1) and cord blood RhD phenotyping for gestational ages of ≥ 27 weeks.

		Cord Rh Phenotype		
		Positive	Negative	Total
Whole blood dqPCR	Positive	0	0	0
	Negative	5	3	8
	Total	5	3	8

Table 34: Contingency table for NIPT pilot study comparing whole blood dqPCR fetal RhD prediction (based on interpretation Algorithm 2) and cord blood RhD phenotyping for all gestational ages.

		Cord Rh Phenotype		
		Positive	Negative	Total
Whole blood dqPCR	Positive	0	1	1
	Negative	9	5	14
	Total	9	6	15

Table 35: Contingency table for NIPT pilot study comparing whole blood dqPCR fetal RhD prediction (based on interpretation Algorithm 2) and cord blood RhD phenotyping for gestational ages of ≥ 27 weeks.

		Cord Rh Phenotype		
		Positive	Negative	Total
Whole blood dqPCR	Positive	0	0	0
	Negative	5	3	8
	Total	5	3	8

Plasma dqPCR

The plasma dqPCR reaction patterns, RhD predictions, and corresponding cord blood RhD phenotype results for the 15 samples are shown in Table 36. There were nine samples with positive reactions, of which six had positive reactions in more than one *RHD* target.

Contingency tables for Algorithm 1 (Table 37 and Table 38) reveal that, irrespective of the gestational age, the algorithm failed to correctly identify samples for which the cord phenotype was D-positive, although several of the samples had positive reactions. For Algorithm 2, six of the nine D-positive cord blood phenotypes were correctly predicted by plasma dqPCR (Table 39) with four of them belonging to the subset of samples with gestational ages of 27 weeks or greater (Table 40).

Table 36: Results table for the plasma dqPCR arm of the NIPT pilot study sorted by gestational age at the time of sample collection.

Sample	Number of positive reactions D5	D7	D10	ALG 1 *RHD* prediction	ALG 2 *RHD* prediction	Gestational Age (weeks)	Cord Rh Type
N002	1	1	1	INDET	POS	8.9	POS
N023	2	3	0	INDET	POS	10.7	POS
N011	0	0	0	NEG	NEG	10.9	NEG
N029	0	0	1	NEG	NEG	22.9	NEG
N168	0	0	0	NEG	NEG	23	POS
N160	0	0	0	NEG	NEG	24.7	NEG
N145	0	1	1	NEG	NEG	25	POS
N032	0	0	0	NEG	NEG	27.3	POS
N024	1	1	0	NEG	POS	28.7	POS
N025	0	0	1	NEG	NEG	29.3	NEG
N018	2	2	0	INDET	POS	29.7	POS
N007	1	1	1	INDET	POS	30.3	POS
N092	0	2	0	INDET	POS	30.4	POS
N103	0	0	0	NEG	NEG	30.7	NEG
N101	0	0	0	NEG	NEG	35	NEG

Table 37: Contingency table for NIPT pilot study comparing plasma dqPCR fetal RhD prediction (based on interpretation Algorithm 1) and cord blood RhD phenotyping for all gestational ages.

		Cord Rh Phenotype		
		Positive	Negative	Total
Plasma dqPCR	Positive	0	0	0
	Negative	4	6	10
	Indeterminate	5	0	5
	Total	9	6	15

Table 38: Contingency table for NIPT pilot study comparing plasma dqPCR fetal RhD prediction (based on interpretation Algorithm 1) and cord blood RhD phenotyping for gestational ages of ≥ 27 weeks.

		Cord Rh Phenotype		
		Positive	Negative	Total
Plasma dqPCR	Positive	0	0	0
	Negative	2	3	5
	Indeterminate	3	0	3
	Total	5	3	8

Table 39: Contingency table for NIPT pilot study comparing plasma dqPCR fetal RhD prediction (based on interpretation Algorithm 2) and cord blood RhD phenotyping for all gestational ages.

		Cord Rh Phenotype		
		Positive	Negative	Total
Plasma dqPCR	Positive	6	0	6
	Negative	3	6	9
	Total	9	6	15

Table 40: Contingency table for NIPT pilot study comparing plasma dqPCR fetal RhD prediction (based on interpretation Algorithm 2) and cord blood RhD phenotyping for gestational ages of ≥ 27 weeks.

		Cord Rh Phenotype		
		Positive	Negative	Total
Plasma dqPCR	Positive	4	0	4
	Negative	1	3	4
	Total	5	3	8

Comparison of whole blood and plasma NIPT pilot study results

To facilitate comparison, the contingency table data from both arms of the NIPT pilot study were utilized to create Figure 37 and Figure 38. Regardless of the interpretation algorithm, there were more false negative results with WB dqPCR than with PL dqPCR. The lowest number of false negatives occurred in the ≥27 weeks' gestation subgroup tested by PL dqPCR (Figure 38, panel B).

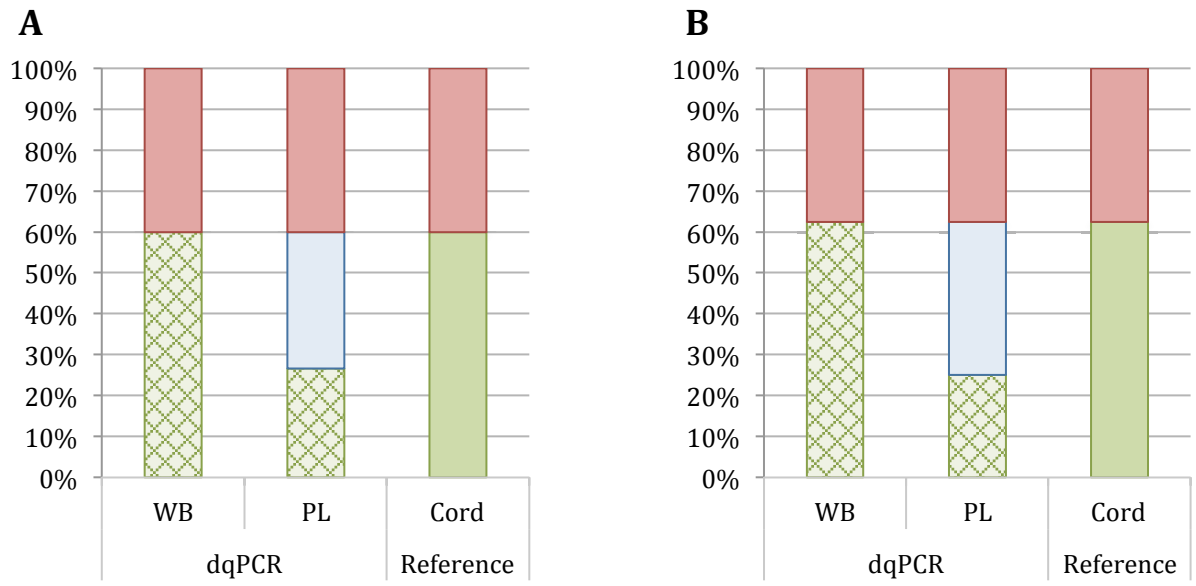

Figure 37: Comparison of the number of positive (green), negative (red), false positive (red crosshatch), false negative (green crosshatch) and indeterminate (blue) fetal RhD type predictions (**algorithm #1**) by WB and PL dqPCR to cord blood phenotype results for all gestational ages (panel A) and the ≥27 weeks' gestation subgroup (panel B).

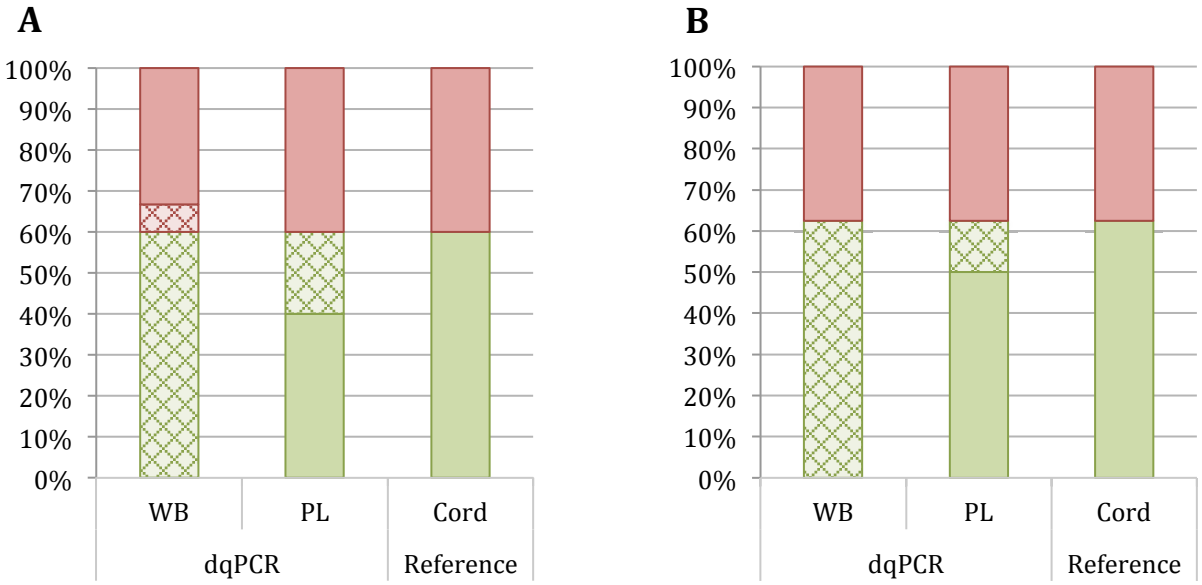

Figure 38: Comparison of the number of positive (green), negative (red), false positive (red crosshatch), and false negative (green crosshatch) fetal RhD type predictions (**algorithm #2**) by WB and PL dqPCR to cord blood phenotype results for all gestational ages (panel A) and the ≥27 weeks' gestation subgroup (panel B).

Comparison of reaction efficiency and LOD for PL dqPCR and WB dqPCR

In determining which dqPCR protocol to use for the remainder of the perinatal samples, direct comparisons were made using data from PCR efficiency and limit of detection experiments. Figure 39 and Figure 40 compare PCR efficiency and limit of detection, by target, for WB dqPCR and PL dqPCR and were prepared from data collected in previously described experiments. PCR efficiencies were similar for the two protocols; however, the limits of detection appear to be quite different, with PL dqPCR values being lower as well as having tighter confidence intervals than WB dqPCR.

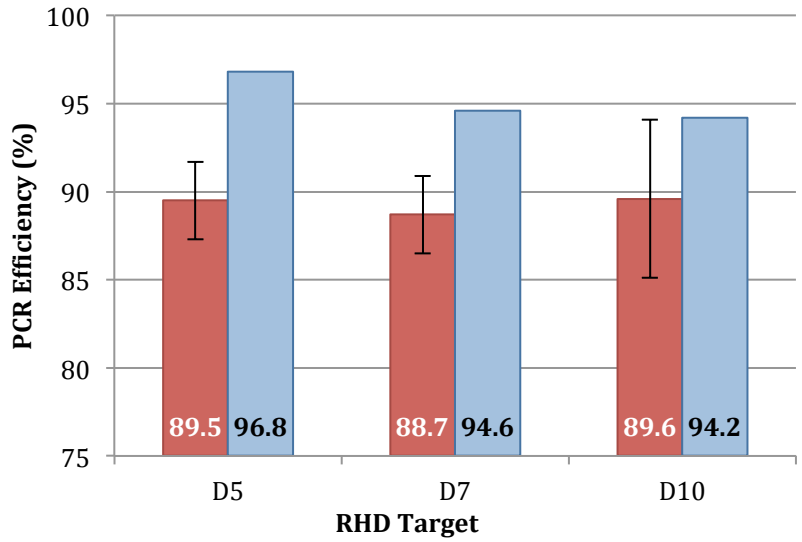

Figure 39: Comparison of reaction efficiencies for whole blood (red) and plasma (blue) dqPCR. Data for WB dqPCR depicts the mean PCR efficiency observed for three standard curve replicates and error bars show the standard deviation. PL dqPCR is for a single standard curve.

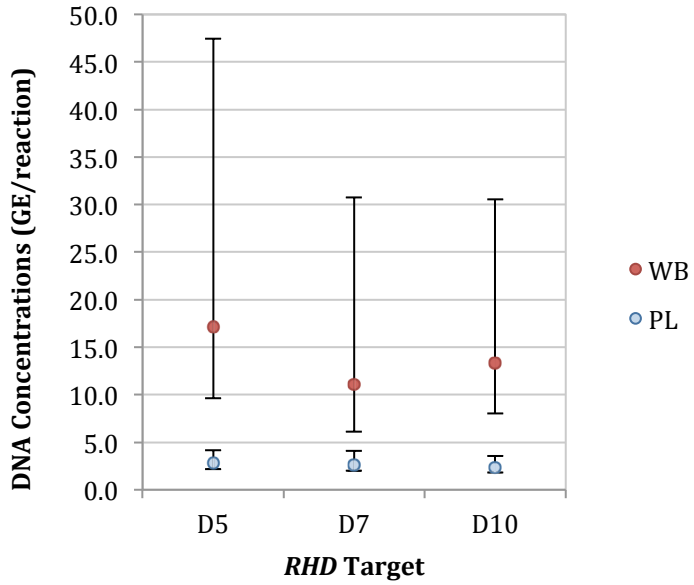

Figure 40: Comparison of limits of detection (95% LOD) for whole blood (red) and plasma (blue) dqPCR. Error bars depict the upper and lower limits of the 95% confidence intervals.

Plasma dqPCR NIPT study

The clinical NIPT study was the final experiment of this project. Of the 205 samples tested, cord blood RhD phenotype results were obtained for 177, of which 109 were D-positive and 68 were D-negative. For the subset of samples collected at ≥ 27 weeks gestation (n = 81), cord blood phenotypes were D-positive for 47 and 34 were D-negative. Figure 41 shows the distribution of gestational age at time of sample collection of the samples for which cord results were obtained.

Considering the entire sample set, 13.8% of D-positive and 95.6% of D-negative cord samples were correctly predicted using Algorithm 1 (Table 41). For the subset of samples drawn at ≥ 27 weeks gestation, the RhD prediction made using Algorithm 1 was correct for all D-negative cord bloods samples and the proportion of correct predictions for D-positive cord blood samples increased to 17.0% (Table 42). With Algorithm 2, 78.5% of D-positive cord bloods and 78.9% D-negative cord bloods were correctly predicted overall (Table 43). The percentage of correct RhD type predictions increase to 84.6% and 84.0% for D-positive and D-negative cord bloods for the subset of prenatal samples collected at ≥ 27 weeks gestation (Table 44). Figure 42 compares the two interpretation algorithms. Table 45 shows the sensitivity, specificity, and other analytical performance measures for both interpretation algorithms.

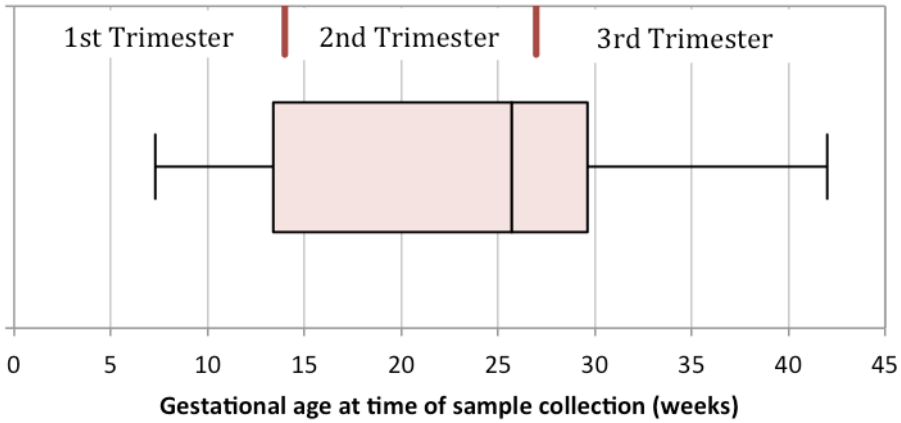

Figure 41: Gestational age distribution of samples included in the NIPT study (n=177).

Table 41: Contingency table NIPT study comparing plasma dqPCR fetal RhD prediction (based on Algorithm 1) and cord blood RhD phenotyping for all gestational ages.

		Cord Rh Phenotype		
		Positive	Negative	Total
Plasma dqPCR	Positive	15	0	15
	Negative	53	65	118
	Indeterminate	41	3	44
	Total	109	68	177

Table 42: Contingency table NIPT study comparing plasma dqPCR fetal RhD prediction (based on Algorithm 1) and cord blood RhD phenotyping for gestational ages of ≥ 27 weeks.

		Cord Rh Phenotype		
		Positive	Negative	Total
Plasma dqPCR	Positive	8	0	8
	Negative	17	34	51
	Indeterminate	22	0	22
	Total	47	34	81

Table 43: Contingency table NIPT study comparing plasma dqPCR fetal RhD prediction (based on Algorithm 2) and cord blood RhD phenotyping for all gestational ages.

		Cord Rh Phenotype		
		Positive	Negative	Total
Plasma dqPCR	Positive	84	14	98
	Negative	25	54	79
	Total	109	68	177

Table 44: Contingency table NIPT study comparing plasma dqPCR fetal RhD prediction (based on Algorithm 2) and cord blood RhD phenotyping for gestational ages of ≥ 27 weeks.

		Cord Rh Phenotype		
		Positive	Negative	Total
Plasma dqPCR	Positive	39	6	45
	Negative	8	28	36
	Total	47	34	81

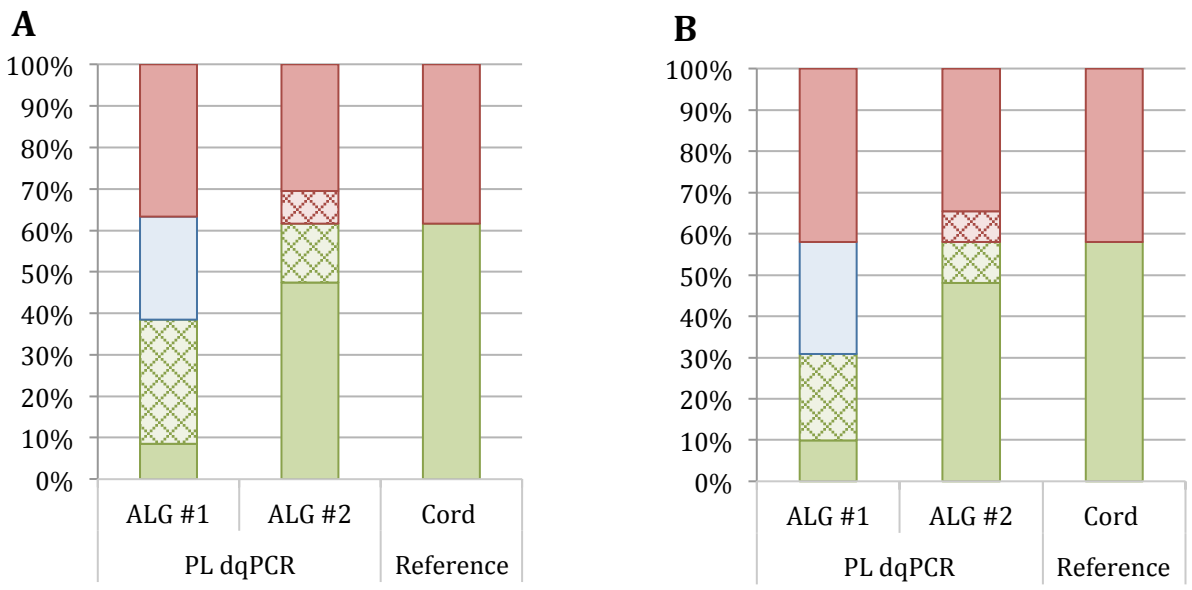

Figure 42: Plasma dqPCR NIPT study. Comparison of the number of positive (green), negative (red), false positive (red crosshatch), false negative (green crosshatch) and indeterminate (blue) fetal RhD type predictions by PL dqPCR using the two interpretation algorithms to cord blood phenotype results for all gestational ages (panel A) and the ≥27 weeks' gestation subgroup (panel B).

Table 45: Analytical performance measures for plasma dqPCR NIPT study.

	Algorithm 1		Algorithm 2	
Parameter	**all gest. ages**	**≥ 27 weeks**	**all gest. ages**	**≥ 27 weeks**
Sensitivity	0.14	0.17	0.77	0.83
Specificity	0.96	1.00	0.79	0.82
Accuracy	0.45	0.52	0.78	0.83
False Positive Rate	0.04	0.00	0.21	0.18
False Negative Rate	0.86	0.83	0.23	0.17
Positive Predictive Value	0.83	1.00	0.86	0.87
Negative Predictive Value	0.41	0.47	0.68	0.78

Chapter 4: Discussion

Though not routinely available in Canada, RHD NIPT is used in a number of regions world wide for fetal RhD type prediction to assess the risk of HDFN or to determine maternal eligibility for RhIg prophylaxis. It is possible that cost and protocol complexity contribute to slow adoption of the method; however, dqPCR can simplify the testing protocol by eliminating the DNA extraction step and its associated costs. The aim of this thesis was to investigate the hypothesis that dqPCR using maternal blood from D-negative women could accurately predict fetal RhD type at or before 28 weeks gestation. In this chapter, I explore and discuss the results and their significance. The chapter is divided into two main sections. In the first, I focus on experimental outcomes for each of the specific research aims (SRA) listed in Chapter 1. The second section is a broader discussion of the research.

Discussion of the Specific Research Aims

SRA A-1: Investigating the impact of sample matrix on whole blood dqPCR

In general, PCR using extracted DNA is approached with the aim of eliminating inhibition. With dqPCR, inhibitory substances present in the sample are an inherent part of the reaction mixture, necessitating investigation of their impact on the reaction. Hemoglobin is of special concern due to its optical properties and the natural variation observed in samples submitted to the laboratory for transfusion related testing. Dilution and interference studies were performed to investigate the impact of hemoglobin on dqPCR.

The purpose of the dilution studies was to explore any impact that hemoglobin variation might have on whole blood dqPCR. The two dilution approaches were chosen for specific reasons. The plasma dilution series was meant to mimic the situation that exists in patients with varying degrees of clinical anemia. In these patients, hemoglobin levels can be quite low, but plasma constituents are usually normal. Dilution with water, while attaining similar hemoglobin levels as dilution with plasma, dilutes plasma constituents as well. Therefore the water dilution series cannot be considered an appropriate mimic of clinical samples from anemic patients. Instead, it acts as a comparison for the plasma dilution series.

The decrease in peak derivative fluorescence observed with increasing Hb concentration (Figure 4) could be related to the greater opacity of the reaction mixture with higher Hb concentrations.

Another possibility is that inhibition may still be occurring. The lower C_q results seen with lower Hb concentrations (Figure 6) suggest that higher Hb concentrations may be inhibiting the reaction. Indeed, a commonly suggested approach to confirm suspected inhibition in PCR is to test the sample using a 10-fold dilution, the assumption being that dilution reduces the effect of the inhibitor resulting in higher C_q values. This is precisely the effect observed in the WB dqPCR water dilution series.

To investigate the effects observed in the dilution studies, I performed interference studies looking for any interactions that might be occurring between DNA, the reporter dye, and the samples matrix (represented by Hb). The SG-Hb interactions observed in the interference study agree with the dilution study observations; the same inverse relationship between Hb concentration and T_m was observed in both. The interference study showed that the effect was greater with higher SG concentrations. This observation highlights the need for optimized SG concentrations in WB dqPCR protocols. Although Taylor et al. found that 40x SG was optimal for their protocol targeting *Plasmodium spp*.[100], perhaps the optimal SG concentration isn't universal for all OmniKlentaq reactions, but rather depends on the target or other factors.

Due to the interaction between SG and Hb, I investigated an alternative dye to determine if the effect was unique to SG. With absorption and emission peaks at 500 nm and 530 nm, respectively[105], EvaGreen is spectrally similar to SG, allowing its use with the StepOne system. The data indicate that EvaGreen may be a viable alternative to SYBR Green I and other researchers have reported sharper, stronger melt peaks and lower T_m with EvaGreen[105]. Such an approach may require custom calibration and may not be an option available with all qPCR instruments. A probe-based assay would eliminate the problem entirely, however this approach cannot be used with OKT polymerase as the enzyme, like all klentaq fragment polymerases, lacks the required exonuclease activity.

While I interpreted my experiments in terms of Hb level, other sample constituents could contribute to the observed T_m shift. Both plasma and water dilutions showed the same pattern of T_m shift, suggesting that the effect is related to the cellular fraction of the sample. It is known that salts, particularly monovalent cations, affect T_m[106-108] and red blood cells contain sodium and potassium[109]. Whether they contain enough salts to contribute to the observed effect is unknown. The fact that EvaGreen reactions do not show a T_m shift in relation to sample dilution suggests that the effect is more complicated than simple changes in salt concentration. As with T_m, the observed statistical

interaction between Hb and SG may actually be due to the dye interacting with another constituent of whole blood. As SG is known to inhibit PCR and affect T_m when used in high concentrations[110], it is possible that both the effect I observed on T_m and the dye interaction are characteristics of SG dye itself. Further study is needed to determine the mechanism leading to these observations.

The inverse relationship between T_m and Hb concentration that was observed in the dilution study (Figure 5) and the interaction between SG and Hb in the interference study (Figure 7) suggest that the use of T_m to verify the correct PCR product may be problematic, depending upon the range of hemoglobin encountered for the specific application of whole blood dqPCR. The ability of an assay to identify the correct product, or the presence of an unexpected one, is important in transfusion medicine as many of the blood group system genes have a significant number of variant alleles with altered antigen expression.

To address the sample-dependent effect on T_m, I explored the use of an amplicon control, wherein known product sequences are added to a reaction with the unknown sample. The T_m of this control reaction then becomes the comparator for all reactions with the same sample. All but one of the target/Hb combinations that were tested showed agreement between the amplicon control and the unknown reactions. I suspect that the statistical difference seen in the 50% Hb level for exon 7 is due to the low number of replicates and that this difference would disappear with a full work up.

A significant drawback to this approach, as seen in the WB dqPCR/DNA qPCR comparison study (Discussion SRA A-3), is the potential for cross contamination that exists with the use of previously amplified product. An alternative approach might be to empirically establish T_m ranges for a number of Hb ranges, tying T_m analysis directly to the Hb concentration of the particular sample being tested. Dilution study data (Figure 5) suggests that patient samples with Hb of ≥110 g/L should have a different T_m range that patient samples with Hb less than 100 g/L. Precisely where the cut-offs should be between Hb ranges and what, if any, overlap there might be in T_m ranges is unknown.

SRA A-2: Determining PCR efficiency and limit of detection of whole blood dqPCR

Efficiency is important for dqPCR because the concentration of inhibitory substances in blood, such as hemoglobin, can vary from person to person and from sample to sample for a given individual. The Hb levels I chose for evaluation of reaction efficiency, 100%, 70% and 50%, are representative

of clinically normal Hb, mild to moderate anemia and severe anemia respectively. Given that the dilution studies suggested the presence of residual inhibition related to the HB concentration in the reaction, it may be somewhat surprising that reaction efficiencies were not statistically different; however, Figure 13 shows that the entire standard curve shifts downward, with minimal changes to the slope, as the Hb concentration decreases. The small variation in slope explains the lack of differences in efficiency and makes sense, as any inhibition would be expected to be relatively constant for a given Hb concentration.

The range of PCR reaction efficiencies that were observed, 87% to 92% for all *RHD* targets, falls at the lower end of the generally acceptable range of 90-110% and could be attributed to the inhibitory effect of high SG concentrations[110]. The efficiency results were slightly higher than the 84% reported by Taylor et al.[100] for a malaria target using OKT polymerase and PEC. Comparing dqPCR results to efficiencies of traditional qPCR for *RHD* is difficult due to a dearth of information in literature. This may be because qPCR in transfusion medicine is most often used for assays that identify the presence or absence of the blood group genes and thus predict the expression of the corresponding antigen on the red blood cells. Using qPCR like this is akin to endpoint PCR without having to perform electrophoresis. I expect to see more reports of PCR reaction efficiencies in blood group genotyping as compliance with MIQE guidelines[111] increases. The efficiencies obtained for *RHD* exon 5 and exon 7 were comparable to those reported by Javadi et al.[112] using the same exon 5 primers and exon 7 primers with very little difference in sequence. I was unable to find any literature that reported efficiencies for *RHD* exon 10 reactions.

OmniKlentaq polymerase is marketed as being inhibitor resistant and appropriate for a number of "dirty" sample types; however, that does not mean that 100% function is attained at all or any concentrations of the various inhibitors that may be present in such samples. The potential for residual inhibition combined with patient-to-patient and sample-to-sample variability draws attention to a significant limitation of PCR analysis using the StepOne instrument software. With the StepOne system, PCR efficiency can only be determined at the assay level, using standard curves. This commonly used approach assumes that all amplifications occur with the same efficiency as the standard curve predicts, which is unlikely to be the case for dqPCR reactions, given the complexity of the sample matrix. Although less of an issue for presence/absence assays such as those used in this thesis, quantitative dqPCR assays would likely benefit from an analysis approach that included determination of efficiency for individual reactions and employed a method to normalize

amplification plots to facilitate comparison of reactions with different efficiencies. Such an approach would likely be of benefit when determining limits of detection as well.

Limit of detection is important to consider for non-invasive prenatal testing by dqPCR because cell-free fetal DNA makes up a very small portion of the DNA in maternal circulation. With the addition of maternal cellular DNA, the amount of cell-free fetal DNA in maternal whole blood is less than the 6-10% reportedly present in maternal plasma[113]. It is difficult to compare the LOD for dqPCR to reported concentrations of cell-free fetal DNA as they are reported in terms of fetal DNA in maternal plasma. However, for quantification of circulating fetal DNA by TaqMan PCR, Zimmerman et al.[114] suggest that 95% LOD should be approximately 4-10 target copies per reaction. Although the LOD results obtained were not in this range, increasing the volume of sample added to each reaction and using plasma instead of whole blood may improve out LODs without losing the benefits of dqPCR.

SRA A-3: Comparing whole blood dqPCR, DNA qPCR, and serologic RhD phenotyping

To be useful in a clinical setting, blood typing predictions made by dqPCR must agree with those obtained by other methods, particularly serologic phenotyping, which is considered the gold standard in transfusion medicine. A caveat to such a comparison is that variant phenotypes, especially those known to give discrepant results with different serologic reagents, will contribute to discrepancies between molecular methods and phenotyping. Nevertheless, method comparison is a vital part of validating a new testing technique. Ideally, a full validation should include variant phenotypes as well as "normal" samples; the small number of samples available for the WB dqPCR/DNA qPCR method comparison did not include any D variants.

Although proposed as a method to evaluate the agreement for categorical data derived from different observers[115], American Clinical Laboratory Improvement Amendments (CLIA) regulations suggest the use of kappa statistics for method comparison studies during validation and verification of laboratory-developed tests[116]. In general, kappa values of 1, -1, and 0 indicate perfect agreement, no agreement, and agreement due to chance alone, with further interpretation of the quality of agreement being somewhat subjective (Table 46). According to McHugh[117], kappa values (Table 23 & Table 27) indicate almost perfect agreement between whole blood dqPCR and DNA PCR for each *RHD* target as well as RhD type prediction.

Table 46: Interpretations of kappa statistic

Value of κ	Quality of agreement	Value of κ	Quality of agreement	Value of κ	Quality of agreement
< 0.00	Poor			< 0.20	Poor
0.00 - 0.20	Slight	0 - 0.20	None		
0.21 - 0.40	Fair	0.21 - 0.39	Minimal	0.21 - 0.40	Fair
0.41- 0.60	Moderate	0.40 - 0.59	Weak	0.41- 0.60	Moderate
0.61 - 0.80	Substantial	0.60 - 0.79	Moderate	0.61 - 0.80	Good
0.81 - 1.0	Almost Perfect	0.80 - 0.90	Strong	0.81 - 1.0	Very Good
		> 0.90	Almost Perfect		
Source	Landis & Koch[115]	Source	McHugh[117]	Source	Kwiecien et al.[118]

False positive and false negative reactions are a concern because, instead of providing clarification, false reactions could further complicate the interpretation of serologic blood typing discrepancies. With specificity of 91.3%, CI(79.3, 103.3), the margin of error for whole blood dqPCR RhD prediction is 12%. Hess et al. point out that there is no consensus on what constitutes an acceptable margin of error for sensitivity and specificity and guidelines for reporting these values in medical literature do not exist[103]. However, this margin of error seems high and I had expected the specificity to be higher.

Investigation of the two unresolved indeterminate whole blood dqPCR RhD predictions discovered identical patterns of positive reactions. Both were unequivocally negative for D5 and D10 but all three D7 replicates were positive. Given the complexity of *RHD* genetics, the observed pattern could be due to an unexpected D-negative variant. However, such variants are rare and finding two in a sample set of 60 would be unlikely. Because many of the samples used for this comparison were also used for other experiments, contamination is most likely the cause of the false positive reactions. Further investigation revealed that both samples were used on the same day that previously amplified D7 PCR product was used in an amplicon control experiment. Contamination of the whole blood samples with D7 amplicon would explain both the reaction pattern and why these two specific samples were affected. Omitting the contaminated samples from analysis, specificity and accuracy become 100% and all kappa values become 1.000. For this small comparison, WB dqPCR performed as well as DNA qPCR for prediction of RhD type.

SRA B-1: Modifying the whole blood dqPCR protocol for use with plasma samples

In developing the plasma dqPCR protocol, I opted to begin with a simple substitution of reagents and sample type into the whole blood dqPCR protocol. The manufacturer of OKT reagents recommends the use of PEC-2 for plasma dqPCR applications but the differences between PEC-1 and PEC-2 are not explicitly disclosed. Examination of the material safety data sheets (MSDS) for the enhancer cocktails indicates that PEC-2[119] contains a very small amount of heparin sodium salt that is not listed on the MSDS for PEC-1[120]. Heparin is generally considered to inhibit PCR [121]; however, it has been shown to reduce the inhibitory effect of IgG and lactoferrin in direct PCR while having no effect on inhibition due to hemin[99], thus explaining the difference in recommended PEC formulations for PCR reactions containing unprocessed whole blood and plasma.

One of the goals of the first trial of plasma dqPCR was to assess the options for analysis settings (i.e. baseline and threshold). When the StepOne software was set for automatic baseline, the results were unpredictable, seemingly due to the "ramp up" effect seen in the first several cycles. This resulted in inconsistent amplification plots for identical samples, especially negative samples, where the entire amplification plots for some D-negative samples were above the threshold (Figure 17). The basic assumption of setting the baseline is that there is little or no change in fluorescent signal during the early stages of PCR. While the assumption holds true for WB dqPCR (Figure 19), it does not for PL dqPCR (Figure 17 and Figure 18). Even the default manual baseline setting (cycles 3 - 15), was insufficient to bypass the "ramp up" effect seen in PL dqPCR amplification plots. For these reasons, automatic baseline setting was not used for subsequent PL dqPCR experiments.

The development of the PL dqPCR protocol proceeded as a series of optimization experiments. Since hemoglobin was no longer a factor, it seemed reasonable that the concentration of the SYBR Green reporter dye could be reduced and that doing so might reduce or eliminate the "ramp up" effect observed in the initial PL qdPCR experiment. The melt temperature shift noted with different SG concentrations (Figure 21) was expected, but given that all D-positive reactions in the initial PL dqPCR experiment showed amplification, the lack of amplification in the 40x SG reactions in the dye titration experiment was surprising. The data revealed an inverse relationship between SG concentration and C_q value, while the magnitude of the fluorescent signal was directly related to SG concentration. At first glance, this would suggest that higher SG concentrations would be better, however, as seen with WB dqPCR, greater SG concentration contributes to a T_m increase. SG is also known to inhibit PCR at higher concentrations. Despite the inhibitor resistant nature of the

reagents used in this project, it seemed pertinent to reduce inhibitors where possible. Thus, optimization of SG concentration meant balancing the positive effects of higher amounts of SG (higher fluorescent signal and lower C_q values) with the negative (T_m bias). The relatively small T_m shift observed for 2.5x and 5x SG concentrations (up to 2 °C positive bias when compared with T_m for 1x SG) while T_m were shifted by as much as 5 °C for 20x SG reactions suggested that the optimum SG concentration, with respect to T_m, fell between 1x and 5x SG. I opted to proceed using 5x SG.

Sample volume was the next factor that I investigated in the development of the PL dqPCR protocol. Without the contribution from white blood cells, plasma has less DNA than whole blood. In the context of dqPCR, which lacks the concentrating effect of DNA extraction, the only way to increase the amount of target DNA is to increase the amount of sample added to each reaction. The combination of OmniKlentaq polymerase and a PCR enhancement cocktail has been shown to allow amplification with unprocessed sample accounting for as much as 25% of the reaction mixture[99]. I approached this experiment by adding the maximum sample volume possible, 25.5%, which was determined by the concentrations of the various PCR reagents and the volume required to bring the reaction volume to 10 µL. Amplification was observed at the higher sample volume, though the use of single reactions meant that statistical comparison was not possible. Despite this, I chose to continue the protocol development using the high sample volume because of the theoretical advantage of greater target DNA molecules.

The purpose of the second dye titration experiment was two fold. First, I wanted to confirm that 5x SG was still appropriate with the increased sample volume. An additional aim was to investigate the possibility that EvaGreen could be used instead. Although the melt curves for EG reactions (Figure 25) appear to be better defined than those for SG (Figure 24), particularly at 10x, the gradual and sustained increase in background fluorescence observed in EG reactions (Figure 30) suggest that EG may not be the best reporter dye for PL dqPCR. With baseline setting applied to avoid the "ramp up" region of the curves, the EG amplification plots take on an overall convex shape (Figure 28), which shifts the positive plots downward, likely contributing to the higher C_q values observed for EG reactions compared to SG reactions (Figure 26 panel A). When the same baseline settings are applied to SG amplification plots, the region of the curves beyond the 8-cycle "ramp up" remains relatively flat (Figure 27), though a very slight gradual increase in background fluorescence was also observed (Figure 29).

Although EG has been shown to be superior to SG in qPCR using extracted DNA[110], little is known about the behaviour of either dye in the context of dqPCR. However, a full characterization of the dyes was not necessary to determine which was most appropriate for PL dqPCR. With the goal of applying dqPCR to non-invasive fetal RhD type prediction, anything that might artificially increase C_q values has the potential to negatively impact the LOD of the assay; therefore, I opted to continue using SG as the reporter dye for PL dqPCR. As in the previous SG titration experiment, the optimum SG concentration was arrived at by balancing the C_q values and T_m; however, I also considered the background fluorescence. The 10x SG concentration was eliminated as an option due to wide melt peaks, high background fluorescence and large T_m bias, while the 1x concentration was eliminated because of higher C_q values. The 5x SG reactions had the lowest C_q but higher background fluorescence and T_m than reactions containing 2.5x SG. Considering all these variables, I chose 2.5x as the optimum SG concentration for PL dqPCR in reactions containing 25% plasma.

The aim of the final experiment in the development of the PL dqPCR protocol was to address the "ramp up" effect observed in the amplification plots. Without knowing the cause of the "ramp up" effect, my approach was to see if eliminating collection of the fluorescence data from the affected cycles would allow the StepOne to correctly assign baselines automatically. Even with the modified run method, the auto baseline setting resulted in erroneous C_q values (Figure 33).

Although mean C_q values for were similar for reactions with standard and modified run methods, the small sample size did not allow evaluation of the variability of the "ramp up" effect; therefore, the effect on C_q cannot be predicted. In addition, the precise way in which the baseline is applied by the StepOne software is not known (proprietary) and cannot be adjusted. As a result of these factors and the unknown cause of the "ramp up" effect, the only way to ensure the effect does not impact interpretation is to avoid collecting fluorescence data for the affected cycles. For this reason, the finalized PL dqPCR protocol uses the modified run method.

SRA B-2: Determining PCR efficiency and limit of detection of plasma dqPCR

According to Scott Adams, a perfect PCR assay has "a slope of -3.32 (100% efficiency), a y-intercept between 33 and 37 cycles and an r^2 of 1.00" [122]. In such an assay, the amplification factor is 2.00, indicating that the amount of product doubles with each cycle. With slopes, R^2 values and amplification factors close to the ideal (Figure 35), PL dqPCR appears to be a good assay, although the y-intercepts are low. Scott Adams attributes high y-intercepts to underestimation of target

quantity, possible due to template degradation but doesn't specifically address low y-intercepts[122]. One might logically determine that, if high y-intercepts indicate underestimation, that low y-intercepts would signal overestimation.

But is PL dqPCR truly prone to overestimation of target quantity? Scott Adams bases y-intercept on the detection limit of free FAM[122], a reporter dye commonly used in probe-based PCR assays. If y-intercept is related to properties of the reporter dye and the signal detection system in the qPCR analyzer, then it's possible that the comparatively low y-intercepts observed with PL dqPCR are not indicative of erroneous quantification. Rather, they could be a result of unique interactions between sample matrix and SYBR Green I, which is used as significantly higher concentrations in PL dqPCR than are normally used with DNA-based assays. For this thesis, the question of incorrect quantification might be considered mute, as dqPCR was applied in a presence/absence assay instead of a quantitative one. A more significant concern might be the potential for stochastic results, due to the interplay of LOD and cffDNA concentration, when dqPCR is applied to RhD NIPT.

For PL dqPCR, 95% LOD estimates for all three targets, ranging from 2.4 to 2.8 GE/PCR (Figure 36), translate to 960-1120 GE/mL of plasma. Comparing the LOD to reported concentrations of cffDNA in maternal plasma is difficult because there is disagreement about the concentration partially due to variations in testing platforms (qPCR vs microfluidic digital PCR) and the impact of cffDNA fragmentation on differences in PCR product length. The cffDNA concentrations, as determined by qPCR, were 3.3-69.4 GE/mL of maternal plasma (mean 25.4) in early pregnancy, while concentrations in late pregnancy were 76.9-769 GE/mL (mean 292.2)[113]. Considering these values, one would expect PL dqPCR to be ineffective at detecting cffDNA. However, cffDNA concentrations were approximately twice as high when measured by microfluidic digital PCR[123]. Sikora et al. reasoned that the differences seen with the two quantification methods might be related to the size of the PCR product, as they observed higher concentrations with shorter products and attributed the finding to the fragmented nature of cffDNA[124]. This could potentially impact the application of dqPCR, either plasma or whole blood, to RhD NIPT because the exon 7 product is approximately 40 bp longer than the other two products, which is similar to the difference in product lengths of the qPCR (137 bp[124]) and microfluidic digital PCR (87 bp[123]). In terms of a presence/absence assay, it is possible that such an effect would not be noticed unless the cffDNA concentration was very close to the LOD. In this case, the patterns may be evident by negative reactions for exon 7 and positive

reactions for exons 5 and 10. Ultimately, the best way to determine whether the LOD of dqPCR is sufficient to detect cffDNA is to perform a clinical study using prenatal samples.

SRA C-1: Evaluation of whole blood and plasma dqPCR for RhD NIPT (pilot study)

The intent of the clinical pilot study was to provide information that would aid in the determining which of the dqPCR assays, whole blood or plasma, would be most appropriate for RhD NIPT. The data (Figure 37 and Figure 38) clearly illustrate the difference between whole blood and plasma dqPCR with respect to clinical application. There were fewer false negative results with PL dqPCR than with WB dqPCR, regardless of the interpretation algorithm or the gestational age subgroup. Given that the LOD and efficiencies were similar for the three targets, one would expect the number of false negative reaction to be similar; however, the total number of PL dqPCR false negative reactions for D7 (123 bp product) was 13 while D5 (82 bp product) and D10 (74 bp product) were 20 and 19, respectively (determined from Table 36). Although the sample size is very small, this seems to refute the effect of smaller PCR product size on determination of cffDNA concentration discussed earlier in this thesis, which suggests that more false negative reactions should be seen with longer PCR products.

While it's quite clear that WB dqPCR was not sensitive enough for RhD NIPT, failing to correctly predict a single RhD type regardless of the prediction algorithm, PL dqPCR performed better, correctly predicting up to 12 of the 15 RhD types depending on the prediction algorithm used.

SRA C-2: Comparing plasma and whole blood dqPCR in the context of NIPT

Although there appears to be a difference in PCR efficiency for D5 and D7 targets (Figure 39), with only one data point for PL dqPCR efficiency, statistical comparison would not be meaningful. However, if a similar magnitude of variance exists for PL dqPCR as was observed for WB dqPCR, it is possible that no statistical difference would be observed. Assuming that they are the same for the two assays, then PCR efficiency is not a helpful parameter in deciding whether one assay might be better for *RHD* NIPT.

Such is not the case for 95% LOD, where the two assays differ by approximately 10 GE/PCR for all three targets (Figure 40). With LOD that were lower and had much tighter confidence intervals, it is

not surprising that greater numbers of positive reactions were observed for PL dqPCR in the NIPT pilot study

Based on these comparisons and the NIPT pilot study, PL dqPCR appears to be the better of the two methods for NIPT.

SRA C-3: To compare dqPCR performed on clinical prenatal samples to cord blood RhD phenotyping

In the RhD NIPT clinical study, agreement between cord blood phenotypes and PL dqPCR RhD type predictions was dependent upon the interpretation algorithm (Figure 42). With algorithm 1, the specificity was near 100% overall and for the ≥27 weeks' gestation subgroup, while the sensitivities were less than 20%. Comparatively, sensitivity and specificity were near 80% for algorithm 2 regardless of the gestational age grouping.

By requiring at least one positive reaction for each target, algorithm 1 resulted in greater specificity for RhD type predictions, but there were more false negative and indeterminate predictions. While algorithm 2 resulted in fewer false negative RhD type predictions, the ability of the assay to differentiate common non-functional *RHD* alleles from the standard D-positive gene sequence was lost.

This study highlighted the importance of the prediction algorithm. Although I was unable to find any published guidelines for determining interpretation algorithms for presence/absence PCR assays based on multiple targets, the choice of algorithm for RhD type prediction should be approached in the context of the population being tested as well as the purpose of testing. For populations in which the frequency of non-functional alleles is high, retaining the additional specificity afforded by an algorithm similar to algorithm 1 will be important. Failing to detect the presence of non-functional alleles may lead to higher than expected false positive rates for RhD type predictions.

False positive and false negative rates are important to consider when placing the RhD type prediction algorithm in the context of testing purpose. If determining RhIg prophylaxis eligibility, false negatives would result in patients not receiving RhIg when they need it, increasing the risk of alloimmunization and subsequent development of HDFN. Too many missed doses could undermine

the effectiveness of a prophylaxis program. False positive RhD type predictions would have comparatively little effect on individual patients, as they would receive the same treatment as in they would have without RhD NIPT. However, in a prophylaxis program employing RhD NIPT, too many false positives may negate the benefits of RhD NIPT, namely reduced product usage and its related costs.

If the purpose of RhD NIPT testing is to assess treatment needs for anti-D alloimmunized pregnant women, false positive results may trigger unnecessary follow up, which may include higher risk procedures such as amniocentesis or chorionic villus sampling. Beyond the impact to individual patients, excessive unnecessary follow up can increase costs to the healthcare system and the increased demand on services may impede access to services for patients that truly require them. False negative results may lead to missed or delayed identification of the need for additional follow up. This can have potentially disastrous outcomes if symptoms of HDFN go untreated. Fortunately, there are other means to assess HDFN risk for alloimmunized patients, such as maternal antibody titrations and Doppler velocimetry to identify fetal anemia[125].

Unlike HDFN risk assessment, there is no redundancy in a system that relies on RhD NIPT for determination of RhIg prophylaxis eligibility. A highly sensitive assay coupled with an RhD type prediction algorithm designed to minimize false negatives would best meet the objectives of such a program. For HDNF risk assessment, both scenarios described above are undesirable. To limit the impact of false results on anti-D alloimmunized patients, the combined effect of PCR assay and RhD type prediction algorithm should balance sensitivity and specificity.

Summary Discussion

The use of inhibitor resistant reagents in real-time PCR can eliminate the need for DNA extraction but there may be sample matrix effects not directly related to the function of the polymerase enzyme. Using Omni Klentaq polymerase and PCR Enhancement Cocktail, I demonstrated *RHD* genotyping using qPCR technology without any sample processing. I examined the effect of whole blood sample matrix on reaction efficiency and melt temperature and determined the analytical and diagnostic sensitivity for detection of three targets specific to the *RHD* gene as well as RhD type prediction. In addition, I developed a dqPCR assay using plasma in place of whole blood and evaluated its use for non-invasive fetal RhD type prediction.

While the NIPT pilot study showed that WB dqPCR is not sensitive enough for such an application, it could be used in place of DNA qPCR for donor antigen typing. In this situation, the observed melt temperature shift that occurred with lower levels of hemoglobin would not be a significant issue as the minimum hemoglobin level for donation eligibility falls above the affected range. Recipient antigen typing could also be performed using WB dqPCR if appropriate T_m ranges were established based on specific sample hemoglobin ranges. Beyond transfusion medicine, any genetic test for which the target DNA would normally come from circulating blood cells could be performed using WB dqPCR. WB dqPCR may also facilitate identification and susceptibility testing for positive blood cultures. Performing PCR for bacterial identification and sensitivity directly from the blood culture vial could eliminate the need for additional culture-based testing.

The NIPT clinical study revealed the potential of PL dqPCR for applications that target cell-free DNA, though it's clear that the sensitivity must be improved. To carry the method forward, a simple strategy to increase sensitivity would be to increase the reaction volume, thereby increasing the amount of target DNA in each reaction. Alternately, coupling inhibitor resistant reagents with a digital PCR method would offer absolute quantification of cffDNA as well as potentially improve sensitivity for RhD NIPT.

Whether testing is performed on whole blood or plasma, dqPCR is a unique approach to DNA testing in transfusion medicine and a novel approach to non-invasive fetal testing.

REFERENCES

1. Daniels G. Human blood groups. 3rd ed. Chichester: Wiley-Blackwell; 2013.
2. Clarke CA, Finn R, Lehane D, McConnell RB, Sheppard PM, Woodrow JC. Dose of anti-D gamma-globulin in prevention of Rh-haemolytic disease of the newborn. Br Med J. 1966 ;1(5481):213-4.
3. ISBT, Red Cell Immunogenetics and Blood Group Terminology Working Party. Table of blood group antigens v.5_151222.
4. Maxwell MJ, Wilson MJA. Complications of blood transfusion. Continuing Education in Anaesthesia, Critical Care & Pain. 2006;6(6):225-9.
5. Levine P, Katzin EM, Burnham L. Isoimmunization in pregnancy: Its possible bearing on the etiology of erythroblastosis foetalis. J Am Med Assoc. 1941;116(9):825-7.
6. de Haas M, Thurik FF, Koelewijn JM, van der Schoot CE. Haemolytic disease of the fetus and newborn. Vox Sang. 2015;109(2):99-113.
7. Fung Kee Fung K, Eason E, Crane J, Armson A, De La Ronde S, Farine D, et al. Prevention of Rh alloimmunization. Journal of Obstetrics & Gynaecology Canada: JOGC. 2003;25(9):765-73.
8. Watanabe KK, Busch MP, Schreiber GB, Zuck TF. Evaluation of the safety of Rh immunoglobulin by monitoring viral markers among Rh-negative female blood donors. Vox Sang. 2000;78(1):1-6.
9. Reid ME. Transfusion in the age of molecular diagnostics. Hematology. 2009:171-7.
10. Westhoff CM. Review: the Rh blood group D antigen... dominant, diverse, and difficult. Immunohematology. 2005;21(4):155-63.
11. Daniels G. Molecular blood grouping. Vox Sang. 2004;87 Suppl1:63-6.
12. Alfirevic Z, Sundberg K, Brigham S. Amniocentesis and chorionic villus sampling for prenatal diagnosis. Cochrane Database of Systematic Reviews. 2003(3).
13. Clausen FB, Christiansen M, Steffensen R, Jørgensen S, Nielsen C, Jakobsen MA, et al. Report of the first nationally implemented clinical routine screening for fetal RHD in D– pregnant women to ascertain the requirement for antenatal RhD prophylaxis. Transfusion 2012;52(4):752-8.
14. de Haas M, van der Ploeg CPB, Scheffer PG, Verlinden DA, Hirschberg H, Abbink F, et al. A nation-wide fetal RHD screening programme for targeted antenatal and postnatal anti-D. ISBT Science Series. 2012;7(1):164-7.
15. Mercier B, Gaucher C, Feugeas O, Mazurier C. Direct PCR from whole blood, without DNA extraction. Nucleic Acids Res. 1990;18(19):5908.
16. Landsteiner K, Wiener AS. An agglutinable factor in human blood recognized by immune sera for rhesus blood. Proc Soc Exp Biol Med. 1940;43:223.
17. Reid ME, Lomas-Francis C, Olsson ML. The blood group antigen factsbook. 3rd ed. Oxford: Academic Press; 2012.
18. Denomme GA. The structure and function of the molecules that carry human red blood cell and platelet antigens. Transfus Med Rev. 2004;18(3):203-31.
19. Daniels G. Rh Blood Group System. Human Blood Groups: Blackwell Science Ltd; 2007. p. 195-274.
20. Avent ND, Ridgwell K, Tanner MJ, Anstee DJ. cDNA cloning of a 30 kDa erythrocyte membrane protein associated with Rh (Rhesus)-blood-group-antigen expression. The Biochemical Journal. 1990;271(3):821-5.
21. Le Van Kim C, Mouro I, Chérif-Zahar B, Raynal V, Cherrier C, Cartron JP, et al. Molecular cloning and primary structure of the human blood group RhD polypeptide. Proceedings of the National Academy of Sciences of the United States of America. 1992;89(22):10925-9.

22. Avent ND, Madget TE, Lee ZE, Head DJ, Maddocks DG, Skinner LH. Molecular biology of Rh proteins and relevance to molecular medicine. Expert Reviews in Molecular Medicine. 2006;8(13):1-20.

23. Iwamoto S. Molecular aspects of Rh antigens. Legal Med. 2005;7(4):270-3.

24. Callebaut I, Dulin F, Bertrand O, Ripoche P, Mouro I, Colin Y, et al. Original article: Hydrophobic cluster analysis and modeling of the human Rh protein three-dimensional structures. Analyse des amas hydrophobes et modélisation de la structure tridimensionnelle des protéines humaines (French). 2006;13:70-84.

25. Tilley L, Green C, Poole J, Gaskell A, Ridgwell K, Burton NM, et al. A new blood group system, RHAG: three antigens resulting from amino acid substitutions in the Rh-associated glycoprotein. Vox Sang. 2010;98(2):151-9.

26. Chérif-Zahar B, Mattei MG, Le Van Kim C, Bailly P, Cartron JP, Colin Y. Localization of the human Rh blood group gene structure to chromosome region 1p34.3-1p36.1 by in situ hybridization. Hum Genet. 1991;86(4):398-400.

27. Wagner FF, Flegel WA. RHD gene deletion occurred in the Rhesus box. Blood. 2000;95(12):3662-8.

28. Avent ND, Reid ME. The Rh blood group system: a review. Blood. 2000;95(2):375-87.

29. Wagner FF, Gassner C, Muller TH, Schonitzer D, Schunter F, Flegel WA. Molecular basis of weak D phenotypes. Blood. 1999;93(1):385-93.

30. Stratton F. A new Rh allelomorph. Nature. 1946;158:25-6.

31. Flegel WA. Molecular genetics of RH and its clinical application. Transfus Clin Biol. 2006;13(1-2):4-12.

32. Garcia F, Rodriguez M-A, Goldman M, Azcarate M-N, Rodriguez M-I, Muniz-Diaz E, et al. New RHD variant alleles. Transfusion [Report]. 2015;55(2):427-9.

33. Wagner FF, Frohmajer A, Flegel WA. RHD positive haplotypes in D negative Europeans. BMC Genet. 2001;2:10.

34. Flegel WA, Wagner FF. Molecular biology of partial D and weak D: implications for blood bank practice. Clinical laboratory. 2002;48(1-2):53-9.

35. Okubo Y, Yamaguchi H, Tomita T, Nagao N. A D variant, D_{el}? Transfusion 1984;24(6):542.

36. Körmöczi GF, Gassner C, Shao CP, Uchikawa M, Legler TJ. A comprehensive analysis of DEL types: partial DEL individuals are prone to anti-D alloimmunization. Transfusion 2005;45(10):1561-7.

37. Wagner FF, Moulds JM, Flegel WA. Genetic mechanisms of Rhesus box variation. Transfusion 2005;45(3):338-44.

38. Singleton BK, Green CA, Avent ND, Martin PG, Smart E, Daka A, et al. The presence of an RHD pseudogene containing a 37 base pair duplication and a nonsense mutation in africans with the Rh D-negative blood group phenotype. Blood. 2000;95(1):12-8.

39. Avent ND. RHD genotyping from maternal plasma: Guidelines and technical challenges. Methods Mol Biol. 2008;444:185-201.

40. Harmening D, editor. Modern blood banking and transfusion practices. 5th ed. Philadelphia: F.A. Davis; 2005.

41. Gunson HH, Stratton F, Phillips PK. The primary Rho(D) immune response in male volunteers. Br J Haematol. 1976;32(3):317-29.

42. Kim K-H, Kim K-E, Woo K-S, Han J-Y, Kim J-M, Park KU. Primary anti-D immunization by DEL red blood cells. Korean Journal Of Laboratory Medicine. 2009;29(4):361-5.

43. Wagner T, Körmöczi GF, Buchta C, Vadon M, Lanzer G, Mayr WR, et al. Anti-D immunization by DEL red blood cells. Transfusion 2005;45(4):520-6.

44. Yasuda H, Ohto H, Sakuma S, Ishikawa Y. Secondary anti-D immunization by D_{el} red blood cells. Transfusion 2005;45(10):1581-4.

45. Bowman J. Thirty-five years of Rh prophylaxis. Transfusion 2003;43(12):1661-6.

46. Darrow RR. Icterus gravis (erythroblastosis) neonatorum - An examination of etiologic considerations. Archives of Pathology. 1938;25:378-417.

47. Levine P, Stetson RE. An unusual case of intra-group agglutination. JAMA: The Journal of the American Medical Association. 1939;113(2):126-7.

48. Levine P. Serological factors as possible causes in spontaneous abortions. J Hered. 1943;34(3):71-80.

49. Geifman-Holtzman O, Wojtowycz M, Kosmas E, Artal R. Female alloimmunization with antibodies known to cause hemolytic disease. Obstetrics and Gynecology. 1997;89(2):272-5.

50. Liverpool Medical Association. The Lancet. 1960;275(7123):526-7.

51. Kleihauer E, Braun H, Betke K. Demonstration von fetalem Hämoglobin in den Erythrocyten eines Blutausstrichs. Klinische Wochenschrift. 1957;35(12):637.

52. Finn R, Clarke CA, Donohoe WTA, McConnell RB, Sheppard PM, Lehane D, et al. Experimental Studies On The Prevention Of Rh Haemolytic Disease. The British Medical Journal. 1961;1(5238):1486-90.

53. Clarke CA, Donohoe WT, McConnell RB, Woodrow JC, Finn R, Krevans JR, et al. Further experimental studies on the prevention of Rh haemolytic disease. Br Med J. 1963;1(5336):979-84.

54. Wegmann A, Glück R. The history of rhesus prophylaxis with anti-D. Eur J Pediatr. 1996;155(10):835-8.

55. Chown B, Duff A, Buchanan D, Beck R, deVeber L, Cunningham T, et al. Prevention of primary Rh immunization - first report of the Western Canadian Trial, 1966-1968. Canadian Medical Association Journal. 1969;100(22):1021-4.

56. Bowman JM, Chown B, Lewis M, Pollock J. Rh isoimmunization, Manitoba, 1963-75. Canadian Medical Association Journal. 1977;116(3):282-4.

57. Brinc D, Denomme GA, Lazarus AH. Mechanisms of anti-D action in the prevention of hemolytic disease of the fetus and newborn: What can we learn from rodent models? Curr Opin Hematol. 2009;16(6):488-96.

58. Westhoff CM. Rh complexities: serology and DNA genotyping. Transfusion 2007;47:17S-22S.

59. Judd WJ. Practice guidelines for prenatal and perinatal immunohematology, revisited. Transfusion 2001;41(11):1445-52.

60. Coombs RRA, Mourant AE, Race RR. A new test for the detection of weak and "incomplete" Rh agglutinins. British Journal of Experimental Pathology. 1945;26(4):255-66.

61. Noizat-Pirenne F, Verdier M, Lejealle A, Mercadier A, Bonin P, Peltier-Pujol F, et al. Weak D phenotypes and transfusion safety: Where do we stand in daily practice? Transfusion 2007;47(9):1616-20.

62. Denomme GA, Dake LR, Vilensky D, Ramyar L, Judd WJ. Rh discrepancies caused by variable reactivity of partial and weak D types with different serologic techniques. Transfusion 2008;48(3):473-8.

63. Martinez BA, Crews E, Dowd AM, McMahan M. Comparative testing for weak expression of D antigen: Manual tube testing vs. a semiautomated IgG gel system. Immunohematology. 2003;19(1):7-9.

64. Flegel WA, Denomme GA, Yazer MH. On the complexity of D antigen typing: a handy decision tree in the age of molecular blood group diagnostics. Journal of obstetrics and gynaecology Canada. 2007;29(9):746-52.

65. Daniels G, Poole G, Poole J. Partial D and weak D: can they be distinguished? Transfus Med. 2007;17(2):145-6.

66. Dean L. The ABO blood group. Blood Groups and Red Cell Antigens: NCBI; 2005.

67. Judd WJ, Moulds M, Schlanser G. Reactivity of FDA-approved anti-D reagents with partial D red blood cells. Immunohematology. 2005;21(4):146-8.

68. Knowles SM, Milkins CE, Chapman JF, Scott M. The United Kingdom National External Quality Assessment Scheme (blood transfusion laboratory practice): trends in proficiency and practice between 1985 and 2000. Transfus Med. 2002;12(1):11-23.

69. Lai M, Grasso C, Boschi I, D'Onofrio G, Pascali V, Leone G. Characterization of anti-D monoclonal antibody reagents based on their reactivity with the weak D phenotype. Transfusion 2009;49(5):937-42.

70. Scott M. Section 1A: Rh serology. Coordinator's report. Transfus Clin Biol. 2002;9(1):23-9.

71. Flegel WA. How I manage donors and patients with a weak D phenotype. Curr Opin Hematol. 2006;13(6):476-83.

72. Denomme GA, Wagner FF, Fernandes BJ, Li W, Flegel WA. Partial D, weak D types, and novel RHD alleles among 33,864 multiethnic patients: implications for anti-D alloimmunization and prevention. Transfusion 2005;45(10):1554-60.

73. Ghidini A, Sepulveda W, Lockwood CJ, Romero R. Complications of fetal blood sampling. American Journal of Obstetrics & Gynecology. 1993;168(5):1339-44 6p.

74. Christiansen M, Samuelsen B, Christiansen L, Morbjerg T, Bredahl C, Grunnet N. Correlation between serology and genetics of weak D types in Denmark. Transfusion 2008;48(1):187-93.

75. Seltsam A, Doescher A. Sequence-Based Typing of Human Blood Groups. Transfus Med Hemother. 2009;36(3):204-12.

76. Polin H, Danzer M, Hofer K, Gassner W, Gabriel C. Effective molecular RHD typing strategy for blood donations. Transfusion 2007;47(8):1350-5.

77. Gassner C, Schmarda A, Kilga-Nogler S, Jenny-Feldkircher B, Rainer E, Muller TH, et al. RHD/CE typing by polymerase chain reaction using sequence-specific primers. Transfusion 1997;37(10):1020-6.

78. Atamaniuk J, Stuhlmeier KM, Karimi A, Mueller MM. Comparison of PCR methods for detecting fetal RhD in maternal plasma. Journal of clinical laboratory analysis. 2009;23(1):24-8.

79. Daniels G, Finning K, Martin P, Soothill P. Fetal blood group genotyping from DNA from maternal plasma: an important advance in the management and prevention of haemolytic disease of the fetus and newborn. Vox Sang. 2004;87(4):225-32.

80. Simsek S, Faas BHW, Bleeker PMM, Overbeeke MAM, Cuijpers HTM, Vanderschoot CE, et al. Rapid Rh D genotyping by polymerase chain reaction-based amplification of DNA. Blood. 1995;85(10):2975-80.

81. Daniels G, Finning K, Martin P, Massey E. Noninvasive prenatal diagnosis of fetal blood group phenotypes: Current practice and future prospects. Prenatal Diagn. 2009;29(2):101-7.

82. Finning K, Martin P, Summers J, Massey E, Poole G, Daniels G. Effect of high throughput RHD typing of fetal DNA in maternal plasma on use of anti-RhD immunoglobulin in RhD negative pregnant women: Prospective feasibility study. BMJ. 2008;336(7648):816-8.

83. Wang YH, Chen JC, Lin KT, Lee YJ, Yang YF, Lin TM. Detection of RhD(el) in RhD-negative persons in clinical laboratory. Journal of Laboratory & Clinical Medicine. 2005;146(6):321-5.

84. Lo YMD, Bowell PJ, Selinger M, Mackenzie IZ, Chamberlain P, Gillmer MDG, et al. Prenatal determination of fetal RhD status by analysis of peripheral blood of rhesus negative mothers. The Lancet. 1993;341(8853):1147-8.

85. Lo YM, Corbetta N, Chamberlain PF, Rai V, Sargent IL, Redman CW, et al. Presence of fetal DNA in maternal plasma and serum. Lancet. 1997;350(9076):485-7.

86. Anstee DJ. Red cell genotyping and the future of pretransfusion testing. Blood. 2009;114(2):248-56.

87. Bills VL, Soothill PW. Fetal blood grouping using cell free DNA – An improved service for RhD negative pregnant women. Transfusion and Apheresis Science. 2014;50(2):148-53.

88. Teitelbaum L, Metcalfe A, Clarke G, Parboosingh JS, Wilson RD, Johnson JM. Costs and benefits of non-invasive fetal RhD determination. Ultrasound in Obstetrics and Gynaecology. 2015;45:84-8.

89. IBGRL Molecular Diagnostics. [2016 30Mar]. Available from: http://ibgrl.blood.co.uk/ReferenceServices/Genotyping/MolecularDiagnostics2015.htm.

90. Finning K, Martin P, Daniels G. The use of maternal plasma for prenatal RhD blood group genotyping. Methods Mol Biol. 2009;496:143-57.

91. Finning K. User guide for referring samples to the IBGRL Molecular Diagnostics Laboratory [Internet]. NHS Blood and Transplant; 04Feb2016 [cited 29Mar2016]. Available from: http://ibgrl.blood.co.uk/ReferenceServices/UserGuides/INF1135%20User%20Guide%20for%20the%20genotyping%20laboratory.pdf

92. Finning K. Fetal RHD screening to determine requirement for anti-D prophylaxis during pregnancy [Internet]. NHS Blood and Transplant; 10Mar2015 [cited 29Mar2016]. Available from: http://ibgrl.blood.co.uk/ReferenceServices/UserGuides/INF1259.pdf

93. Nishimura N, Nakayama T, Tonoike H, Kojima K, Kato S. Direct polymerase chain reaction from whole blood without DNA isolation. Ann Clin Biochem. 2000;37:674-80.

94. Panaccio M, Georgesz M, Lew AM. FoLT PCR: a simple PCR protocol for amplifying DNA directly from whole blood. BioTechniques. 1993;14(2):238-43.

95. McCusker J, Dawson MT, Noone D, Gannon F, Smith T. Improved method for direct PCR amplification from whole blood. Nucleic Acids Res. 1992;20(24):6747.

96. Panaccio M, Lew A. PCR based diagnosis in the presence of 8% (v/v) blood. Nucleic Acids Res. 1991;19(5):1151.

97. Hall AT, Zovanyi AM, Christensen DR, Koehler JW, Minogue TD. Evaluation of Inhibitor-Resistant Real-Time PCR Methods for Diagnostics in Clinical and Environmental Samples. PLoS ONE. 2013;8(9).

98. Miura M, Tanigawa C, Fujii Y, Kaneko S. Comparison of six commercially-available DNA polymerases for direct PCR. Rev Inst Med Trop Sao Paulo. 2013;55(6):401-6.

99. Zhang Z, Kermekchiev MB, Barnes WM. Direct DNA amplification from crude clinical samples using a PCR enhancer cocktail and novel mutants of Taq. J Mol Diagn. 2010;12(2):152-61.

100. Taylor BJ, Martin KA, Arango E, Agudelo OM, Maestre A, Yanow SK. Real-time PCR detection of Plasmodium directly from whole blood and filter paper samples. Malar J. 2011;10:244.

101. Lo YM, Hjelm NM, Fidler C, Sargent IL, Murphy MF, Chamberlain PF, et al. Prenatal diagnosis of fetal RhD status by molecular analysis of maternal plasma. New Engl J Med. 1998;339(24):1734-8.

102. Geneious version 5.6.4 created by Biomatters. Available from www.geneious.com

103. Hess AS, Shardell M, Johnson JK, Thom KA, Strassle P, Netzer G, et al. Methods and recommendations for evaluating and reporting a new diagnostic test. European journal of clinical microbiology & infectious diseases : official publication of the European Society of Clinical Microbiology. 2012;31(9):2111-6.

104. Al-Soud WA, Rådström P. Purification and characterization of PCR-inhibitory components in blood cells. J Clin Microbiol. 2001;39(2):485-93.

105. Mao F, Leung W-Y, Xin X. Characterization of EvaGreen and the implication of its physicochemical properties for qPCR applications. BMC Biotechnol. 2007;7:76.

106. Owczarzy R, You Y, Moreira BG, Manthey JA, Huang LY, Behlke MA, et al. Effects of sodium ions on DNA duplex oligomers: Improved predictions of melting temperatures. Biochemistry. 2004;43(12):3537-54.

107. Doktycz MJ. Nucleic Acids: Thermal Stability and Denaturation. eLS. Chinchester: John Wiley & Sons, Inc; 2002.

108. Schildkraut C, Lifson S. Dependence of the melting temperature of DNA on salt concentration. Biopolymers. 1965;3(2):195.

109. Beilin LJ, Knight GJ, Munro-Faure AD, Anderson J. The sodium, potassium, and water contents of red blood cells of healthy human adults. J Clin Invest. 1966;45(11):1817-25.

110. Eischeid AC. SYTO dyes and EvaGreen outperform SYBR Green in real-time PCR. BMC Res Notes. 2011;4:263.

111. Bustin SA, Benes V, Garson JA, Hellemans J, Huggett J, Kubista M, et al. The MIQE guidelines: Minimum information for publication of quantitative real-time PCR experiments. Clin Chem. 2009;55(4):611-22.

112. Javadi A, Verduin EP, Brand A, Schonewille H. Comparison of different blood sample processing methods for sensitive detection of low level chimerism by RHD real-time PCR assay. Chimerism. 2013;4(1):9-14.

113. Lo YMD, Tein MSC, Lau TK, Haines CJ, Leung TN, Poon PMK, et al. Quantitative analysis of fetal DNA in maternal plasma and serum: Implications for noninvasive prenatal diagnosis. Am J Hum Genet. 1998;62(4):768-75.

114. Zimmermann BG, Maddocks DG, Avent ND. Quantification of circulatory fetal DNA in the plasma of pregnant women. Methods Mol Biol. 2008;444:219-29.

115. Landis JR, Koch GG. The Measurement of Observer Agreement for Categorical Data. Biometrics. 1977;33(1):159-74.

116. Burd EM. Validation of laboratory-developed molecular assays for infectious diseases. Clin Microbiol Rev. 2010;23(3):550-76.

117. McHugh ML. Interrater reliability: the kappa statistic. Biochemia Medica. 2012;22(3):276-82.

118. Kwiecien R, Kopp-Schneider A, Blettner M. Concordance Analysis: Part 16 of a Series on Evaluation of Scientific Publications. Deutsches Ärzteblatt International. 2011;108(30):515-21.

119. PCR Enhancer Cocktail 2. [Online]. DNA Polymerase Technology I, St. Louis, USA. 28Aug2010. [cited 09Jan2016] Available from: http://www.klentaq.com/products/pcr_enhancer_cocktail_2.

120. PCR Enhancer Cocktail 1. [Online]. DNA Polymerase Technology I, St. Louis, USA. 28Aug2015. [cited 09Jan2016] Available from: http://www.klentaq.com/products/pcr_enhancer_cocktail_1.

121. Yokota M, Tatsumi N, Nathalang O, Yamada T, Tsuda I. Effects of heparin on polymerase chain reaction for blood white cells. Journal Of Clinical Laboratory Analysis. 1999;13(3):133-40.

122. Scott Adams P. Data analysis and reporting. In: Dorak MT, editor. Real-time PCR. New York: Taylor & Francis Group; 2006. p. 39-62.

123. Lun FMF, Chiu RWK, Allen Chan KC, Yeung Leung T, Kin Lau T, Dennis Lo YM. Microfluidics Digital PCR Reveals a Higher than Expected Fraction of Fetal DNA in Maternal Plasma. Clin Chem. 2008;54(10):1664-72.

124. Sikora A, Zimmermann BG, Rusterholz C, Birri D, Kolla V, Lapaire O, et al. Detection of Increased Amounts of Cell-Free Fetal DNA with Short PCR Amplicons. Clin Chem. 2010;56(1):136-8.

125. Mari G, Deter RL, Carpenter RL, Rahman F, Zimmerman R, Moise KJJ, et al. Noninvasive Diagnosis by Doppler Ultrasonography of Fetal Anemia Due to Maternal Red-Cell Alloimmunization. New Engl J Med. 2000;342(1):9-14.

Appendix A

DNA Extraction Protocol – QIAamp DNA Blood Mini Kit

Objective
To isolate DNA from a small volume of blood (whole blood, buffy coat or plasma) in preparation for PCR.

Materials & Equipment

- EDTA whole blood sample (7 mL)
- QIAamp DNA Blood Mini kit
  - Mini spin columns
  - collection tubes (2 mL)
  - Buffer AL (see note 1)
  - Buffer AW1
  - Buffer AW2
  - Buffer AE
  - QIAGEN Protease (see note 2)
- microtubes (1.5 mL)
- PCR grade water
- anhydrous ethanol (see note 3)
- 56°C heating block
- pipette
- sterile pipette tips (aerosol barrier)
- centrifuge
- microcentrifuge (see note 4)
- sterile glass Pasteur pipettes (aerosol barrier)
- clean pipette bulb
- RNAse A (100 mg/mL)

Safety
DO NOT add bleach or acidic solutions to DNA extraction waste. Guanidine hydrochloride in Buffers AL and AW1 can form highly reactive compounds when combined with bleach.

Procedure
I. Preparation

Step	Action
1	Gather all samples and reagents. Allow them to come to room temperature.
2	Ensure heating block is turned on and at 56°C.
3	Clean bench and equipment (ie. pipettes, pipette tip boxes, tube racks, etc) first with Percept, then with 70% ethanol allowing both to air-dry.

II. DNA Extraction & Purification

Step	Action
1	Label 2 microtubes for the extracted DNA with sample number, DNA, date and initials.
2	Label a protease aliquot with sample number, date and initials.
3	Transfer 200 µL of sample (whole blood (see note 5), buffy coat or plasma) to the protease tube. Pulse vortex for 15 s.
4	Add 4 µL RNAse A (100 mg/mL). Pulse vortex for 15 s and centrifuge briefly to remove any drops from the lid.
5	Add 200uL of buffer AL. Pulse vortex for 15 s (see notes 1 and 6).
6	Incubate at 56°C for 10 minutes. Record temperature of heating block at time of incubation (see note 7).
7	Briefly centrifuge the 1.5 ml microtube to remove drops from the inside of the lid.
8	Add 200 µL of ethanol, pulse vortex for 15 s and centrifuge briefly to remove any drops from the lid (see note 3).
9	Open a new spin column and write sample number on column lid. Without wetting the rim, apply mixture to spin column (with column in a collection tube). Close the lid tightly.
10	Spin at 6000 x *g* for 1 min. For buffy coat samples, spin at 16000 x *g* to avoid clogging.

Step	Action
11	Discard filtrate tube and replace with a clean collection tube (see note 8).
12	Add 500 µL buffer AW1 to the spin column.
13	Spin at 6000 x *g* for 1 min.
14	Discard filtrate tube and replace with a clean collection tube (see note 8).
15	Add 500 µL buffer AW2 to the spin column.
16	Centrifuge at 16000 x *g* for 4 min (see note 9).
17	Discard filtrate tube and replace with a collection tube (see note 10).
18	Centrifuge at 16000 x *g* for 2 min.
19	Discard filtrate tube and place spin column into one of the DNA microtubes labeled in step 1. Remove the lid and keep for later use (see note 10).
20	Add 200uL of PCR grade water and let sit at room temperature for 5 minutes.
21	Centrifuge at 6000 x *g* for 1 minute.
22	Transfer all but about 5 µL of eluate to the other DNA microtube from step 1.
23	Cap and retain tube with 5 µL of DNA extract for yield and purity check.
24	Store DNA extracts in -20 °C freezer.

Notes:

1. A precipitate may form in Buffer AL. Dissolve by incubating at 56 °C.
2. Reconstituted QIAGEN protease is stored as 20 µL aliquots in the -20°C freezer.
3. Anhydrous ethanol is a controlled substance. Be sure to record usage on the log sheet attached to the container.
4. All centrifugation steps for DNA extraction are carried out at room temperature (15–25°C).
5. Extraction from 200 µL of whole blood yields 3–12 µg of DNA. Preparation of buffy coat is recommended if a higher yield is required.
6. Do not add QIAGEN Protease or proteinase K directly to Buffer AL.
7. DNA yield reaches a maximum after lysis for 10 min at 56°C. Longer incubation times have no effect on yield or quality of the purified DNA.
8. Buffers AL and AW1 are NOT compatible with bleach.
9. This is a modification of the QIAamp DNA Blood Mini kit instructions. Time has been increased because full speed of Acker lab microcentrifuge is not 20000 x *g*.
10. When spinning the column in a microtube, high speeds can cause the lid to detach from the tube and may result in damage to specimen tubes or the centrifuge. Remove the mictotube lid before spinning.

References

This protocol was adapted from the manufacturer's instructions provided with the kit; QIAamp DNA Mini and Blood Mini Handbook, QIAGEN, 3rd ed, Apr2010.

Appendix B

DNA Isolation – FlexiGene DNA Kit – Buffy Coat

Objective
To isolate DNA from 1.0 mL or 100 µL of buffy coat sample using the Qiagen FlexiGene DNA kit

Materials

- buffy coat samples
- Qiagen FlexiGene DNA kit
  - Buffer FG1 (lysis buffer)
  - Buffer FG2 (denaturation buffer)
  - Buffer FG3 (hydration buffer)
  - Qiagen Protease
- centrifuge with swing-out rotor
- vortex mixer
- 100% isopropanol
- 70% ethanol
- conical tubes, 15 mL
- microtubes
- pipettes and sterile filter tips
- 65 °C water bath (or heating block)

Safety
DO NOT add bleach or acidic solutions to extraction waste containing Buffer FG2. Guanidine hydrochloride in Buffer FG2 can form highly reactive compounds when combined with bleach. If liquid containing Buffer FG2 is spilt, clean with suitable laboratory detergent and water. If the spilt liquid contains potentially infectious agents, clean the affected area first with laboratory detergent and water, and then with 1% (v/v) sodium hypochlorite.

Reagent Storage
All buffers and reagents can be stored at room temperature (15–25°C) for up to 24 months without reduction in performance.

Lyophilized QIAGEN Protease can be stored at room temperature (15–25°C) for up to 24 months without reduction in performance. For storage longer than 24 months or if ambient temperatures frequently exceed 25°C, QIAGEN Protease should be stored dry at 2–8°C.

Reconstituted QIAGEN Protease is stable for 2 months when stored at 2–8°C.

Incubating the QIAGEN Protease stock solution at room temperature for prolonged periods of time should be avoided. Storage at –20°C will prolong its life, but repeated freezing and thawing should be avoided. Dividing the solution into aliquots and storage at –20°C is recommended.

Notes:

1. The Buffer FG2/Protease solution should be used within 1 hour of preparation.
2. Samples may be fresh or frozen. Thaw frozen samples quickly in a 37°C water bath with mild agitation.
3. All centrifugation steps should be carried out at room temperature in a swing-out rotor.
4. When processing multiple samples, vortex each tube immediately after addition of Buffer FG2/QIAGEN Protease. Do not wait until buffer has been added to all samples before vortexing. Usually 3–4 pulses of high-speed vortexing for 5 s each are sufficient to homogenize the pellet. However, traces of pellet with a jelly-like consistency (often barely visible) may remain. If these traces are seen, add a further 300 µL Buffer FG2 and vortex.

Procedure

Step	Action
1	Calculate the total volume of buffy coat to be processed in the batch.
2	Prepare Buffer FG2/Protease solution. For every 1 mL of buffy coat to be processed, combine 1 mL of Buffer FG2 and 10 µL of protease.

Step	Action		
3	Add buffy coat samples (mL) to a labelled conical tube.	1.0 mL	100 µL
4	Add Buffer FG1 and mix by inverting 5 times.	2.5 mL	250 µL
5	Centrifuge for 5 minutes at 2000 *x g*.		
6	Discard the supernatant and leave tube inverted on a clean absorbent paper for 2 minutes, taking care that the pellet remains in the tube.		
7	Add Buffer FG2/protease solution. Close the tube and vortex immediately until the pellet is completely homogenized. **See Note 4**.	1.0 mL	100 µL
8	Invert the tube 3 times, place in a water bath and incubate at 65°C for 10 minutes.		
9	Add 100% isopropanol and mix thoroughly by inversion until DNA precipitate becomes visible as threads or a clump.	1.0 mL	100 µL
10	Centrifuge for 3 minutes at 2000 *x g*. If pellets are loose, increase time or *x g*.		
11	Discard the supernatant and briefly invert the tube onto a clean absorbent paper, taking care that the pellet remains in the tube.		
12	Add 70% ethanol and vortex for 5 seconds.	1.0 mL	100 µL
13	Centrifuge for 3 minutes at 2000 *x g*. If pellets are loose, increase time or centrifuge speed.		
14	Discard the supernatant and leave the tube inverted on a clean absorbent paper for at least 5 minutes, taking care that the pellet remains in the tube.		
15	Air-dry the DNA pellet until all the liquid has evaporated (at least 5 minutes). Over-drying the DNA pellet will make the DNA difficult to dissolve.		
16	Add Buffer FG3, vortex for 5 seconds at **low speed**.	300 µL	200 µL
17	Dissolve the DNA by incubating in a water bath at 65°C for 1 hour. If necessary, increase incubation time until DNA is completely dissolved.		
18	Transfer DNA to appropriately labelled microtubes and store at -20°C.		

References

This protocol was adapted from the manufacturer's instructions provided with the kit; FlexiGene DNA Handbook, QIAGEN, May 2010.